Universitetet i Stavanger

FACULTY OF SCIENCE AND TECHNOLOGY

MASTER'S THESIS

Study programme/specialisation: **Petroleum Engineering / Natural Gas Engineering**	**Spring semester, 2019** **Open**/~~Confidential~~
Author: **Saeed Sajedi** Student Number: **243879**	**Digital Submission** (~~signature of author~~)
Programme coordinator: **Rune Wiggo Time** Supervisor(s): **Rune Wiggo Time (Uis), Arild Fosså (EXPRO)**	
Title of master's thesis: **Accuracy of gas condensate ratio (CGR) based on fluid sampling analyses, Case study: Ormen Lange field**	
Credits: **30 ECTS**	
Keywords: **Condensate to gas ratio (CGR)** **PVT analysis** **Wireline fluid sampling methods** **Modular dynamic tester (MDT)** **Drill stem test (DST)** **Clean-up test**	Number of pages: **143** + supplemental material/other: **0** Stavanger, **15th June 2019**

ABSTRACT

Accuracy of condensate to the gas ratio (CGR) is one of the most significant issues in the petroleum industry. In this study, Ormen Lange field was the case study for checking the accuracy of CGR based on fluid samples from different fluid sampling methods. By analyzing the cleanup test data of nine development wells which were provided by EXPRO from 2007 to 2009, the CGR of each development well was corrected with regards to the total volume correction factor (TVCF) of intended development well. In addition, corrected CGRs were normalized based on missing gas volume of stoke tank oil from cleanup test process due to the missing gas development wells. Hence, by checking the validity of average normalized CGR from the cleanup test with actual production data, liquid and gas phases of test separator sample (cleanup test sample) were recombined together with validated normalized CGR by PVT.SIM software. Consequently, this study showed that the measured CGRs of collected samples by MDT method needed further investigation due to the fact that the average relative error of CGRs from MDT samples was approximately 40% as compared to the average CGR of DST and test separator samples (cleanup test sample). Besides, this significant relative error can result in possible consequences for planning and fluid modelling.

ACKNOWLEDGEMENTS

I would like to represent my gratitude to the people who supervised me to do my master thesis:

- First and foremost, I would like to thank my internal supervisor at the University of Stavanger, **Professor Rune Wiggo Time**; for giving me this opportunity to do my thesis with his supervision.
- To **Arild Fosså**, DST manager of EXPRO in Tananger and my co-supervisor, thank you very much for guiding and teaching me.
- To **Kim Andre Nesse Vorland**, head engineer at the University of Stavanger, thank you very much for helping me to learn PVT.SIM software.
- To **Andreas Habel**, Senior engineer, thank for providing me useful input data from DISKOS database for PVT analyses.

Lastly, I really like to thank **my family** who has supported me in every moment of my life.

Saeed Sajedi

Stavanger 2019

CONTENTS

LIST OF FIGURES

LIST OF TABLES

NOMENCLATURE

Symbol	***Meaning / Units***
CGR	Condensate to Gas Ratio (STB/MMSCF)
GOR	Gas to Oil Ratio (Sm3/ Sm3)
W_r	Angular Velocity
K	Geometric Coefficient
Q_o	Oil Flow Rate (m^3/day)
Q_g	Gas Flow Rate (m^3/day)
MF	Meter Factor
Shr	Shrinkage Factor
BS&W	Base Sediment and Water
CMSCF	Combined Meter Shrinkage Factor
VCF_T	Volume Correction Factor (Temperature)
VCF_p	Volume Correction Factor (Pressure)
C'	Orifice Factor Constant
H_W	Differential Flow
P_f	Following Pressure (Kpa)
F_b	Basic Orifice Factor
F_r	Reynolds Number Factor
F_{pb}	Pressure Base Factor
F_{tb}	Temperature Base Factor
F_{tf}	Following Temperature Factor
F_{gr}	Specific Gravity Factor
F_{pv}	Super compressibility Factor
Y	Expansion Factor
R_F	Response Factor

Accuracy of condensate to gas ratio based on fluid sampling analyses

W_s	Weight of iso-Octane (i-C_8)
A_s	Area of iso-Octane (i-C_8)
W_I	Weight of Component (I)
A_I	Area of Component (I)
X_i	Mole Fraction of Liquid Phase (%)
Y_i	Mole Fraction of Gas Phase (%)
Z_i	Mole Fraction of Reservoir Fluid (%)
γ_{rig}	Specific gas gravity at rig
Z_{Lab}	Compressibility factor at laboratory
Z_{rig}	Compressibility factor at rig
γ_{Lab}	Specific gas gravity at laboratory
Mw	Molecular Weight (gr/mole or kg/kg mole)
F_i	Hoffmann factor for I component
R	Gas Constant ($8.3145\frac{Kpa\,.\,m^3}{K.\ kg\ mole}$)
T_{bi}	Boiling Temperature for i Component (R)
T_{sep}	Temperature of separator (R)
P_{sep}	Pressure of Separator (psi)
T_{Ci}	Critical Temperature of i Component (R)
A_0	Intercept at the plot
A_1	Slope of the line at plot
$\dot{M}_{wf}$	Mass flow rate well fluid (kg/day)
$\dot{M}_{mg\ Sep}$	Mass flow rate missing gas from separator (kg/day)
$\dot{M}_{C\ sep}$	Mass flow rate condensate from separator (kg/day)
Q_{wf}	Volume flow rate of condensate from separator (m3/day)

ρ_{wf}	Density of condensate from separator (g/cm3)
$Q_{mg\ sep}$	Volume flow rate of missing gas from separator (m3/day)
$\rho_{mg\ sep}$	Density of missing gas from separator (g/cm3)
$Q_{C\ sep}$	Volume flow rate of condensate from separator (m3/day)
$\rho_{C\ sep}$	Density of condensate from separator (g/cm3)
$Q_{water\ sep}$	Volume flow rate of water from separator (m3/day)
$\rho_{water\ sep}$	Density of water from separator (g/cm3)
$\dot{M}_{CS}$	Mass flow rate condensate from separator (kg/day)
$\dot{M}_{mg\ STK}$	Mass flow rate missing gas from stock tank oil (kg/day)
$\dot{M}_{C\ STK}$	Mass flow rate condensate from stock tank oil (kg/day)
$Q_{C\ Sep}$	Volume flow rate of condensate from separator (m3/day)
$\rho_{C\ Sep}$	Density of condensate from separator (g/cm3)
$Q_{mg\ STK}$	Volume flow rate of missing gas from stock tan oil (m3/day)
$\rho_{mg\ STK}$	Density of missing gas from stock tank oil (g/cm3)
$Q_{C\ STK}$	Volume flow rate of condensate from stock tank oil (m3/day)
$\rho_{C\ STK}$	Density of condensate from stock tank oil (g/cm3)

ABBREVIATIONS

WFTs	Wireline Fluid Testers
PVT	Pressure, Volume, Temperature
CGR	Condensate to Gas Ratio
MDT	Modular Dynamic Tester
DST	Drill Stem Test
TVCF	Total Volume Correction Factor
NPD	Norwegian Petroleum Directorate
EOS	Equation of State
CME	Constant Mass Expansion
CVD	Constant Volume Depletion
BHS	Bottom-hole Sample
CQG	Crystal Quartz Gauge
GOR	Gas to Oil ratio
VCF	Volume Correction Factor
FID	Flame Ionization Detector
GC	Gas Chromatography
TCD	Thermal Conductivity Detector
TD	Top Depth
STK	Stoke Tank Oil
NACL	Sodium Chloride
KCL	Potassium Chloride
N2	Nitrogen

1 . Chapter 1 Introduction

1.1 Introduction

Gas condensate reservoir is one of the most significant sources of hydrocarbon reserves. However, production from this hydrocarbon resource encounters some challenges. Collecting representative fluid samples from gas condensate reservoirs has a specific principle due to the behavior of in-situ reservoir fluid. There is a diversity of fluid sampling methods and selecting the appropriate approach relies on the type of the reservoir fluid. Gas condensate reservoirs are categorized into two following types; lean gas condensate and rich gas condensate, so choosing the proper fluid sampling method for each type of the gas condensate reservoir is a noteworthy issue. For gas condensate reservoirs, there are two types of fluid sampling methods, namely bottom-hole sampling method and surface sampling method. When the reservoir fluid is a very lean gas condensate, surface sampling method is the best technique for collecting the representative fluid samples because bottom-hole fluid sampling techniques, specifically wireline fluid sampling methods (WFTs) cannot collect enough volume of reservoir fluids for PVT analyses but bottom-hole sampling methods can be utilized for rich gas condensate. Condensate to gas ratio (CGR) measurement is one of the issues about lean gas condensate reservoir fluids, so when the CGR of lean gas condensate is gauged incorrectly the behavior of reservoir fluid will be determined wrongfully. Hence integrating the reservoir model and estimating the production of the reservoir will result in a big standard deviation from actual production. Eventually, incorrect CGR will have irrecoverable consequences with regards to the financial issue in the foreseeable future such as wasting investments for constructing unsuitable plants and refineries due to the fact that the volume of production is estimated based on inaccurate CGR.

1.2 Background study

(Minhas et al., 2009)studied the first high pressure and high temperature (HPHT) gas condensate field from offshore East Malaysia for checking the accuracy of condensate to the gas ratio (CGR). There were some key challenges in that operation. The development wells were spudded with oil based mud (OBM), so the probability of filtrate or contamination in bottom-hole

samples could be high. (Minhas et al., 2009) checked the quality of bottom-hole samples, specifically WFT samples concerning compositional analyses and cleanup test data. Although,(Bjørn Dybdahl & Hans Petter Hjermstad, 2001) stated that wireline fluid sampling methods(WFTs) are not suitable for collecting the fluid samples from gas condensate reservoirs, (Minhas et al., 2009)has verified that WFT samples from rich gas condensate reservoir from offshore East Malaysia have shown good quality as representative fluid samples of in-situ reservoir fluid.

1.3 Motivation

One of the most noticeable reasons that this thesis focuses on the accuracy of condensate to the gas ratio (CGR) is due to the importance of accurate production estimation. In other words, petroleum companies which are defined as operators sometimes estimate the production of oil and gas fields based on inaccurate CGR. Moreover, the second reason which creates motivation for emphasizing on the accuracy of CGR is selecting the most suitable fluid sampling methods for gas condensate reservoirs. Last but not least, the development wells from Ormen Lange field were spudded with water-based mud (WBM) which might have less contaminations or filtrate in fluid samples and that is why the Ormen Lange field has been chosen as a case study for this thesis.

1.4 Objective of the project

This thesis aims to illustrate the accuracy of condensate to gas ratios (CGRs) of fluid samples collected of exploration wells from Ormen Lange field in 1998 by Modular Dynamic Tester (MDT) which was the most advanced wireline fluid sampling method in 1990s and cleanup test sample which was attained by EXPRO. In addition, Consequences of incorrect CGRs can affect making the decision on estimating the production. So, in this project, it has been shown that how measuring the CGR accurately is important.

1.5 Data source for analyses

EXPRO provided cleanup test data of candidate development wells from Ormen Lange field which is the case study in this Thesis and due to the fact that Norwegian Petroleum Directorate (NPD) has not published the cleanup test data, we cannot attach them to the thesis, in

the other words they are confidential. In addition, for fluid sampling analyses of exploration wells from Ormen Lange field, we gathered the PVT data from DISKOS database which has been provided by NPD, and the University of Stavanger has access to this data source.

1.6 Appropriate software for PVT simulation

In this Thesis, PVT.SIM which is a versatile equation of state (EOS) modeling software was utilized to simulate fluid properties and experimental PVT data. This software is the primary commercial software owned, marketed and developed by Calsep Company. Moreover, there are some following reasons that this software was used for PVT analyses:

- Simulating PVT properties of fluid samples without the consideration of experimental data for calibration.
- Consists of nine cubic equation of states (EOS)
- Cutting-edge flash and regression algorithms make the PVT.SIM software the most robust simulator.

2. Chapter 2 Theory

2.1 Flow behavior

2.1.1 Phase behavior of gas condensate

The behavior of gas condensate fluid depends on two elements; the phase envelope and reservoir conditions which can be shown by P-T diagram (figure 2.1). The phase envelope consists of two lines (one line is bubble point line and the other one is dew point line) meet each other in one point which is called critical point. For pressure higher than the cricondenbar line and for temperature more than the cricondentherm line, the reservoir fluid is single phase flow. At the critical point the properties of Liquid and vapor phase cannot be different anymore. With increasing the percentage of heavier components (pseudo components &plus fraction) in reservoir fluid, the critical point will move clockwise round phase envelope curve, then the behavior of reservoir fluid will change(Wall, 1982).

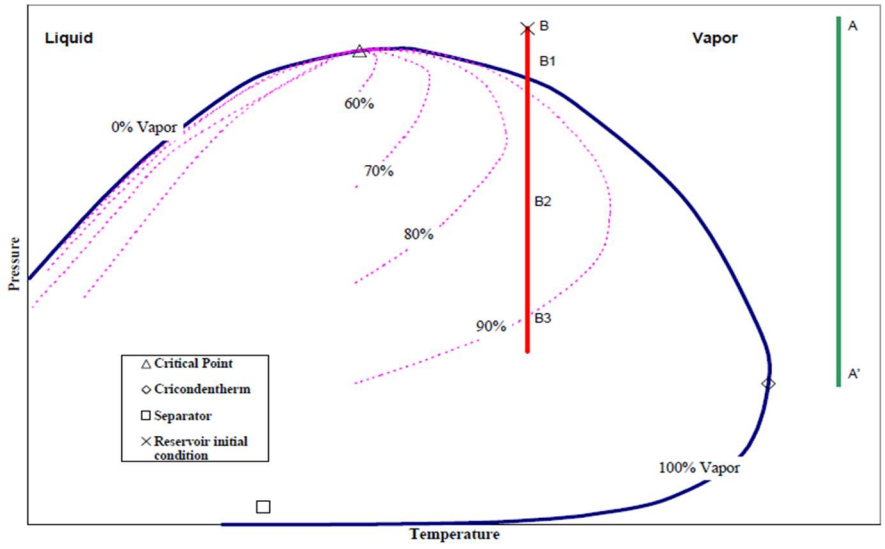

Figure 2.1. Typical gas condensate phase envelope (Fan et al., 2005) & (Roussennac, 2001).

Based on figure 2.1 which shows a typical gas condensate phase envelope, type of the reservoir fluid can be detected by initial conditions of reservoir, so gas and gas condensate reservoirs can be different with regards to their own initial conditions(Roussennac, 2001):

- Gas reservoirs: if the initial temperature and pressure of reservoir are higher than the cricondentherm and cricondenbar, respectively and the standard condition of the reservoir is also is out of the two-phase envelope, this reservoir is **dry gas reservoir** which is indicated with AA' line in figure 2.1. But if the standard condition of the reservoir is in the two-phase envelope that reservoir is the **wet gas reservoir**.

- Gas condensate reservoirs: if initial pressure of the reservoir is more than cricondenbar but reservoir temperature is between cricondentherm and critical temperature, retrograde condensation will appear in the reservoir. In figure 2.1 from B to B1, the reservoir fluid is a single phase but by pressure drop lower than dew point line, which is the outcome of natural depletion, the liquid will drop out in the reservoir. Furthermore, when the reservoir is in the production process, the composition of gas condensate is changing by the time. Because when the condensate saturation is at a low level the mobility of liquid phase is almost zero and only gas will flow through the reservoir until the maximum condensate saturation (B2, see figure 2.1). Likewise, gas condensate reservoirs are divided into the categories **lean gas condensate reservoirs** (when the condensate to the gas ratio (CGR) is lower than 500 $Sm^3/SMMm^3$) and **rich gas condensate reservoirs** (when CGR is higher than 500 $Sm^3/SMMm^3$)(C. H. J. F. d. Whitson & Hydro, 1998). So, if the CGR is measured incorrect, the type of reservoir fluid cannot be determined accurately.

2.1.2 Static and dynamic values of Gas Condensate Systems

The most important aspect of gas condensate systems is identifying the values of static and dynamic properties. Static values are the properties of gas condensate fluid at the given location of reservoir and given time for describing the state of gas condensate system. But dynamic properties are different over the time, for example, the compositions of fluid from wellhead samples are different from the overall compositions in the reservoir, however, they can show the changes of reservoir fluid (gas-condensate system)(Shi, 2009). Likewise, the difference between

static and flowing values of gas condensate fluid can be shown by considering two neighboring grid blocks in a flow simulation (see figure 2.2). In top part of the figure 2.2 represent volume fraction of oil and gas in cells 1 and 2 at given time which is a static value but in the middle of the two cells there is not any physical location and it just shows that only gas flows from cell 1 to cell 2 which represents flowing value, so it can be figured out that the oil mobility is almost zero. Furthermore, the volume fraction of oil in grid block 2 is higher than grid block 1, because of the pressure drop(Roussennac, 2001).

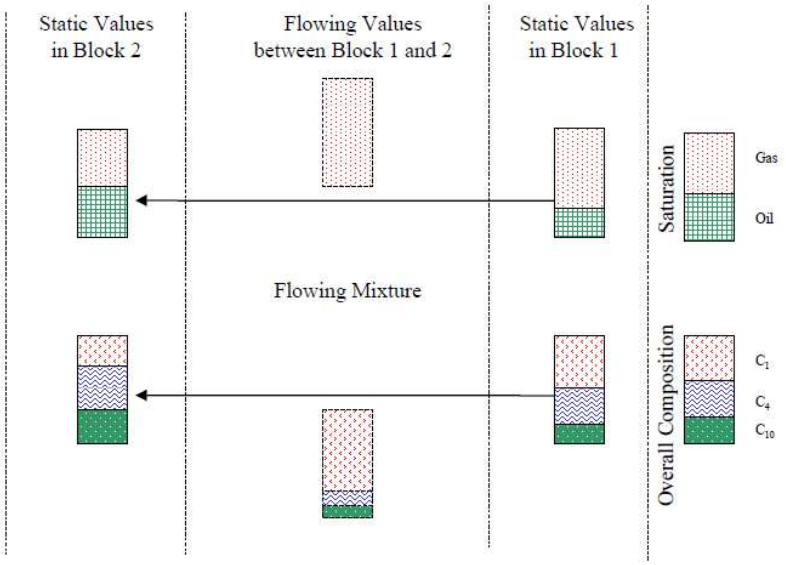

Figure 2.2. Difference between Static and Dynamic (flowing) Values (Roussennac, June 2001).

The other properties like viscosity, density and specifically condensate-gas ratio (CGR) will be different if there is a flowing mixture.

2.1.3 Depletion in gas condensate reservoirs

Gas condensate wells which undergo depletion consist of three regions(Fevang & Whitson, 1996):

- Region 1: this zone is close to wellbore where oil and gas flow at the same time by different velocities. In this region condensate to the gas ratio (CGR) is constant throughout. It means that the gas phase fluid which enters to region 1 has the same composition as produced well stream fluid. The most significant feature about this

region is productivity loss of gas condensate due to the condensate buildup. Therefore drop-out liquid will be a barrier for producing more gas phase fluid.

- Region 2: a region where reservoir pressure decreases lower than dew point pressure, so liquid drops in the reservoir. In this section gas only is flowing and the condensate phase is immobile because the condensate saturation is not high enough to flow. Moreover, if heavier components (plus fraction) which have a high molecular weight drop into this region, leaner single-phase gas will flow through this region.

- Region 3: this section just consists of original reservoir gas because the reservoir pressure is higher than the dew point pressure, so there is a single gas phase. Also, the composition of reservoir fluid is constant in this zone.

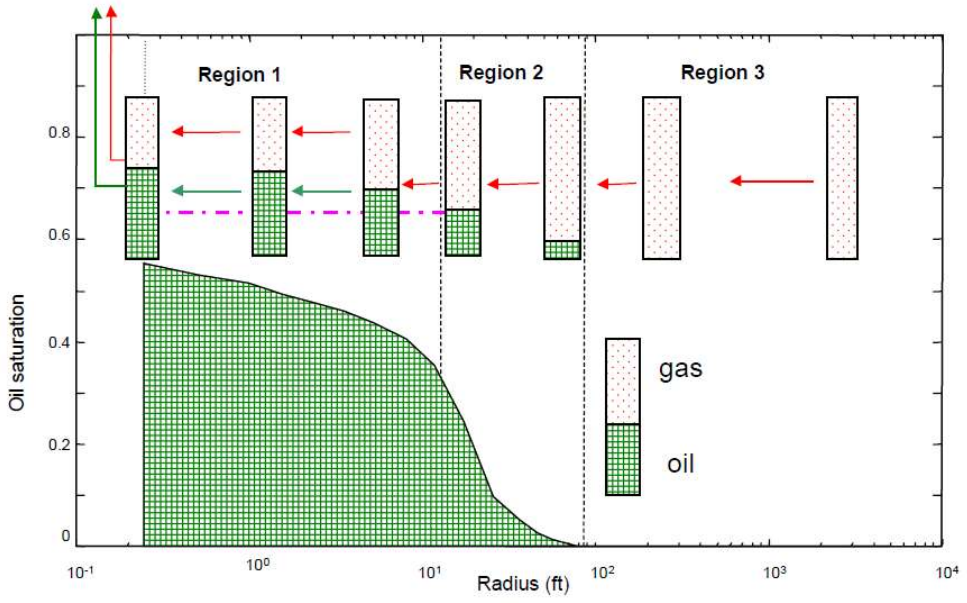

Figure 2.3. Schematic gas condensate behavior in three regions (Roussennac, June 2001).

The behavior of gas condensate in three regions is illustrated in figure 2.3 and it can be figured out that in region 1 the saturation of gas condensate is high enough (condensate buildup) to allow condensate to flow, However, in region 2 the mobility of liquid phase is approximately zero. Furthermore, region 3 where is far from the well the reservoir pressure is more than dew point pressure, so based on figure 2.1 the reservoir fluid in this region is a single gas phase(Roussennac, 2001).

So, for analyzing the accuracy of condensate to gas ratio from one field, the flow behavior of gas condensate should be considered, specifically when there is flowing mixture in reservoir regions and CGR is a dynamic value.

2.2 Fluid Sampling

2.2.1 Why Fluid Sampling?

Fluid sampling aims to collect a representative fluid sample from reservoir fluid. And this sample used in a laboratory for determining PVT behavior of fluid both at reservoir and surface conditions. Furthermore, an adequate volume of representative fluid should be gathered for processing analysis which is necessitated for designing required plants and crude assay for refinery processes. A standard set of the measurement performed on the representative sample from gas condensate reservoir would include PVT analysis, viscosity, specific gravity, condensate to the gas ratio (CGR) and multistage separation tests (Constant Mass Expansion (CME) & Constant Volume Depletion CVD). Moreover, for having the consistent fluid sampling program, reservoir fluid should be single-phase and contaminations which are introduced by drilling and completion fluids should be minimized substantially as well. A wide range of the techniques, tools, and procedures exist for fluid sampling program. Though, there are some following issues which should be considered: type of fluid sampling method, design of consistent equipment, transferring the samples. Likewise, the amount of non-hydrocarbon components or solid components such as wax and asphaltenes which can be formed into wellbore should be measured. one should keep in mind that the representative sample belongs to one point of the formation cannot be taken into account as an overall representative sample of the fluid from gas condensate reservoir (Nagarajan et al., 2006).

Determining accurate sampling method with regards to the type of reservoir fluid is the first step for setting the accurate CGR and divided into two following categories:

2.2.2 Well fluid sampling methods

These kinds of methods collect desired samples directly from pre-selected locations at reservoir conditions. Then the sample chambers are brought to the surface and the samples which were gathered by sample device will be pressurized and restored as a single phase and finally will be sent to the laboratory for properties analysis. In addition, adequate cleaning of near-wellbore regions and controlling drawdown are vital elements for gaining uncontaminated representative samples. due to the fact that controlled drawdown prevents phase split and two-phase flow into the reservoir (Witt, Crombie, & Vaziri, 1999). There are two types of well fluid sampling techniques as following:

- Wireline formation sampling: this kind of sampling may give fine quality samples with an adequate sample volume for PVT analysis of oils but for gas condensate, the volume of sample may be too small for studying the physical and chemical characteristics of gas condensate. Although this type of well fluid sampling method is cost efficient and environmentally friendly (no burning of gas), it has some issues about having a representative fluid sample from reservoir fluid. In order to use wireline formation tester (WFT) when the wellbore is not complete, the fluid sample may be contaminated by drilling fluid filtrate specifically when oil-based drilling mud used in the wellbore. Furthermore, various wireline formation testers have been presented in petroleum industry, such as FIT (formation interval tester) in the 1950s, FMT (formation multi tester) in 1970s, RFT (repeat formation tester) in 1980s and MDT (modular dynamic tester) was the most advanced wireline fluid sampling method in last decades (see figure 2.4). The most significant privileges of utilizing these modern generations of wireline formation test tools are that they reduce the expenses of petroleum industry in fluid sampling and they are also time-efficient due to the fact that some regions can be sampled in one run, however wireline fluid sampling methods cannot be considered as good options for very lean gas condensate reservoir fluids (Proett, Gilbert, Chin, & Monroe, 1999).

- Bottom-hole sampling (BHS): this kind of method sampling can be used after completing the wells. In other words, when drilling mud and any chemical materials

has been removed from the wellbores. And the samples may be taken by wireline or tubing conveyed carrier. Moreover, one of the advantages of tubing conveyed bottom-hole samplers is that they are very time-efficient by rejecting the need for separate sampling flow. Because numerous sampling compartments can be filled in one run. One of the deficiencies of this sampling method is that if the reservoir fluid is two-phase (reservoir pressure is lower than dew point pressure), this sampling method cannot be recommended. Also because of the limited volume of samples by this method the same as wireline formation sampling is not recommended for **lean gas condensates** but it may be used for **rich gas condensates** where the condensate yield is inadequate to gain a good characterization of heavy components (plus fractions) (Bjørn Dybdahl & Hans Petter Hjermstad, 2001).

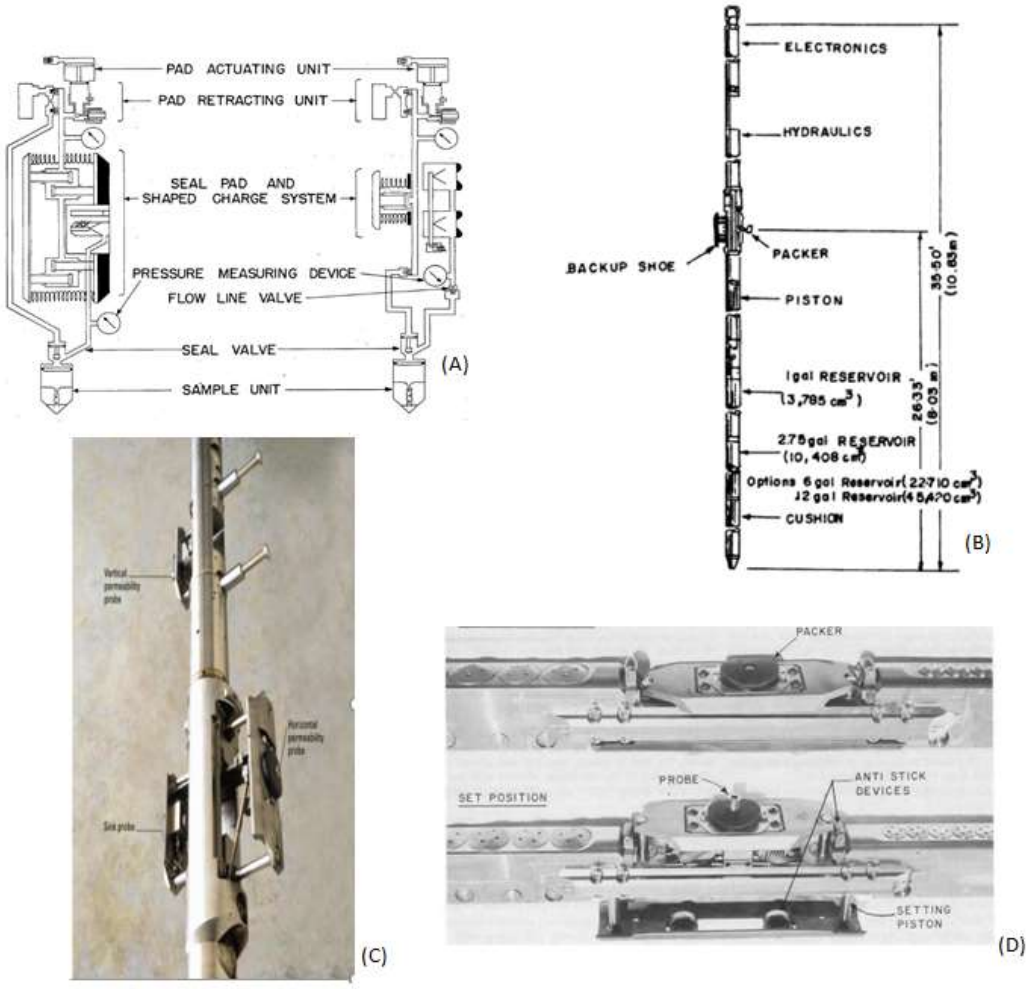

Figure 2.4. Wireline fluid sampling methods: formation interval tester (FIT) (A), formation multi tester (FMT) (B), modular dynamic tester (MDT) (C) and repeat formation tester (RFT) (D).

2.2.3 Surface Sampling methods

The most important step for obtaining a great quality of fluid samples in the surface sampling process is an appropriate well conditioning. It means that flowing the well at an ideal rate with single-phase flow in the reservoir until the constant producing CGR is detected. Besides, accurate oil and gas rate at the surface from separators play the vital roles for acquiring stable producing CGR. However cleaning the near-wellbore regions is one of the critical steps before sampling, it is not a serious concern during the surface sampling operation because of the huge amount of fluids produced before sampling operation (Nagarajan et al., 2006). In addition, there are three types of surface sampling methods as following:

- Wellhead sampling method: samples are collected directly on the wellhead, but it should be known that the well fluid is single-phase. Although this type of surface fluid sampling methods is appropriate for oil and gas condensate, it is not recommended for gas condensate with high wax formation temperatures.

- Separator sampling method: consist of getting the samples of oil and gas by optimum rates from test separators at the same time. In this type of surface sampling methods as soon as wellbore has been conditioned taking the samples from separators should be carried out. Then the two samples (oil & gas) should be recombined together in the same quantity as measured condensate to the gas ratio (CGR) when it is stable at test separator. One of the challenges about this method is determining an accurate recombination ratio. And the positive point is obtaining large volume samples of each phase (gas & oil) easily. So, this method gives a chance for getting adequate fluid to characterize heavy components (plus fraction) in some lean gas condensates. However, if the oil rate from the oil separator is lower than 35 m3/day this method is not suitable for measuring the condensate production rate because lower than this value the uncertainties of liquid rate will be huge which can impact on condensate to gas ratio (CGR) measurement (Bjørn Dybdahl & Hans Petter Hjermstad, 2001).

- Split stream sampling at wellheads: when the wellhead temperatures are low, wax precipitation can exist and influence on representability of fluid sampling at separators. And requiring the injection of inhibitors for hydrate formations is the other issues which can happen during the production. These problems are more considerable for gas condensates than for oils because of the minor heat content of the flow and higher wax formation temperatures. Isokinetic split stream fluid sampling method can reduce these issues through the big operational range for lean gas condensates as compared to test separator (see figure 2.4). Modern generations of this method are equipped by a single fixed probe which can collect the samples from upstream of choke manifold and/or from downstream of test separator. Furthermore, the flow rate from the sampling probe is the same as that of a well-fluid stream. Then, the high-quality samples will be brought to a small-scale separator for establishing accurate condensate gas ratio (CGR). The other advantage of isokinetic split stream fluid sampling method is that it can be used for detecting liquid carry-over in the separator gas outlet which can be observed in gas condensate fields. This method can be applied just for fluids with a CGR of less than 200 STB/MMSCF (Kool et al., 2001).

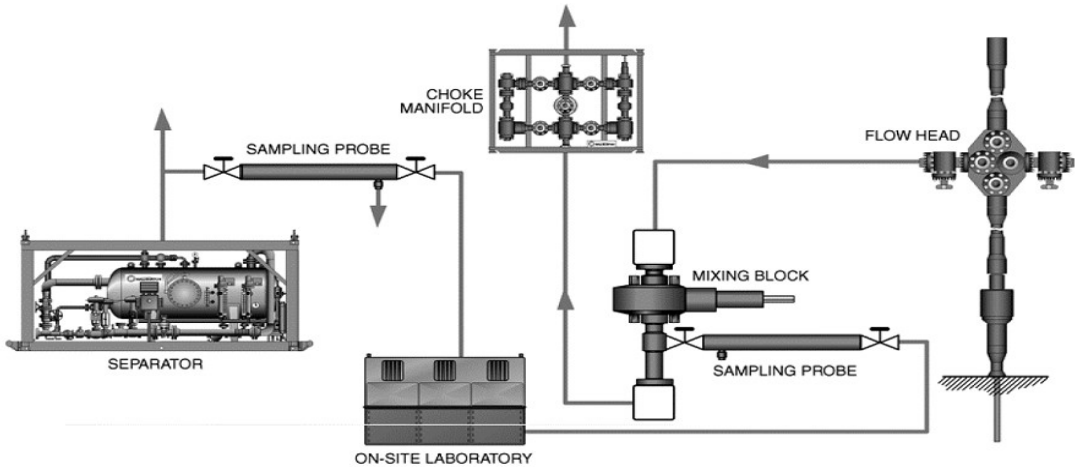

Figure 2.5.Schematic isokinetic split stream fluid sampling method (Kool et al., 2001).

2.2.4 Modular Dynamic Tester (MDT)

The basic purpose of wireline fluid sampling methods is to measure formation pressure and collect samples of formation fluid at discrete depths in the reservoir for analysis and measuring fluid in-situ properties including viscosity, density, specific gravity, gas to oil ratio (GOR). Wireline fluid sampling method has been introduced to the oil and gas industry since 1955 and modular dynamic tester (MDT) is the most advanced wireline fluid sampling method in the petroleum industry now.

This type of wireline formation tester which was introduced by Schlumberger in the 1990s is the most efficient method as compared to the last four decades. Because it provides fast and accurate pressure measurements and high-quality fluid sampling on a single descent in the well. It can also measure permeability anisotropy, so this method offers all requirements at the possible shortest time which are needed for decision making. One of the most significant features about this method is a segmental design which can let the operator modify the tool based on the goals and requirements (Schlumberger, 2002). One of the modules which makes modular dynamic tester (MDT) to be capable to collect fluid samples from thin zones or very low permeability, laminated, fractured and vuggy formations is a dual packer module (see figure 2.6). This module consists of two expandable packers which can seclude a section of formation by 1 to 3.5 m sizes to allow fluids to take out from the formation to the wellbore by high rate without decreasing the pressure lower than saturation pressure. Dual packer module consists of two pressure measurement gauges. One of them is stain gauge which is utilized for measuring the pressure inside the dual packers for checking the setting pressure and the other pressure gauge is Crystal Quartz Gauge (CQG) which is used for measuring the pressure and temperature in the flow line when sampling fluid comes to wireline formation tester, so it can monitor bubble point or dew point pressures of representative fluid (Badry, Head, Morris, & Traboulay, 1993).

The other distinguished module which can determine permeability anisotropy in region 1 of the reservoir (near-wellbore zone) is multiprobe module. This module is equipped with one dual-probe module that consists of two probes (sink probe and horizontal permeability probe) which are in the same segment but back-to-back and one single-probe module (vertical permeability probe). During the simple test, the pre-determined amount of formation fluid is pulled into the pre-test chamber in flow control module from the sink probe for measuring the flow rate of the fluid. And then by determining the pressure in dual-probe and single-probe modules, the

horizontal and vertical permeability can be calculated accurately (see figure 2.6)(Schlumberger, 2002).

The electrical module is the other unit which is responsible to supply power for electrical segments by an electrical bus which is run through all units in modular dynamic tester (MDT). Also, there are some modules which need hydraulic power for operation such as setting and withdrawing single- and dual-probe modules, so hydraulic power module which consists of a hydraulic pump and electric motor is the other power source for supplying power for tools (Mp, Indra, & Prasetyo, 1999).

One of the most important modules for measuring the physical properties of reservoir fluid in flowline is Live Fluid Analyzer. This module is equipped with two analyzing sensors, one spectrometer which employs infrared light for measuring the amount of representative and drilling fluids. This sensor transfers infrared light through the fluid, then some of this light will be absorbed by the fluid. And this amount of absorbed infrared light can determine the composition of the fluid. Figure 2.7 shows the optical density spectra which can be used for determining the type of reservoir fluids(Schlumberger, 2002). The second sensor is gas refractometer which can detect gas from oil, so live fluid analyzer can determine the type of fluid from formation and specify the proportion of oil and free gas to measure gas to oil ratio (GOR)(Mp et al., 1999). Moreover, tables 2.1 and 2.2 show the specifications of the modular dynamic tester and its pressure sensors. As compared to its last generations, this method of wireline fluid sampling is well-organized and time efficient. And, it can be employed in high pressure and temperature wells which is one of the challenges in the petroleum industry. In Ormen Lange field, MDT method with single probe module was employed for collecting reservoir fluids in deferent depth points in 1990s.

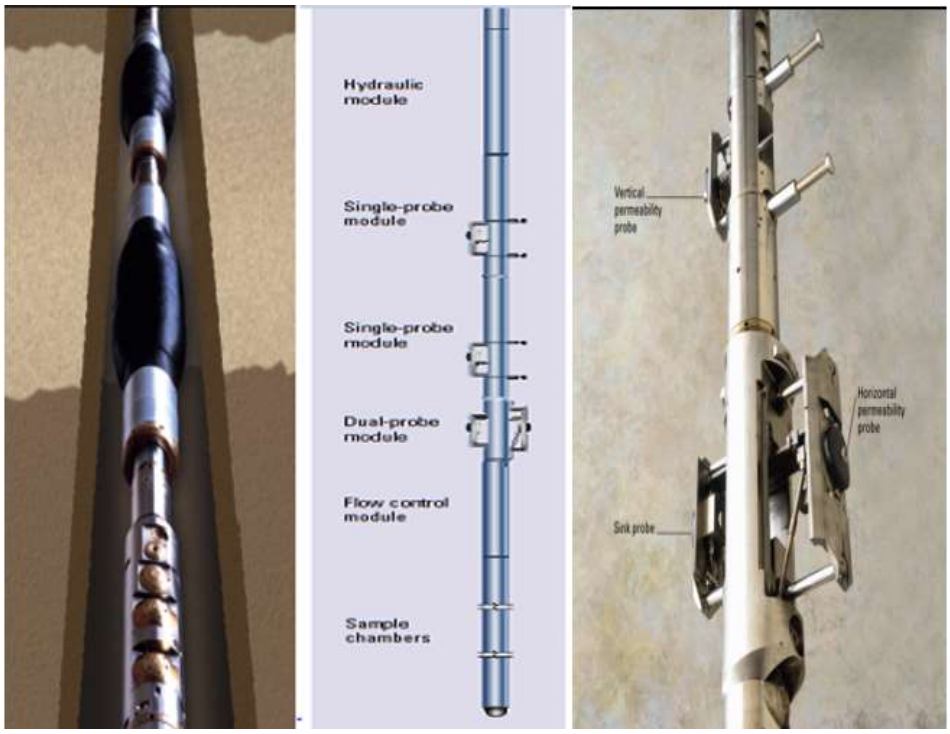

Figure 2.6. Dual packer module (Left-hand side), Multiprobe assembly (middle side) and Dual probe module (Right-hand side)(Schlumberger, 2002).

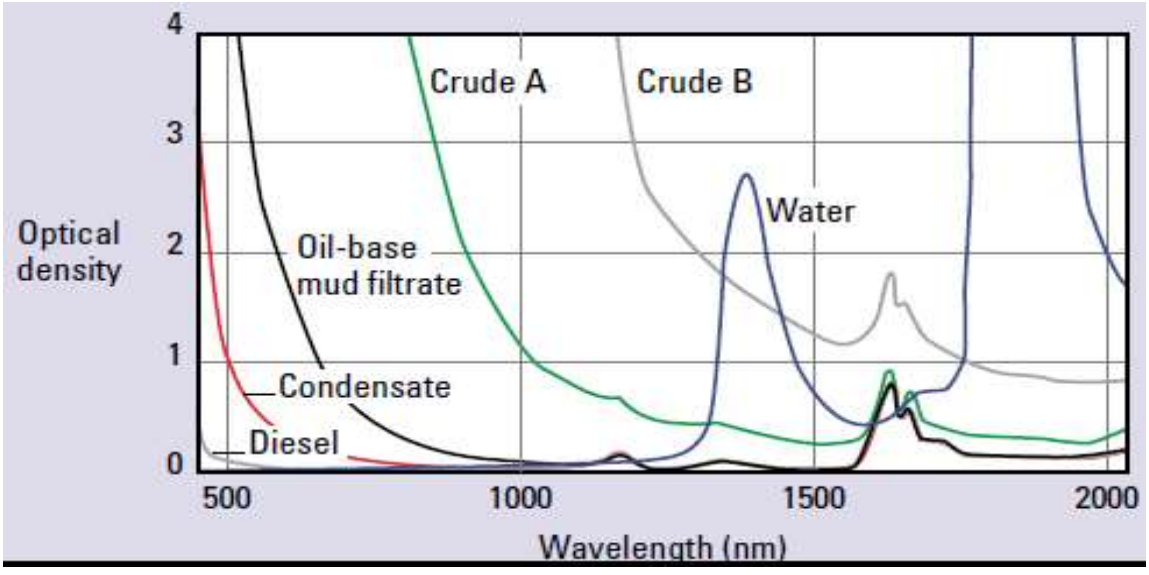

Figure 2.7. Optical density spectra for determining the type of reservoir fluid (Schlumberger, 2002).

Table 2.1. Specifications of Modular Dynamic Tester (MDT)(Schlumberger, 2002).

Specifications	Single Probe Module	Multi Probe Module	Dual Packer Module
Pressure rating (Psi)	25000	25000	25000
Temperature rating (°F)	400	400	325
Maximum hole size (inch)	24	15	14.75
Minimum hole size (inch)	5.875	7.62	5.875
Diameter (in)	4.75	6	5
Formation Type	Consolidated & Unconsolidated	Consolidated & Unconsolidated	Consolidated & Unconsolidated

Table 2.2. Specifications of Strain and Quartz gauges of MDT (Schlumberger, 2002).

Specification	Strain Gauge	Quartz gauge
Calibrated ranges (psi)	0 to 25000	0 to 25000
Resolution (psi)	0.1	0.01
Accuracy	±0.1%	±2 psi
Repeatability	±0.06%	< 1 psi
Temperature rating (F)	400	400

2.3 Cleanup test Process

Before the well testing process, wellbore should be prepared properly. Specifically, in exploration wells, there is some debris which remains during the drilling operation. Because cuttings or mud filtrate can influence well-testing data, especially drawdown test data, so the **cleanup test** can prevent the fluctuations in flow rate and allow the well to flow at the maximum acceptable level. EXPRO is one of the most experienced international companies in cleanup and well testing process. And this company plays a crucial role in providing effective solutions for its clients to improve optimal productions of their reserves(Gundersen, 2015).

2.3.1 Cleanup test equipment

When the well fluid is produced, some tests should be done for characterization and decision making, so there should be some equipment and tools based on pre-determined operations as following(Gundersen, 2015):

- Getting the representative fluid samples of well fluid for PVT analysis at the laboratory.
- Arranging the fluids at the surface based on the eco-friendly approach.
- Separating the phases of the well fluid from each other (oil, gas, and water) and measuring their flow rates at different pressures and temperatures by specific flow meters (Orifice, turbine and Coriolis).

Surface equipment utilized in cleanup test process should be chosen based on client objectives and processing state. But here we discuss primary components which are essential for all cleanup test operations (see figure 2.15).

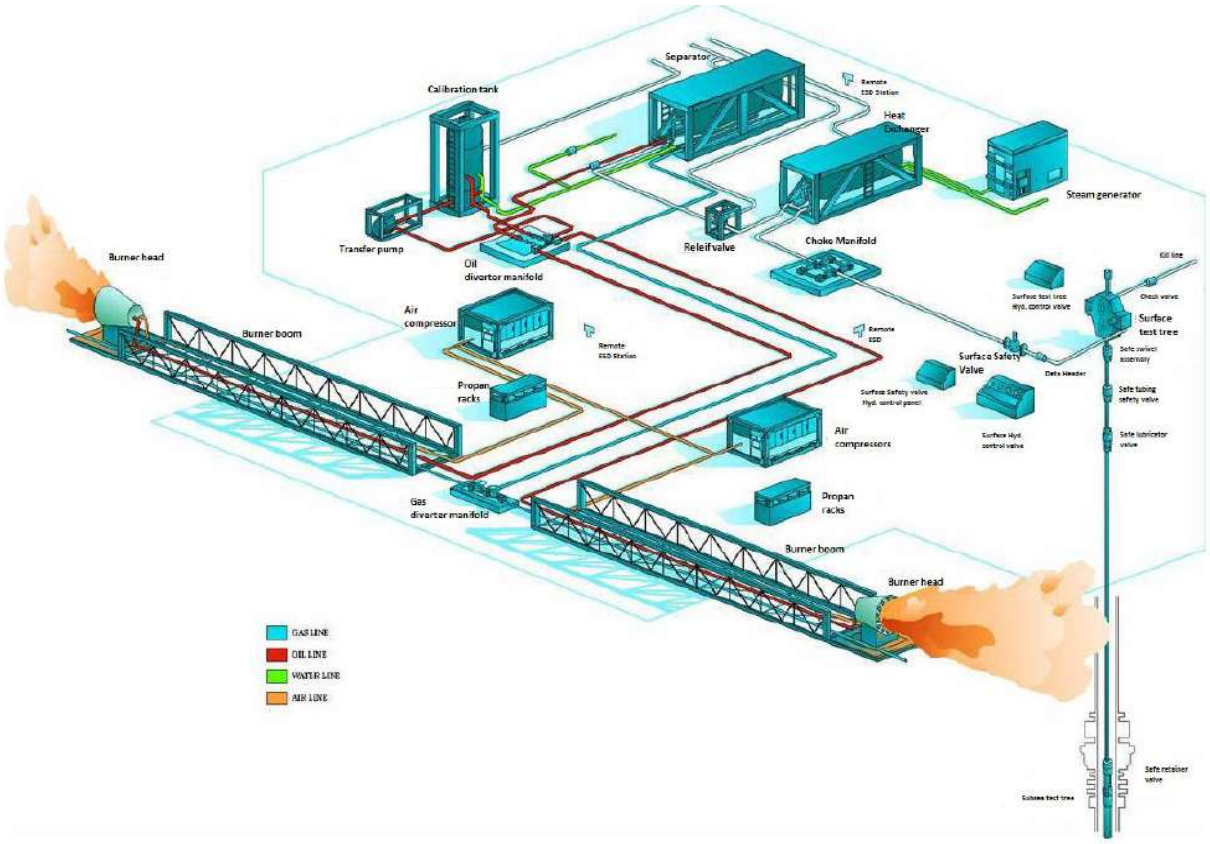

Figure 2.8. Schematic diagram of surface cleanup test equipment (Gundersen, 2015).

2.3.1.1. Choke manifold:

This component can be used for controlling the flow rate of well fluid which comes from wellbore before enters to processing equipment and decreasing the well pressure. Choke manifold has two following types(Gundersen, 2015,Rene Mignot,2003) :

- Adjustable choke which is utilized for the cleanup test or whenever fixed choke needs to be changed.
- Fixed choke is the other type of choke manifold which is a fixed orifice by higher accuracy in flow control as compared to adjustable choke. The sizes of the fixed chokes are termed in 64^{th} and in the next chapter, there are different sizes of fixed chokes which were used in the development wells. Moreover, the reason for using fixed choke is to get the critical flow on the choke which is very important for approving the drawdown pressure test data.

Figure 2.9. Choke Manifold (courtesy of EXPRO, 2007).

2.3.1.2. Heat exchanger:

Because of the pressure loss through choke manifold, there might be some wax, emulsion or hydrate. So, by heating the fluid it can avoid to hydrating, foamy oil and emulsion and also assist to separate phases of the fluids in separators(Gundersen, 2015).

Figure 2.10. A typical heat exchanger (EXPRO)(Gundersen, 2015).

.

2.3.1.3. Separator:

The produced well fluid should transfer to the separator for fluid segregations (oil, gas, and water) and fluid sampling. Generally, separators have three outlets including gas, oil and water outlets which are equipped with flow meters for measuring the flow rates of phase fluids separately. Also, there are some inflatable controls for gauging the pressure and fluid levels accurately in the separator(Gundersen, 2015). However, the flow rates of phase fluids measured by flow meters (Coriolis, turbine, and orifice) are not at standard conditions, therefore EXPRO provided some methods for correcting flow rates in different pressures and temperatures to atmospheric conditions. These methods are used for correcting the cleanup test data in this project which are discussed more in the next chapter.

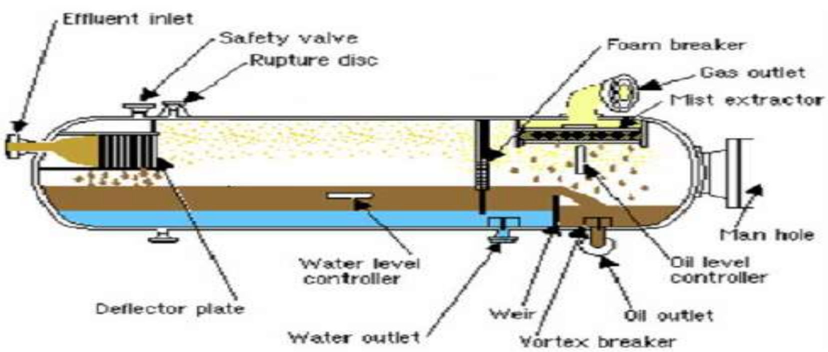

Figure 2.11. Schematic diagram of well testing separator (Gundersen, 2015).

2.3.2 Turbine meter and correction factor

Mostly, there is a multi-bladed rotor in turbine meters which is utilized for measuring the flow rate of the fluid. When the fluid passes through the rotor, it causes the multi-bladed rotor rotates by angular velocity which is roughly proportional to the flow rate of the fluid (see eq.2.1). The blades of the rotor are made of ferromagnetic substances which can make a magnetic circuit with the coil in the turbine housing (see figure 2.12). Then, the generated voltage in the coil is proportional to the angular velocity of multi-bladed rotor, therefore the flow rate can be measured based on the following equation(Bentley, 2005):

$$\omega_r = KQ \quad \ldots\ldots\ldots\ldots\ldots\ldots\ldots\ldots \quad (2.1)$$

ω_r: Angular velocity.

Q: flow rate.

K: is a constant which depends on the geometry of the blades.

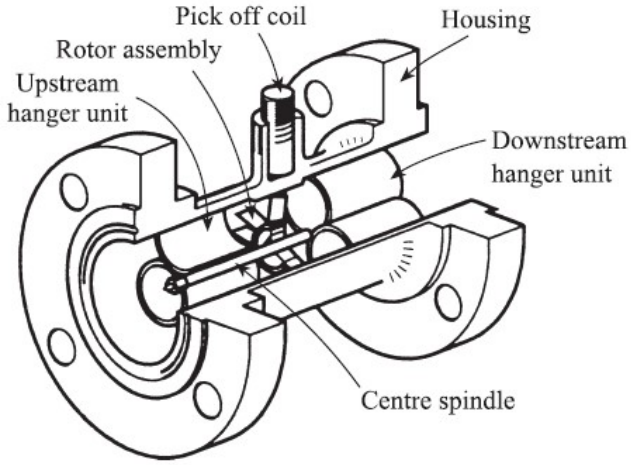

Figure 2.12. Schematic diagram of the turbine meter (Bentley, 2005).

One of the most important factors that should be considered about flow meters is the correction factor. When well fluid transmitted from turbine to calibration tank (stock tank oil) for achieving standard conditions (1 bar, 60 °F), there will be a pressure loss which is created by the level control valve and frictions in the pipelines. Then, pressure drop causes some changes in the oil and precipitations of the gas. Thus, (Worth, 2003)prepared an equation (see eq.2.2) for converting the flow rate at flow meter in different pressures and temperatures to standard conditions (1 bar, 60 °F). Equation 2.2 also consists of shrinkage factor because the pressure loss results in precipitation of the gas and then shrinking of the oil. Volume correction factor (VCF) due to the temperature is the other factor which can affect oil flow rate should be considered as well.

$$Q_{oil}\left(\frac{Sm^3}{day}\right) = V_s * MF * \left(1 - \frac{Shr}{100}\right) * \left(1 - \frac{BS\&W}{100}\right) * VCF \quad \ldots\ldots\ldots\ldots\ldots\ldots\ldots\ldots (2.2)$$

V_s: uncorrected flow rate (m^3/day) taken at meter.

MF: meter factor.

Shr: shrinkage factor.

BS&W: base sediment and water.

VCF: volume correction factor.

In EXPRO, the total volume correction factor (TVCF) can be measured in two ways but in this project, we considered following method which has the highest accuracy(Gundersen, 2015) for correcting the measured oil flow rates from candidate field (Ormen Lange):

$$CMSF = VCF_p = \frac{Final\ tank\ reading - initi\quad tank\ reading}{final\ meter\ reading - initia\ \ meter\ reading} \quad \ldots\ldots\ldots\ldots\ldots\ldots \text{(2.3)}$$

$$VCF_T = 1 - \left\{\left[T_{\circ C} * \left(\frac{9}{5}\right) + 32\right] - 60\right\} * 0.0005 \ldots\ldots\ldots\ldots\ldots\ldots\ldots\ldots \text{(2.4)}$$

$$TVCF = CMSF * VCF_T \ldots\ldots\ldots\ldots\ldots\ldots\ldots\ldots\ldots\ldots\ldots\ldots\ldots\ldots \text{(2.5)}$$

$$Q_{oil}\left(Sm^3/_{day}\right) = V_s * TVCF \ldots\ldots\ldots\ldots\ldots\ldots\ldots\ldots\ldots\ldots\ldots\ldots\ldots\ldots \text{(2.6)}$$

CMSF: combined meter shrinkage factor.

VCF_P: volume correction factor due to the pressure.

VCF_T: volume correction factor due to the temperature.

TVCF: total volume correction factor.

In this method, before a certain volume of oil is diverted to calibration tank (stock tank oil), the initial reading of oil flow rate at turbine meter with oil line properties (pressure, temperature) should be recorded. And the initial volume of calibration tank before the oil is transmitted to the tank must be measured. Then, when the oil in calibration tank reaches atmospheric conditions (1 bar, 60 °F) the second reading of the oil volume in the tank and turbine meter should be carried out (see eq. 2.3) (Gundersen, 2015).

2.3.3 Orifice meter and correction factor

Gas flow rates generally were measured by orifice flowmeters but recently Coriolis flow meter is utilized in the petroleum industry for measuring gas and oil flow rates. EXPRO has

employed Coriolis flow meters from the last decade. In the next subchapter, we will discuss Coriolis flowmeter for measuring gas flow rate.

Orifice flow meter (Daniel Box) consists of two pressure sensors which are connected to orifice flange or fitting measure static and differential pressures. Likewise, there is one orifice plate which is held by orifice flange or fitting is perpendicular to the flow line and can make differential pressure (see figure 2.13 A and 2.20 B)(GPSA, 1998).

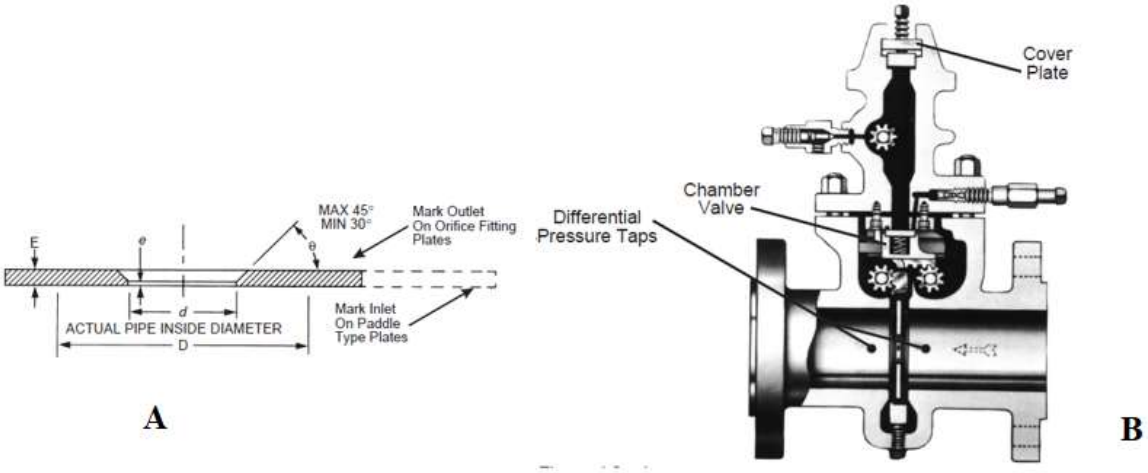

Figure 2.13. Schematic diagram of Orifice plate (A), a typical flange Orifice meter (B) (GPSA, 1998).

so based on the following equation the gas flow rate can be computed(GPSA, 1998):

$$Q_g\left(\frac{m^3}{hr}\right) = C' * \sqrt{H_w P_f} \quad \text{..... (2.7)}$$

C': Orifice factor constant.

H_w: Differential flow.

P_f: Following pressure (Kpa).

$$C' = F_b * F_r * Y * F_{pb} * F_{tb} * F_{tf} * F_{gr} * F_{pv} \quad \text{..... (2.8)}$$

F_b : Basic orifice factor. Y: Expansion factor.

F_r: Reynolds number factor.

F_{pb}: Pressure base factor.

F_{tb}: Temperature base factor.

F_{tf}: Following temperature factor.

F_{gr}: Specific gravity factor.

F_{pv}: Super compressibility factor.

2.3.4 Coriolis meter

Cleanup tests which were carried out by EXPRO for development wells from Ormen Lange field (2007 to 2009) were equipped with Coriolis flow meter for measuring the gas flow rates. This gauging device can also measure mass flow, density, pressure, and temperature of fluid which is passing through the control pipe. Coriolis consists of a tube and some measuring sensors, so when the fluid passes through the tube it will make some vibrations and the measuring sensors will gauge the mass flow based on vibrations. Installation the orientations of Coriolis flowmeter depends on the type of the fluid which is passing through the process control pipe (see figure 2.14).

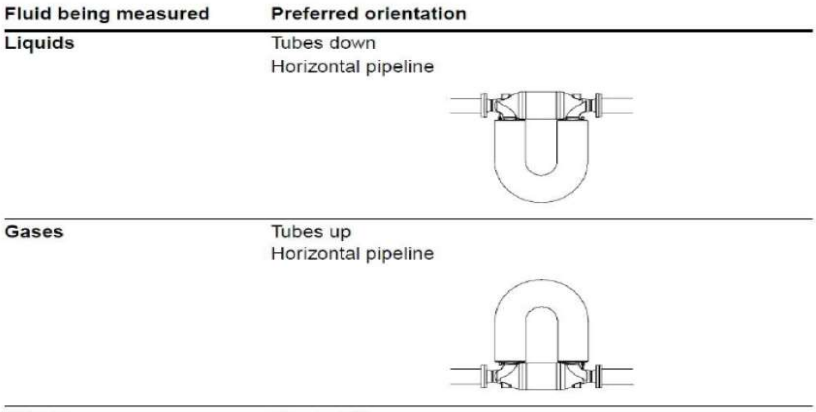

Figure 2.14. Schematic diagram of the orientation of Coriolis meter for different fluids.

EXPRO has been using Edge-X software which can receive the gas flow rates data from Coriolis meters and correct them by calculating the uncertainties which can affect the gas flow rates. So, in this project, because EXPRO utilized Edge-X software in cleanup tests of development wells (Ormen Lange field), we did not need to correct gas flow rates for calculating the normalized condensate to gas ratios (CGRs).

2.4 PVT analysis

When the representative samples are collected by wireline fluid sampling tools or surface fluid sampling methods, they will be transmitted to the laboratory for analyzing the reservoir fluids. In other words, PVT analysis is the study of basic properties of reservoir fluid: pressure, volume and temperature. And the most significant properties which play vital roles for analyzing the representative samples are as following(Curtis H. Whitson, 1983):

- The compositions of reservoir fluid.
- Saturation pressure at reservoir temperature for detecting the behavior of the fluid.
- Density and Viscosity of reservoir fluid.
- Shrinkage factor (B_g) of the gas condensate from the reservoir to standard conditions.

Based on the type of the representative samples, there are some analyses which can be recommended, so for reservoir fluids which are gas condensates there are three standard following analyses(Curtis H Whitson & Brulé, 2000):

- Recombined Separator compositions.
- Constant mass expansion (CME).
- Constant volume depletion (CVD).

2.4.1 Compositional analysis

The components in petroleum reservoir fluids are divided into two categories(Curtis H Whitson & Brulé, 2000):

1. Non-hydrocarbon (non-organic): H_2S, N_2, CO_2.
2. Hydrocarbon (organic): C_1, C_2, C_3, i-C_4, n-C_4… Cn.

The compositional analysis is utilized for some reasons but in this project, the outputs of this analysis are used for simulating reservoir fluid behavior. There are some methods for analyzing the compositions of the representative fluid samples but one of them which was applied for PVT analysis is Gas chromatography.

2.4.1.1. Gas Chromatography (GC):

When the gas condensate fluid which is collected by wireline fluid sampling methods transferred to the laboratory for PVT analysis, it is at reservoir conditions. Therefore, for analyzing the compositions of gas condensate fluid by gas chromatography, firstly it should be flashed to standard conditions. Then some heavier components are separated from the lighter components and create a liquid phase of the representative fluid. Secondly, the liquid phase (condensate) is heated until the boiling temperature and circulated through columns by carrier gas which generally is helium or nitrogen. Then, by increasing the temperature in the stationary phase in columns, lighter compounds are separated from heavier compounds and transmitted by the carrier gas to FID (flame ionization detector) or TCD (thermal conductivity detector). Inflame ionization detector, there is a small air flame which burns the compounds and the ions of each compound are accumulated on the electrodes. Then the quantities of the ions are improved and recorded. But thermal conductivity detector which can be used for inorganic components gauges the heat which is transmitted from the filament to the walls of the detector. After that, the concentration of individual compounds can be measured by thermal conductivity changes. Finally, the concentrations of components are recorded as a series of the chromatographic peaks and the area under each peak is proportional to the weight of each compound individually. In addition, identification of components is based on retention time due to the fact that each compound is kept by columns(Freyss et al., 1989).

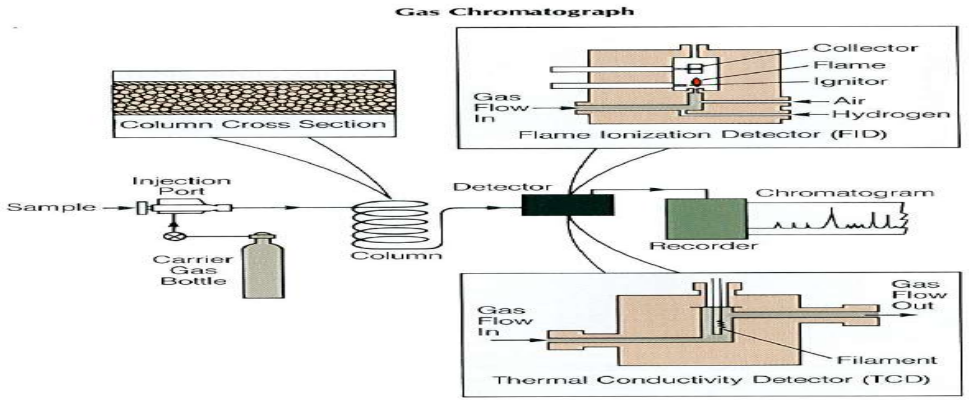

Figure 2.15. Typical gas chromatography with FID or TCD (Freyss et al., 1989).

Also, the gas phase is like liquid phase and it is originally gas and it does not need to be vaporized, so the gas phase is injected to the gas chromatography and circulated by a carrier

gas (He or N2) and compounds of gas phase will be recorded like liquid phase (condensate) which is explained above.

For quantifications of components in GC, there is one standard which is iso-octane (i-C_8) due to the fact that the peak area of iso-octane is recognizable and does not overlap with the peak areas of other components. Therefore, the pre-determined quantity of iso-octane is about 1% weight of fluid which is injected to GC. Then, based on response factor of iso-octane which is calculated by the following formula (see eq. 2.9), the weight of each component can be calculated (see eq. 2.10) (Burke, Chea, Hobbs, & Tran, 1991):

$$R_f = \frac{W_s}{A_s} \quad \text{(2.9)}$$

$$W_i = R_f * A_i \quad \text{(2.10)}$$

R_f: Response factor.

W_s: the weight of iso-octane (i-C_8) in STO.

A_s: Area of iso-octane (i-C_8).

W_i: the weight of component i.

A_i: Area of component i.

Then, the weight of plus fractions (C_{10+}) in the liquid phase can be calculated from the mass balance equation (see eq. 2.11)(Burke et al., 1991):

$$W_{C_{10+}} = W_{STO} - \sum_{i=C_1}^{i=C_9} W_i \quad \text{(2.11)}$$

Consequently, after computing the weight of each component, the molar fraction or weight fraction of components can be calculated by considering their molecular weights.

2.4.1.2. Compositional analysis of representative fluid samples from WFT:

Determining the compositions of representative samples which are collected by bottom-hole sampling tools like wireline fluid sampling testers (WFTs) follows some steps(Curtis H Whitson & Brulé, 2000; C. H. J. F. d. Whitson & Hydro, 1998):

- Firstly, the representative fluid should be flashed to the standard conditions (1 bar, 60 °F).
- Secondly, the quantity of Liquid (Condensate) and gas phases should be gauged at standard conditions.
- The weight fractions of liquid (condensate) and gas phases should be measured by gas chromatography (GC).
- Then, the molecular weight (Mw) of condensate and heavy components (plus fractions) must be calculated.
- Finally, after normalizing the weight or mole fractions of gas (y_i) and liquid phase (x_i) components, they should be recombined together to achieve the reservoir fluid composition (z_i).

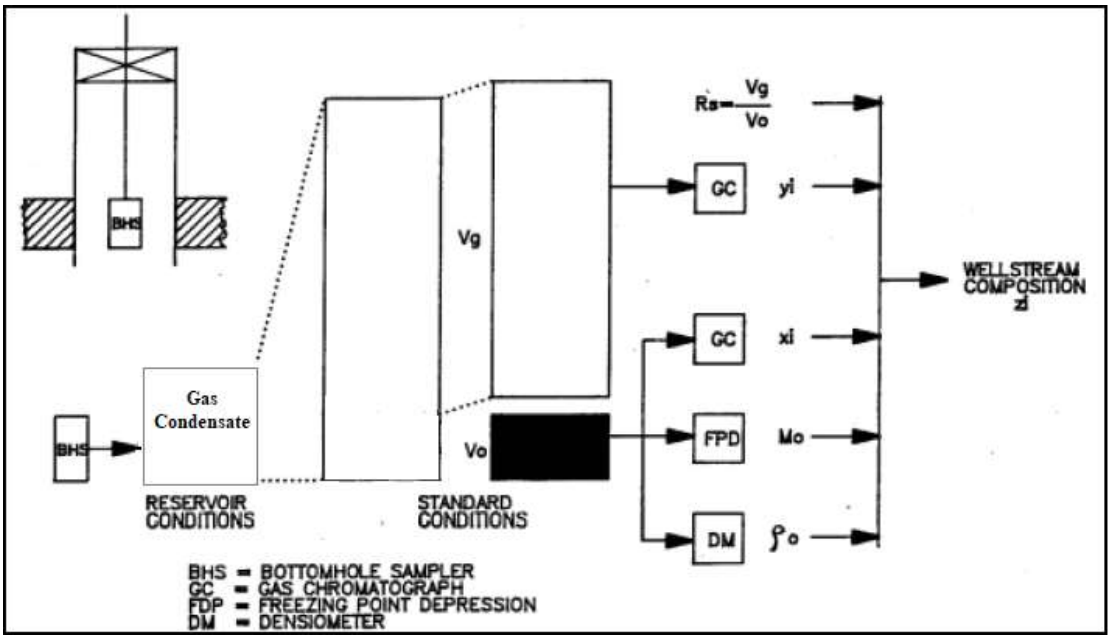

Figure 2.16. Schematic diagram of determining the compositions of bottom-hole sample (Theodosia Fiotodimitraki, February 2016,)

Apart from PVT software (PVT.SIM) which is used for this thesis, there is also mathematical approach for calculating the compositions of reservoir fluid (Gas Condensate) which can be expressed as following(C. H. J. F. d. Whitson & Hydro, 1998):

$$(\text{Mole})_{\text{Reservoir fluid}} * Z_i = X_i * (\text{Mole})_{\text{Liquid phase}} + Y_i * (\text{Mole})_{\text{Gas phase}} \quad \text{(2.12)}$$

$$(\text{Mole})_{\text{Reservoir fluid}} = (\text{Mole})_{\text{Liquid phase}} + (\text{Mole})_{\text{Gas phase}} \quad \text{(2.13)}$$

So, from eq. (2.12) and (2.13) we have:

$$Z_i = X_i * \frac{(\text{Mole})\text{Liquid phase}}{(\text{Mole})\text{Liquid phase} + (\text{Mole})\text{Gas phase}} + Y_i * \frac{(\text{Mole})\text{Gas phase}}{(\text{Mole})\text{Liquid phase} + (\text{Mole})\text{Gas phase}}$$

Then, by dividing the term "(Mole)Liquid phase", the following equation is derived:

$$Z_i = X_i * \frac{1}{1 + \frac{(\text{Mole})\text{Gas phase}}{(\text{Mole})\text{Liquid phase}}} + Y_i * \frac{\frac{(\text{Mole})\text{Gas phase}}{(\text{Mole})\text{Liquid phase}}}{1 + \frac{(\text{Mole})\text{Gas phase}}{(\text{Mole})\text{Liquid phase}}}$$

Considering one substitution (F_g):

$$F_g = \frac{\frac{(\text{Mole})\text{Gas phase}}{(\text{Mole})\text{Liquid phase}}}{1 + \frac{(\text{Mole})\text{Gas phase}}{(\text{Mole})\text{Liquid phase}}} \quad , \quad 1 - F_g = \frac{1}{1 + \frac{(\text{Mole})\text{Gas phase}}{(\text{Mole})\text{Liquid phase}}}$$

Then, we have the final equation for calculating the normalized reservoir fluid compositions:

$$Z_i = X_i * F_g + Y_i * (1 - F_g) \quad \text{(2.14)}$$

2.4.1.3. Compositional analysis of representative fluid samples from surface fluid sampling method:

When the well fluid moves from the bottom-hole to the surface, it enters to multistage separators and by flashing process, liquid and gas phases will be separated from each other. Then

the same as bottom-hole samples (see subchapter 2.4.1.2) the quantity of liquid and gas phases are measured and by gas chromatography the compositions of each phase are identified. But the separator gas and liquid phases will be recombined by gas to oil ratio (GOR). And there is a difference between the gas oil ratio from the rig with the gas oil ratio from the laboratory due to the errors in gauging the gas flow rate by an orifice flow meter (see subchapter 2.3.5) and the carryover of the liquid phase in gas separator or gas phase in condensate separator and oil line. Thus, the GOR should be corrected based on the specific gravity of the gas from rig and laboratory as following(René MIGNOT, 2003):

If $Z_{Lab} * \gamma_{Lab} \neq Z_{rig} * \gamma_{rig}$,

So,

$$GOR_{Correct} = GOR_{rig} * \sqrt{\frac{Z_{Lab}*\gamma_{Lab}}{Z_{rig}*\gamma_{rig}}} \quad \text{..... (2.15)}$$

$GOR_{Correct}$: Corrected gas to oil ratio (gas to oil ratio at the laboratory).

GOR_{rig}: Gas to oil ratio from the rig.

Z_{Lab}: Compressibility factor at the laboratory.

Z_{rig}: Compressibility factor at the rig.

γ_{rig}: Specific gas gravity at the rig.

γ_{Lab}: Specific gas gravity at the laboratory.

Moreover, carryover is the other factor which can affect the recombination of gas and liquid (condensate) phases together. So, for correcting the gas to oil ratio (GOR), the efficiency of separators should be evaluated. Hoffmann plot is one of the methods for quality control of separator samples which will be discussed more in the next subchapter (2.5.2).

2.4.2 Constant mass expansion (CME)(Curtis H Whitson & Brulé, 2000; C. H. J. F. d. Whitson & Hydro, 1998)

Constant mass expansion is a technique that can be utilized in oil and gas reservoirs for measuring **dew point pressure** and **liquid volume** which is proportional to the volume of the reservoir fluid at dew point pressure. Figure 2.17 shows a schematic diagram of constant mass expansion, firstly gas condensate is injected in one cell at a pressure higher than initial reservoir pressure and should be confirmed that the fluid is a single phase. Then, by increasing the volume of the cell stepwise (see figure 2.17), the pressure will also decrease step by step. When the first drop of liquid is separated from the gas condensate that pressure is the dew point pressure of the reservoir fluid. Based on the method, which is shown in figure 2.17, decreasing the pressure of the cell will continue until the standard conditions (1 bar, 60 °F). Finally, by quantifying the gas and liquid at atmospheric conditions, the gas volume factor (B_g) can be computed.

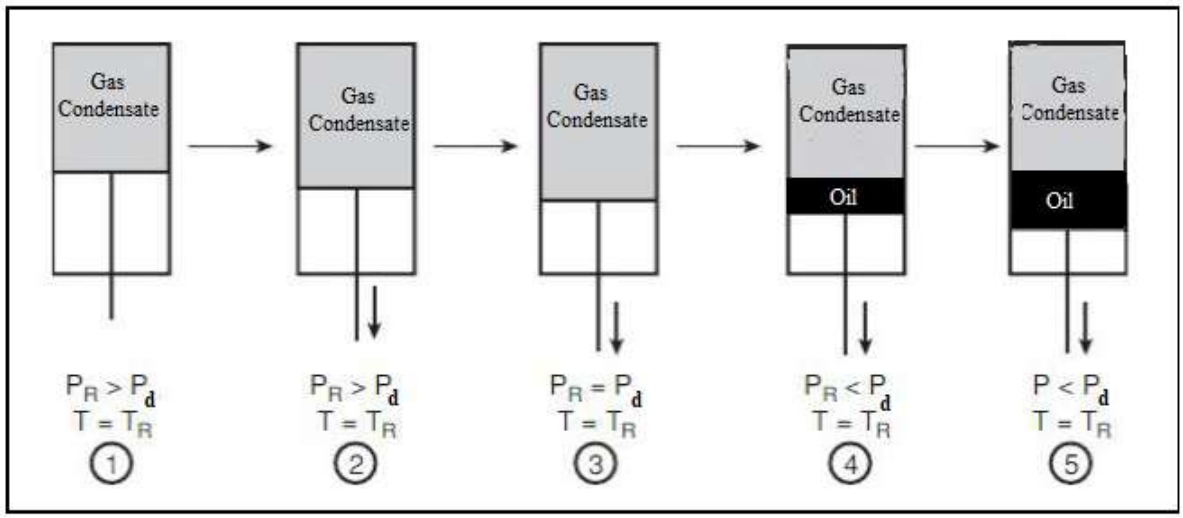

Figure 2.17. Schematic Diagram of Constant Mass Expansion.

2.4.3 Constant volume depletion (CVD)(Curtis H Whitson & Brulé, 2000; C. H. J. F. d. Whitson & Hydro, 1998).

Constant volume depletion is the other technique which can be applied for providing the compositional and volumetric data from representative samples of gas condensate reservoirs. And infrequently, this method can be used for volatile oil reservoirs by natural pressure depletion. The output data from the constant volume depletion experiment is utilized for reservoir engineering computations as following:

- Mean drop-out liquid or vaporization (oil saturation) due to the natural pressure depletion in the gas condensate reservoirs.
- Calculating the wet gas recovery based on mass balance.

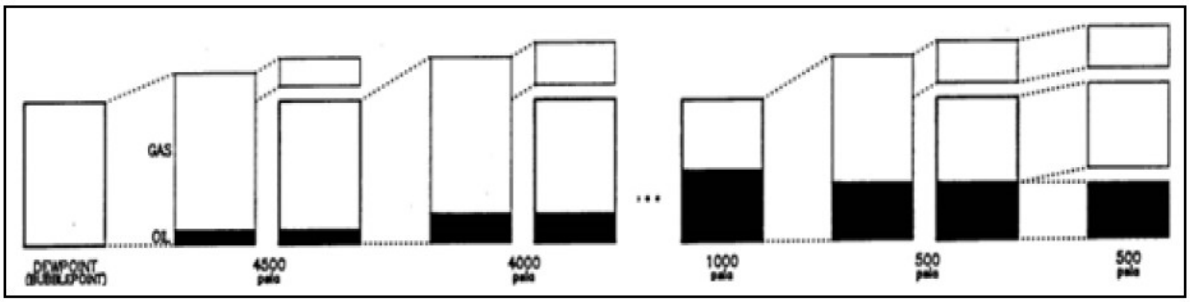

Figure 2.18. . Schematic diagram of Constant volume depletion (CVD) process (Theodosia Fiotodimitraki, February 2016,).

Firstly, gas condensate fluid is injected into the cell at saturation pressure (dew point pressure P_d) which was measured before by constant mass expansion method (CME) (see subchapter 2.4.2). Then, by increasing the volume of the cell stepwise, the pressure will decrease lower than dew point pressure and liquid phase will be separated from the gas phase (see figure 2.18). After that, the specific volume of gas comes out from cell due to the piston of cell moves back to its original saturation volume and then the removed gas will be brought to standard conditions (1 bar, 60 °F) for compositional analysis. This technique will continue in some steps until the atmospheric conditions when the liquid phase is completely separated from the gas phase. Consequently, by measuring the volume of the residual liquid phase in the cell, volume of gas phase which was removed in each step, densities of gas and liquid phase (condensate) and molecular weight of liquid phase, the mole of the gas which was removed from the cell can be calculated as follows:

$$\Delta n_g = \frac{\Delta V_o * \rho_o}{M_o} + \frac{\Delta V_g}{379} \quad \text{..... (2.16)}$$

Then, by the following equation the compressibility factor of gas can be calculated:

$$Z = \frac{\Delta V_g * p}{\Delta n_g * R * T} \quad \text{..... (2.17)}$$

2.5 Quality control of recorded samples

When the fluid samples are collected from the bottom-hole or from the surface, the quality of the samples should be checked properly. In this project, recorded samples can be divided into two categories based on the validity check:

2.5.1 Quality check of bottom-hole samples

One of the most precise methods for validity check of bottom-hole samples used in this project is the measurement of dew point pressure at the reservoir and ambient temperatures. If the dew point pressures of two or three samples have the same saturation pressures at the reservoir and atmospheric temperatures within 2 or 3 % (C. H. J. F. d. Whitson & Hydro, 1998), those samples can be considered as representative samples. Likewise, the dew point pressures which are calculated for each sample should be less than the flowing bottom-hole pressure.

2.5.2 Quality control of surface samples

Hoffmann plot is one of the analytical techniques to control the consistency of compositions of samples from oil and gas separators(Hoffman, Crump, & Hocott, 1953). Based on this method, the vapor pressure of each hydrocarbon component raises exponentially with temperature (see eq. 2.18). Plotting the Log K values of components versus Hoffmann factors (F_i) creates a linear relationship which can show that the sample from the separator is consistent (see eq. 2.19). In addition, although this method can indicate that the samples which are collected from the surface (oil and gas separators) are reliable, it cannot guarantee that the samples are representative fluid samples for entire reservoir fluid (Hoffman et al., 1953; Theodosia Fiotodimitraki, February 2016,).

$$Log(K_i * P_{sep}) = (A_1 * F_i) + A_0 \quad \text{(2.18)}$$

$$F_i = Log\frac{Log\frac{P_{Ci}}{P_{sep}}}{\frac{1}{T_{bi}} - \frac{1}{T_{Ci}}} * \left(\frac{1}{T_{bi}} - \frac{1}{T_{Sep}}\right) \quad \text{(2.19)}$$

$$K_i = \frac{Y_i}{X_i} \quad \text{..... (2.20)}$$

K_i: K value for i Component.

F_i: Hoffmann factor for i Component.

R: gas constant ($8.3145 \frac{Kpa\,.\,m^3}{K.\ kg\ mole}$).

T_{bi}: the boiling temperature for i component (R).

T_{sep}; the temperature of separator (R).

P_{sep}: the pressure of separator (psi).

A_0: intercept at the plot.

A_1: The slope of the line at the plot.

T_{Ci}: Critical temperature of i component (R).

But, when the pressure of separator is lower than 1000 psi and the temperature of separator is between 500 and 663 Rankine, A0 and A1 can be calculated as following(Standing, 1977; Theodosia Fiotodimitraki, February 2016,):

$$A_0 = 0.89 - \left(1.7 * 10^{-4} * P_{sep}\right) - (3.5 * 10^{-8} * P_{sep}^2) \text{..... (2.21)}$$

$$A_1 = 1.2 + \left(4.5 * 10^{-4} * P_{sep}\right) + (15 * 10^{-8} * P_{sep}^2) \text{..... (2.22)}$$

3 Chapter 3 Methodology

In this project, Ormen Lange field is a case study for comparing the MDT results which were achieved by NORSK HYDRO from 1997 to 1998 with cleanup test results by EXPRO from 2007 to 2009 in order to show that even if there has been improvement in wireline fluid sampling methods, there are some errors in their outcomes. Thus, in this chapter, we have divided the methodology into some steps. Firstly, the case study is the Ormen Lange field and its candidate exploration and development wells which will be introduced in the next subchapter (3.1). Secondly, cleanup test data from candidate development wells are identified for correcting and normalizing the condensate to the gas ratio (CGR) of each selected development well. Thirdly, by utilizing PVT.SIM software, representative fluid samples from MDT method, and surface fluid sampling methods are simulated due to analyzing laboratory data. Finally, by considering the results from simulations, the accuracy of condensate to gas ratios (CGRs) of MDT samples can be identified as compared to surface fluid sampling methods (test separator and wellhead methods).

3.1 Case Study

3.1.1 Ormen Lange field

Ormen Lange field located in the south of the Norwegian Sea, and the water depth in this area is different from 800m to 1100m (see figure 1.B). NORSK HYDRO company discovered this field in 1997, and development and operation were approved in 2004. Operating and developing this field was tricky in deep water and encountered some challenges, so some new techniques compared to last decades were implemented. Production from this field started by two templates on the seabed and in 2009 and 2011 added two more templates for development (see figure 3.1A). Therefore, Ormen Lange field consists of 5 exploration wells and 24 development wells. Moreover, this field produces gas and condensate by natural pressure depletion from “EGGA member” in Tang formation which its lithology is sandstone of Paleocene age. The reservoir is located at a depth of 2700 to 2900 meters below the sea level(Norwegian Petroleum Directorate, 2019).

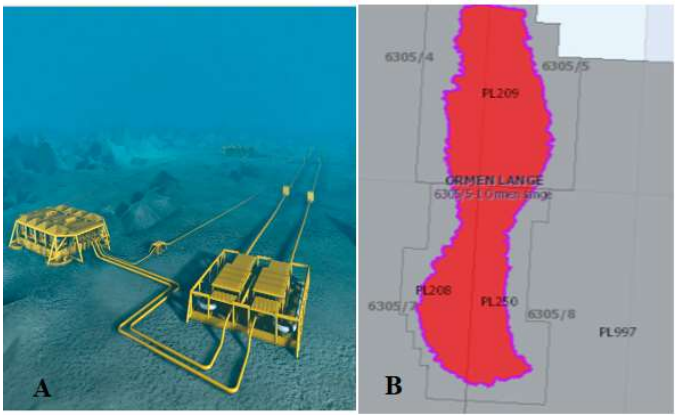

Figure 3.1. Schematic Diagram of templates on the seabed (A) and Geographical picture of Ormen Lange Field (B).

3.1.2 Exploration Wells

Ormen Lange field was explored with five wells by NORSK HYDRO and BP companies. Well 6305/5_1 is a wild cat, and the other four wells are the appraisal. In this project, three exploration wells were chosen as candidate wells for analyzing condensate to gas ratios (CGR) which were measured by MDT method. Because DISKOS database had compsitional and PVT data just for following exploration wells (Norwegian Petroleum Directorate, 2019):

3.1.2.1. Well 6305/5_1:

This well was spudded with a semi-submersible installation called the “Atlantic Ocean” in 1997 and was drilled at the depth around 3100m in Nise formation by NORSK HYDRO company. Drilling mud was water-based with a certain amount of potassium chloride (KCL). This well proved that the Ormen Lange field consists of gas which is in Egga member (Tang formation). Geochemical analyses of gas verified 95 % methane, so the most significant volume of gas in the Ormen Lange field belongs to lighter components. In this well, the reservoir was located in two formations; Egga member in Tang formation (from 2718m to 2771m) and Springar formation (from 2771m to 2780m). In this well, five MDT samples from 2747m to 2789.1m were collected(Norwegian Petroleum Directorate, 2019).

3.1.2.2. Well 6305/7_1:

This well was the second exploration well, which was drilled by BP company in Ormen Lange field, and the most important objectives of the well were to qualify the reservoir fluid and compositional analysis. This well was spudded in the water depth around 850m with the semi-submersible installation the same as well 6305/5_1 but on 6th of July 1998 and was drilled to top

depth (TD) at approximately 3377m in Springar formation (late Cretaceous age). Besides, the drilling mud which was applied for this well was water-based mud with seawater and hivis pills to 1708m and Potassium Chloride (KCl)/ Sodium Chloride (NaCl) mud to the top depth of Springar formation. Top of the Egga member was penetrated at 2911m, and the reservoir was located in the interval 2917m to 3012.5m, so the gross thickness of reservoir was around 95.5m (98% recovery). Two MDT samples were taken from two different depth point (2921m and 2937m in Egga member). Likewise, Geochemical analysis of representative samples from the MDT method showed 93.5 % methane. Also, one drill stem test (DST) was carried out in the interval 2915m to 2931m, and the result from DST confirmed that 93.5 % of gas was methane by CGR around 16.18 STB/MMSCF(Norwegian Petroleum Directorate, 2019).

3.1.2.3. Well 6305/4_1:

The well was spudded in 2002. and the total vertical depth was around 2975m in the late Cretaceous springar formation. This well was drilled with seawater and hi-vis pills to 1756m and KCL/polymer and glycol mud from 1756m to the total depth (2975m). The temperatures of top and base zones of the formation that the reservoir is located in are 72 C and 84 C, respectively. Also, eight MDT samples were taken from the reservoir at 2778.8m. Moreover, all eight samples recovered gas, and one MDT sample recovered water at 2811.1m. One production test was performed by British Petroleum Company (BP), and the measured CGR from this well was around 14.5 STB/MMSCF through the 80/64” choke size at 135 bar(Norwegian Petroleum Directorate, 2019).

3.1.3 Development Wells

In this project, nine development wells were supposed for analysis. EXPRO, which is one of the most experienced international companies in cleanup and well testing process, performed the cleanup test for development wells in the Ormen Lange field from 2007 to 2009. In this project, just nine development wells are analyzed for calculating average normalized condensate to the gas ratios (CGRs).

3.2 Condensate to gas ratio (CGR) from cleanup test data

3.2.1 Stability in fixed choke size

For computing more accurate condensate to the gas ratio (CGR) from cleanup test data, first of all, the choke size should not have high fluctuation in size so the more stable choke size, the more accurate condensate to the gas ratio (CGR) can be attained. Figure 3.2 indicates a schematic diagram of cleanup test data of well 6305/5B-3H from Ormen Lange field, which is a development well. This diagram shows variations of pressure and temperature of gas and oil in the outlets of the separator. Based on the statement, which was mentioned above, when the choke size is stable, the pressure and temperature of fluid lines are almost constant which can give the extra confidence for achieving correct CGR (see figure 3.2, yellow circle).

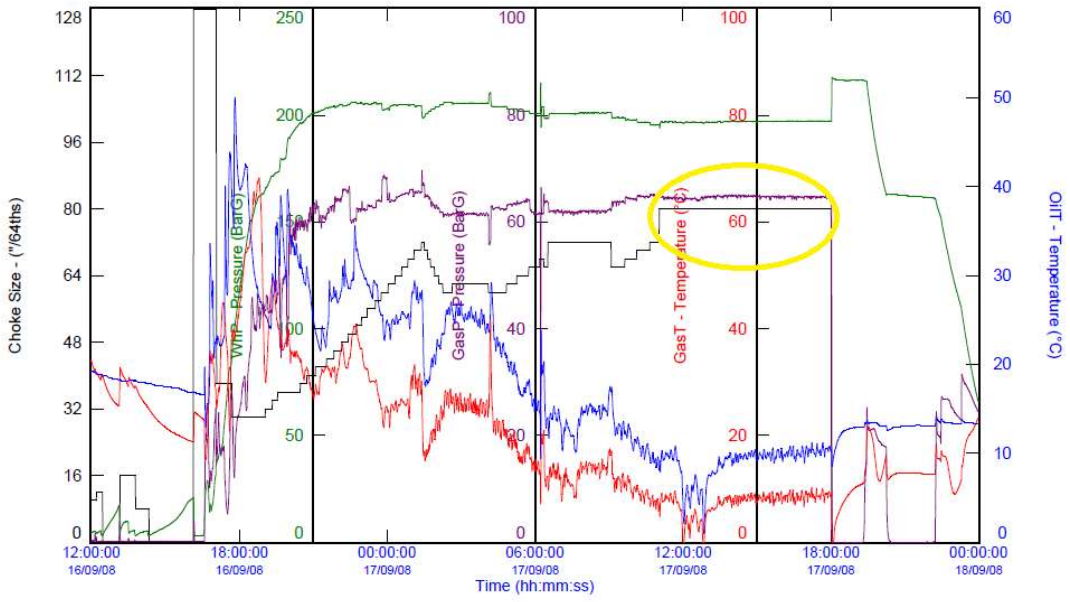

Figure 3.2. Schematic diagram of cleanup test data of development well 6305/5B_3H from Ormen Lange field (Expro, 2007).

3.2.2 Correction of gas and oil flow rates from flow meters

After selecting the stable choke size for calculating the condensate to the gas ratio (CGR), the gas and oil flow rates from flow meters should be corrected which is discussed more in subchapters 2.3.2, 2.3.3 and 2.3.4. Because the oil and gas flow rates from flowmeters are at different pressures, and temperatures and they should be brought to standard conditions (1 bar, 60°F). However, EXPRO utilized Coriolis flow meter for measuring gas flow rates. Moreover, based on the statement that mentioned in subchapter 2.3 EXPRO has been using one software Edge-X from 2006 to receive and organize cleanup test data (gas flow rates) and implement some corrections due to some uncertainties and errors from Coriolis flow meter. Thus, all gas flow rates from cleanup test results were corrected in advance and we did not need to correct them in this project, so we used corrected gas flow rates from cleanup test data for calculating and normalizing the CGR. But for correcting the oil flow rates from cleanup test due to the transition from turbine meter to calibration tank (stock tank oil) for attaining standard conditions (1 bar, 60 °F), equations 2.3 _ 2.6 (see subchapter 2.3.2) can be utilized.

3.2.3 Normalization of condensate to gas ratios (CGRs)

In the cleanup test, for bringing the well fluid to standard conditions (1 bar, 60 °F), there are two types of separator set-up; single stage and multiple stages separator set-up. When liquid and gas phases are separated from each other by separators at different pressures and temperatures, the liquid phase will be sent to the calibration tank (stock tank oil) mentioned in the last subchapter. Then, the gas phase which was removed from the calibration tank sent to burners. However, for calculating the condensate to the gas ratio (CGR), this specific volume of the gas eliminated from the calibration tank was not considered in cleanup test data from EXPRO. Therefore, this volume of missing gas should be estimated.

Figure 3.3 which is a schematic of the process in surface test plant of three development wells of Ormen Lange field indicates that well fluid by passing through some processes enters a single stage separator set-up (see figure 3.3, orange color line). Then, after flashing liquid and gas

phases are separated from each other and gas phase is removed from top of the separator set-up (see figure 3.3, green color line) and liquid phase is taken out from bottom of the separator (see figure 3.3, red color line) and sent to calibration tank (stock tank oil).

So, based on the mass-balance equation, the missing gas from calibration tank can be estimated as follows:

- Mass balance equation for separator:

$$\dot{M}_{wf} = \dot{M}_{mg\ sep} + \dot{M}_{C\ sep} + \dot{M}_{water\ sep} \quad \text{..... (3.1)}$$

$$Q_{wf} * \rho_{wf} = Q_{mg\ sep} * \rho_{mg\ sep} + Q_{C\ sep} * \rho_{C\ Sep} + Q_{water\ sep} * \rho_{water\ sep} \quad \text{..... (3.2)}$$

$\dot{M}_{wf}$: Mass flow rate well fluid (kg/day).

$\dot{M}_{mg\ Sep}$: Mass flow rate missing gas from the separator (kg/day).

$\dot{M}_{C\ sep}$: Mass flow rate condensate from the separator (kg/day).

Q_{wf} : Volume flow rate of condensate from the separator (m3/day).

ρ_{wf}: Density of condensate from the separator (g/cm3).

$Q_{mg\ sep}$: Volume flow rate of missing gas from the separator (m3/day).

$\rho_{mg\ sep}$: Density of missing gas from the separator (g/cm3).

$Q_{C\ sep}$: Volume flow rate of condensate from the separator (m3/day).

$\rho_{C\ sep}$: Density of condensate from the separator (g/cm3).

$Q_{water\ sep}$: Volume flow rate of water from the separator (m3/day)

$\rho_{water\ sep}$: Density of water from the separator (g/cm3)

- mass balance equation for calibration tank (stock tank oil):

$$\dot{M}_{CS} = \dot{M}_{mg\ STK} + \dot{M}_{C\ STK} \quad \text{..... (3.5)}$$

$$Q_{C\ Sep} * \rho_{C\ Sep} = Q_{mg\ STK} * \rho_{mg\ STK} + Q_{C\ STK} * \rho_{C\ STK} \quad \text{..... (3.4)}$$

$\dot{M}_{CS}$: Mass flow rate condensate from the separator (kg/day).

$\dot{M}_{mg\ STK}$: Mass flow rate missing gas from the stock tank oil (kg/day).

$\dot{M}_{C\ STK}$: Mass flow rate condensate from the stock tank oil (kg/day).

$Q_{C\ Sep}$: Volume flow rate of condensate from the separator (m3/day).

$\rho_{C\ Sep}$: Density of condensate from the separator (g/cm3).

$Q_{mg\ STK}$: Volume flow rate of missing gas from the stock tan oil (m3/day).

$\rho_{mg\ STK}$: Density of missing gas from the stock tank oil (g/cm3).

$Q_{C\ STK}$: Volume flow rate of condensate from the stock tank oil (m3/day).

$\rho_{C\ STK}$: Density of condensate from the stock tank oil (g/cm3).

Then, by considering equation (2), gas flow rate, which is missed out of stock tank oil can be calculated as follows:

$$\dot{M}_{mg\ STK} = \dot{M}_{C\ STK} - \dot{M}_{CS} \quad \text{..... (3.5)}$$

$$Q_{mg\ STK} * \rho_{mg\ STK} = Q_{C\ STK} * \rho_{C\ STK} - Q_{C\ Sep} * \rho_{C\ Sep} \text{ ..... (3.6)}$$

$$Q_{mg\ STK} = \frac{Q_{C\ STK} * \rho_{C\ STK} - Q_{C\ Sep} * \rho_{C\ Sep}}{\rho_{mg\ STK}} \text{ ..... (3.7)}$$

But cleanup test data which were provided by EXPRO has some lacks information. Because for calculating the missing gas flow rate from the stock tank oil (see eq.3.4), we need the density of condensate from the separator and the density of missing gas from stock tank oil. Table 3.1 shows available and unavailable data.

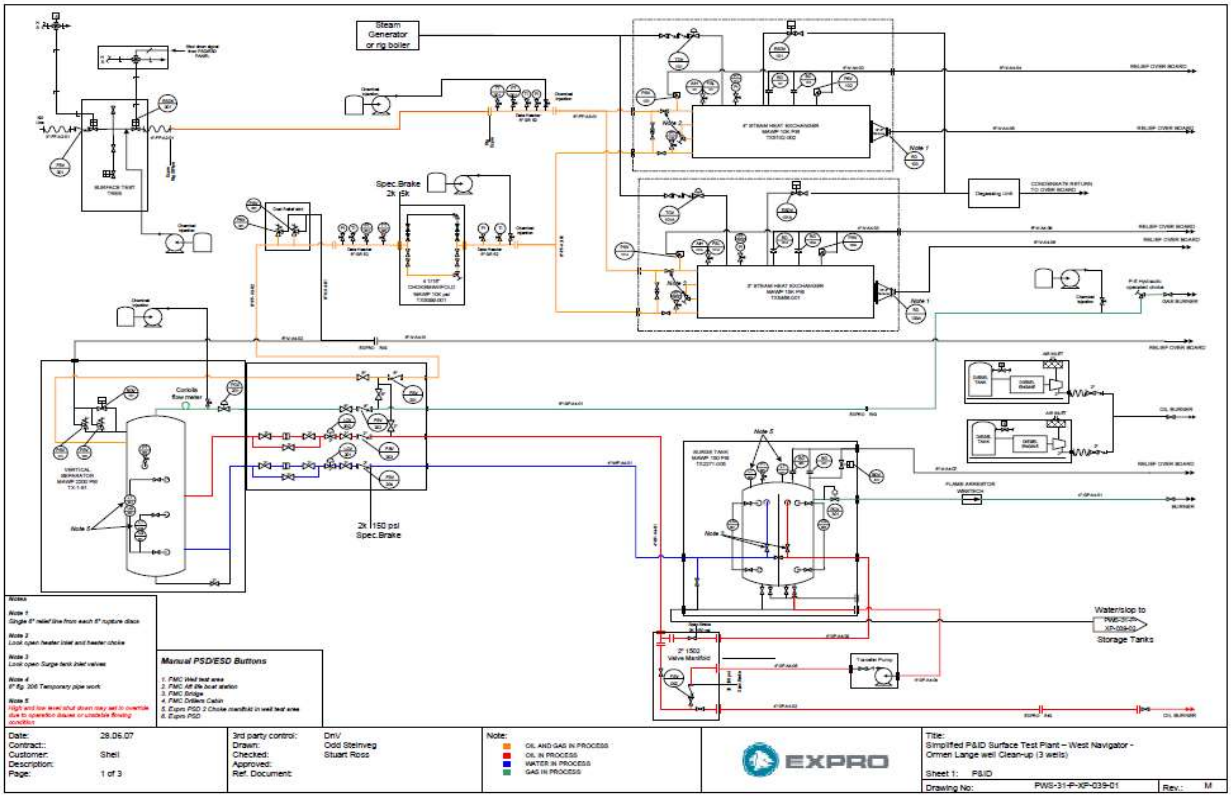

Figure 3.3. Schematic diagram of cleanup test process of development wells (Ormen Lange field) which was done by EXPRO in 2007 for Shell Company.

Table 3.1. Available and unavailable data based on equation 3.4.

Available Data	Unavailable Data
$Q_{C\,Sep}$: flow rate of condensate from the separator (m3/day)	$\rho_{C\,Sep}$: Density of condensate from the separator (g/cm3) at different pressure and temperature.
$Q_{C\,STK}$: flow rate of condensate from stock tank oil (m3/day)	$\rho_{mg\,STK}$: Density of missing gas from stock tank oil (g/cm3) at standard conditions.
$\rho_{C\,STK}$: Density of condensate from stock tank oil (g/cm3).	

Thus, for calculating the missing gas flow rate from stock tank oil, the average density of condensate from the separator ($\rho_{C\,Sep}$) and the average density of missing gas from the stock tank oil at standard conditions ($\rho_{mg\,STK}$) should be estimated. The density of condensate from first stage separator is higher than the density of the missing gas from first stage separator but is lower than the density of condensate from stock tank oil since lighter components are separated from condensate as a gas phase in stock tank oil.

$$\rho_{mg\ Sep} \ll \rho_{C\ Sep} \leq \rho_{C\ STK}$$

Moreover, the density of missing gas from the first stage separator is so close to the density of pure methane ($\rho_{C1} = 0.55\ gr/cm^3$), it means that the highest percentage of missing gas from first stage separator belongs to methane component. However, the density of condensate from stock tank oil shows that the considerable volume of methane is removed from first stage separator.

So,

$\rho_{C\ Sep} \leq \rho_{C\ STK}$ And $\rho_{mg\ Sep} \leq \rho_{mg\ STK}$

Then, after estimating the densities of condensate from the first separator and missing gas from stock tank oil which will be discussed more in next chapter (subchapter 4.1.2), the missing gas flow rate from stock tank oil can be calculated by utilizing equation 3.4.

Thus, based on equation 3.8, the normalized condensate to the gas ratio (CGR) can be computed:

$$CGR_{Normalized} = \frac{Q_{C\ STK}}{Q_{mg\ STK} + Q_{mg\ Sep}} \quad \text{(3.8)}$$

Consequently, by considering the Unnormalized and Normalized condensate to the gas ratios (CGRs), the accuracy of CGR for each development well can be computed.

3.3 PVT simulation

In this project, three exploration wells which were explained in subchapter 3.1.2 are the candidate exploration wells from the Ormen Lange field. NORSK HYDRO Company utilized Modular dynamic tester (MDT) which was the most advanced wireline fluid sampling method in the petroleum industry in 1997 and collected five fluid samples from well 6305/5-1, two fluid samples from 6305/7-1 in different depth points and BRITISH PETROLEUM (BP) gathered nine MDT samples from well 6305/4-1. All these MDT samples were brought to the laboratory for PVT analysis. Firstly, the fluid samples at reservoir conditions were flashed to standard conditions (CME analysis), and the maximum dropout liquid volume of each sample was measured separately (CVD analysis). Secondly, when Liquid and gas phases were separated from each other at standard conditions were sent to gas chromatography (GC) for compositional analysis.

Thus, in this thesis by using PVT.SIM software, the liquid and gas phases of each fluid sample were recombined together with measured CGR from laboratory analysis by implementing the calibrated equation of state (EOS). PVT.SIM software allows to the user to have phase envelope diagram for identifying the behavior of the fluid sample and verifying the representability of fluid sample as a reservoir fluid. After simulating MDT fluid samples, the sample which was collected from cleanup test separator as a test separator sample from one of the development wells (63058-A2H) was simulated by the average normalized CGR which was calculated from the cleanup test data with regards to subchapter 3.2.3. Finally, the results of MDT samples were compared with the results of the cleanup test sample, and the possible consequence of inaccurate CGR was discussed.

4 . Chapter 4 Result and Discussion

4.1 Calculation of condensate to gas ratios (CGRs)

In chapter 3 (methodology) was discussed that for calculating the condensate to gas ratio of development wells from the Ormen Lange field, we should consider the method which was mentioned in subchapter 3.2. Therefore, this method is utilized for computing the CGRs of nine development wells which EXPRO carried out the cleanup test on them.

Firstly, the most stable choke size should be recognized from cleanup test data. Secondly, the gas and liquid flow rates at different pressures and temperatures, which were measured by flow meters (Orifice and turbine) should be corrected. Finally, the calculated condensate to the gas ratios (CGRs) should be normalized.

4.1.1 Correction of oil flow rates (Qo) of nine development wells from the Ormen Lange field

Oil flow rates (Qo) of 9 development wells from the Orman Lange field that EXPRO performed the cleanup test (2007 to 2009) are corrected based on equations 2.3_ 2.6. In figures 4.1 to 4.9, blue curves belong to corrected oil flow rates and orange curves are uncorrected oil flow rates in different periods. Besides, Table 4.1 shows the relative error for each development well as compared to corrected oil flow rates briefly. Thus, the minimum and maximum accuracy due to the fluid conditions in this field (Ormen Lange) is approximately 67% and 95 %, respectively.

Table 4.1. Relative errors of oil flow rates of nine development wells from the Ormen Lange field.

Well no.	Average Uncorrected Qo (m^3/day)	Average corrected Qo (m^3/day)	Relative Error (%)	Well no.	Average Uncorrected Qo (m^3/day)	Average corrected Qo (m^3/day)	Relative Error (%)
63058/A-2H	167.73	104.51	37.69	**6305-8A-4H**	198.77	154.18	22.43
63058/A-7H	328.81	281.79	16.68	**6305- 8A -6H**	250.23	185.86	25.72
63055/B-3H	242.62	233.33	3.82	**6305-8B-7H**	38.84	31.24	19.55
63055/B-A2H	282.88	217.34	23.17	**6305-8B-6H**	210.25	150.54	28.39
6305-8A-5H	373.62	248.21	33.56				

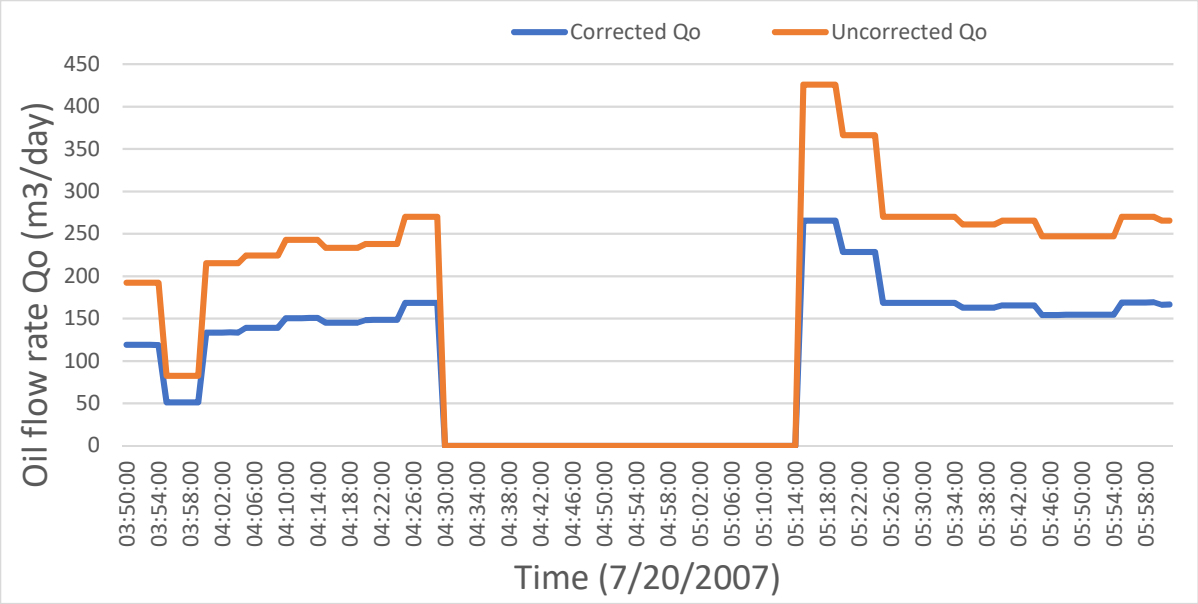

Figure 4.1.Corrected and uncorrected oil flow rate (Qo) of development well 63058/A-2H (Ormen Lange field).

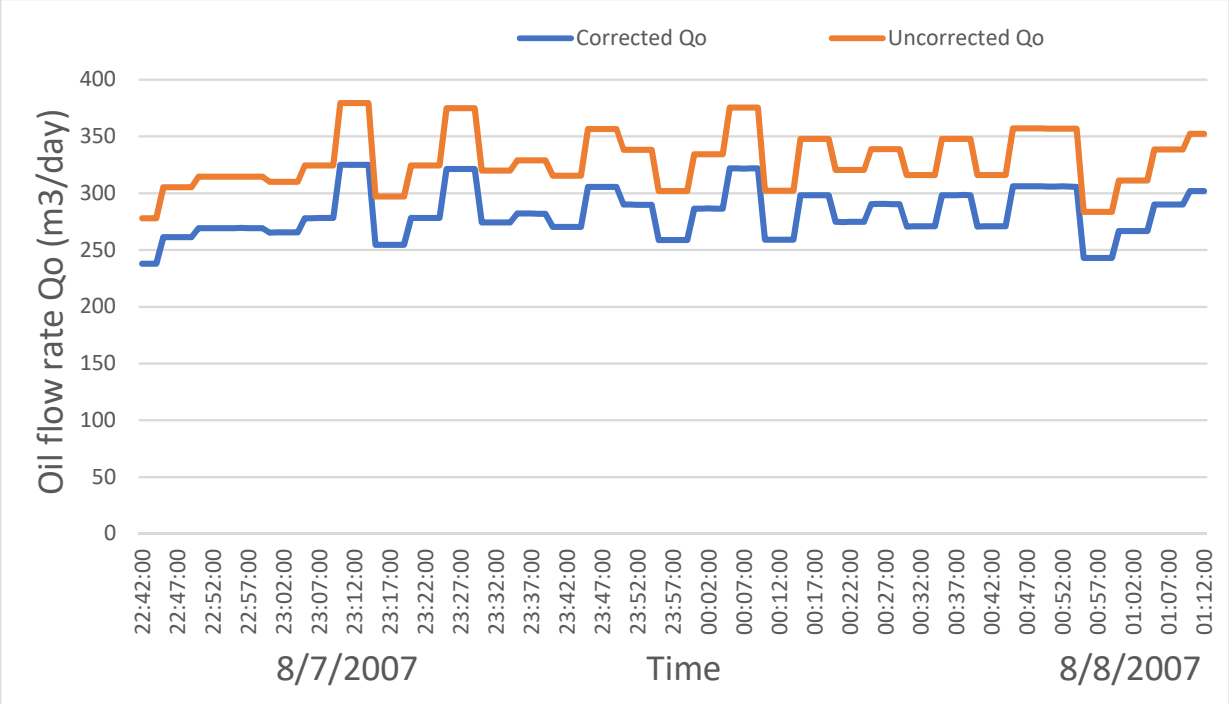

Figure 4.2.Corrected and uncorrected oil flow rate (Qo) of development well 63058/A-7H (Ormen Lange field).

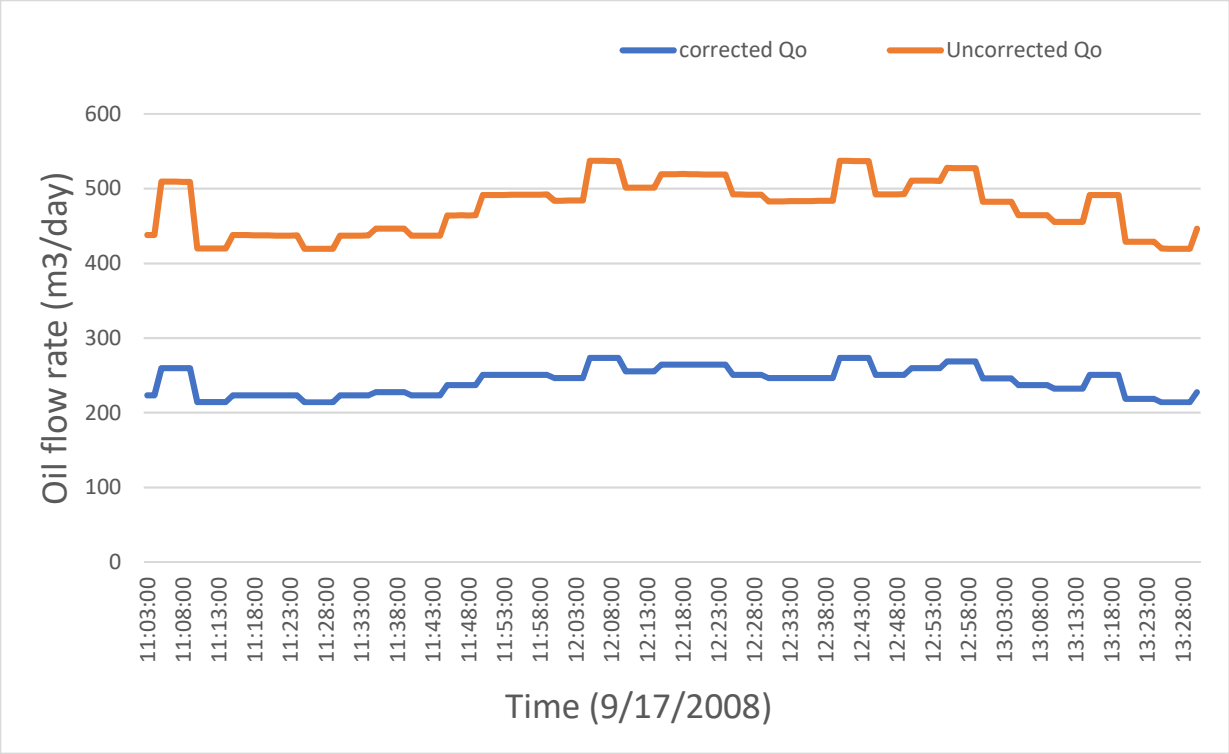

Figure 4.3.Corrected and uncorrected oil flow rate (Qo) of development well 63055/B-3H (Ormen Lange field).

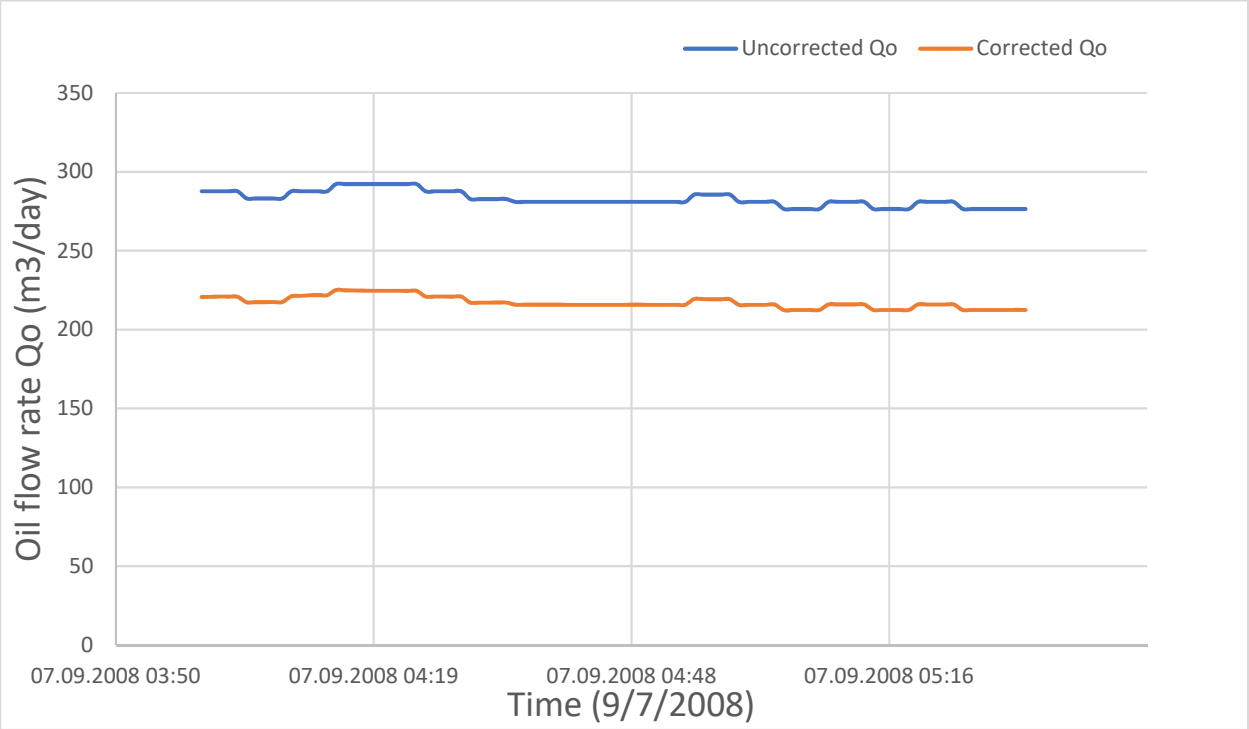

Figure 4.4.Corrected and uncorrected oil flow rate (Qo) of development well 63055/B-A2H (Ormen Lange field).

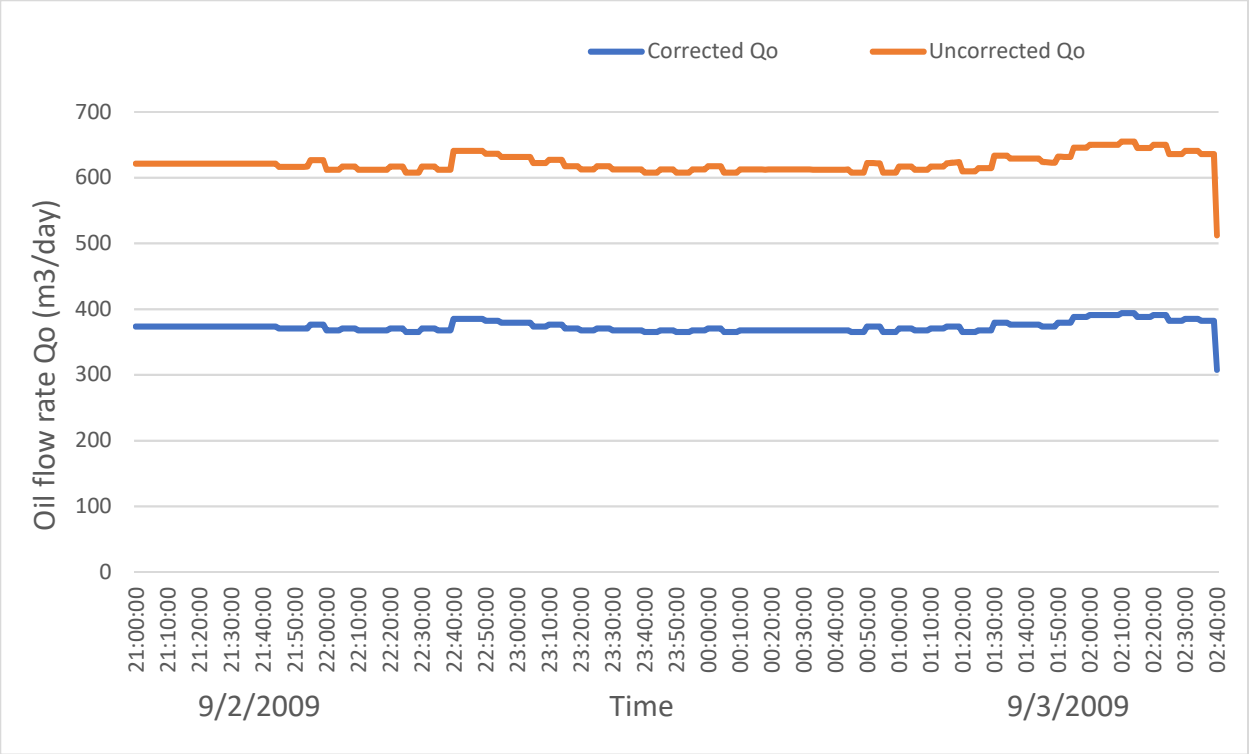

Figure 4.5.Corrected and Uncorrected oil flow rate (Qo) of development well 6305- 8A -5H (Ormen Lange field).

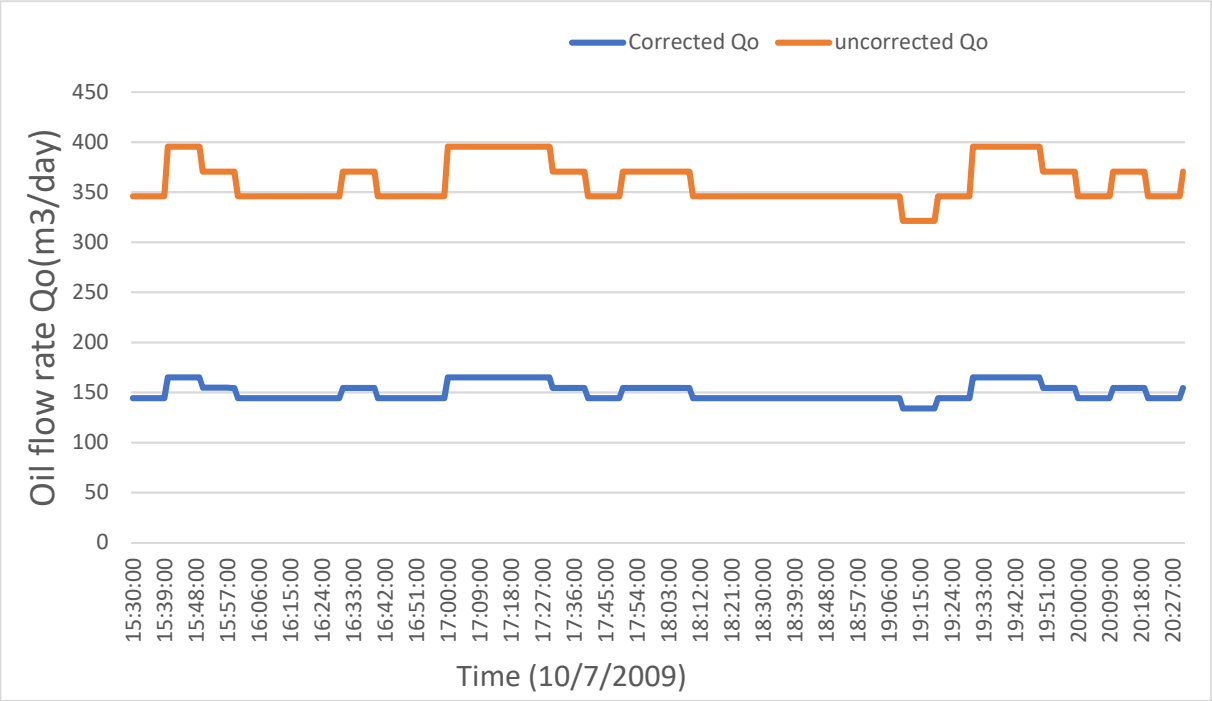

Figure 4.6.Corrected and Uncorrected oil flow rate (Qo) of development well 6305- 8B -6H (Ormen Lange field).

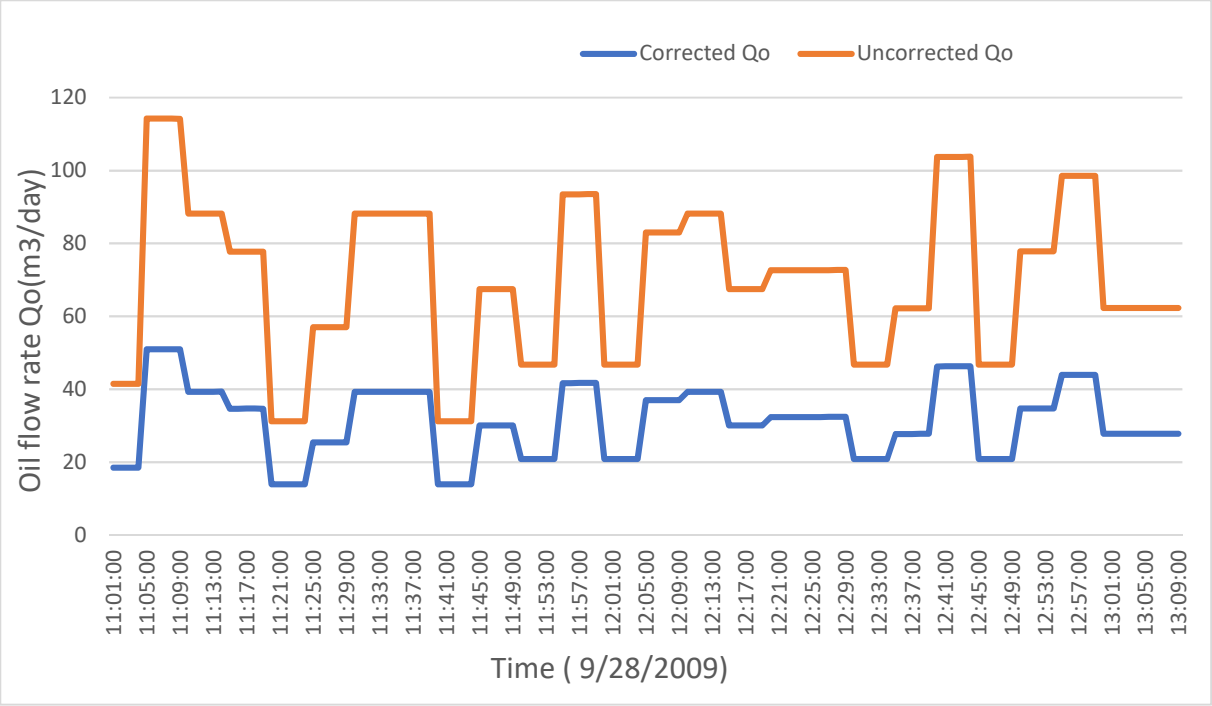

Figure 4.7.Corrected and Uncorrected oil flow rate (Qo) of development well 6305- 8B -7H (Ormen Lange field).

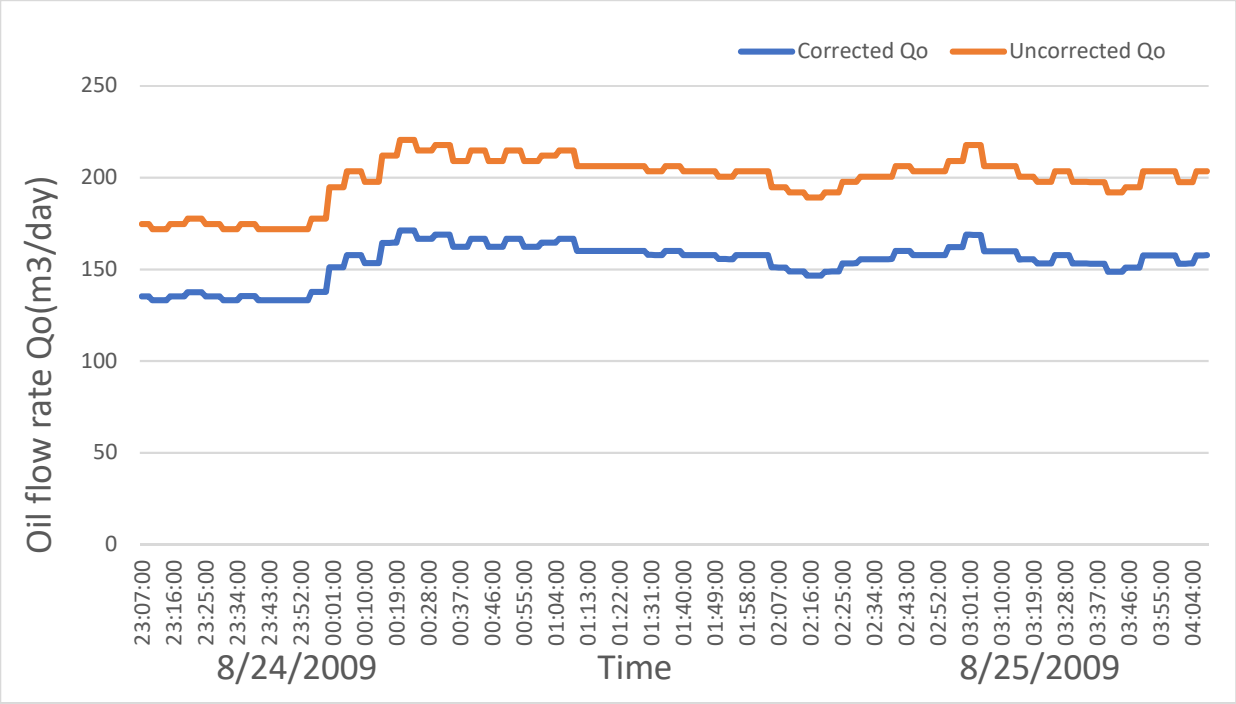

Figure 4.8.Corrected and Uncorrected oil flow rate (Qo) of development well 6305- 8A -4H (Ormen Lange field).

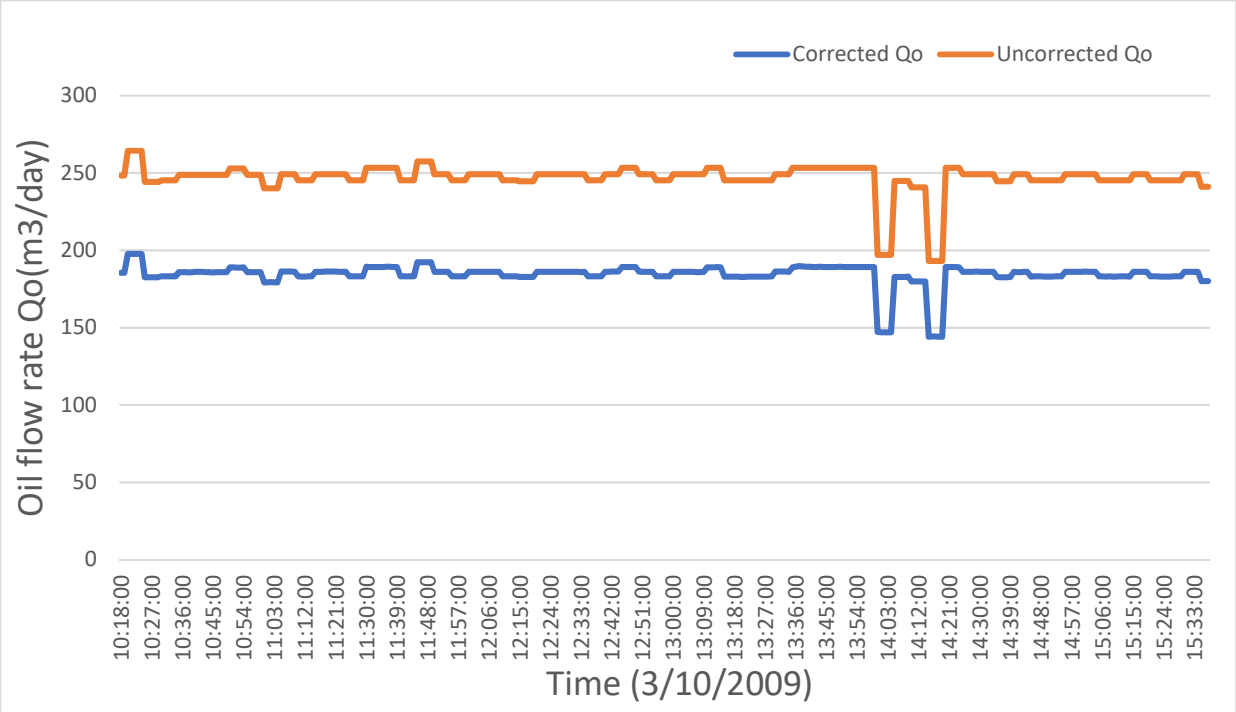

Figure 4.9.Corrected and Uncorrected oil flow rate (Qo) of development well 6305- 8A -6H (Ormen Lange field).

4.1.2 Normalizing the Condensate to gas ratios (CGRs) of nine development wells from Ormen Lange field

In subchapter 3.2 was explained that because of lacks information, the density of condensate from first separator and density of missing gas from stock tank oil should be estimated. So, here one well out of nine development wells from Ormen Lange field has been chosen randomly for normalizing the condensate to gas ratio because the method for estimating the densities and standardizing the CGR of selected well can also be used for the other development wells.

Development Well 63058-A2H (Ormen Lange field) is the candidate for estimating $\boldsymbol{\rho_{C\,Sep}}$ and$\boldsymbol{\rho_{mg\,STK}}$. First, we should calculate the average specific gravity of condensate from stock tank oil and the average specific gravity of missing gas from first stage separator based on cleanup test data (see table 4.2).

Table 4.2. The average specific gravity of condensate from stock tank oil and missing gas from first stage separator.

Average Gas gravity (1st Sep)	**0.59**
Average Oil Gravity (STK)	0.77

By considering the density of methane (0.55 gr/cm3) and plus ethane (1.04 gr/cm3), the percentage of each component in missing gas from first separator and condensate from stock tank oil can be calculated (C_1 = 92.2 %, C_{2+} = 7.8% for missing gas (1st Sep) and C_1= 54%, C_{2+} = 46% for Condensate (STK)). In addition, if we assume that around 40% of methane is removed from first stage separator (based on compositional analyses of gas and liquid phases of test separator sample of exploration well 6305/4_1), then we can estimate the density of condensate from first stage separator ($\boldsymbol{\rho_{C\ Sep}}$= 0.76 gr/cm3). Also, the density of missing gas from stock tank oil ($\boldsymbol{\rho_{mg\ STK}}$ = 0.61 gr/cm3) (see table 4.3).

Table 4.3.the density of condensate and missing gas in first stage separator and stock tank oil of development well 63058-A2H (Ormen Lange field).

	Compositions	Density of pure components (gr/cm3)	Percentage (%)	Density of Fluid (gr/cm3)	Pressure (bar)	Temperature ©
Missing Gas (1st Sep)	C_1	0.55	92.2	0.59	1	15
	C_{2+}	1.04	7.8			
Condensate (STK)	C_1	0.55	54	0.77	1	15
	C_{2+}	1.04	46			
Condensate (1st Sep)	C_1	0.55	58	**0.76**	76.87	14.64
	C_{2+}	1.04	42			
Missing Gas (STK)	C_1	0.55	88.2	**0.61**	1	15
	C_{2+}	1.04	11.8			

Then, by using equation 3.7, the gas flow rate can be calculated:

$$Q_{mg\ STK} = \frac{Q_{C\ STK} * \rho_{C\ STK} - Q_{C\ Sep} * \rho_{C\ Sep}}{\rho_{mg\ STK}}$$

$$(Q_{mg\ STK})_{AVG} = 58.21\ \text{m3/day}$$

Consequently, because the densities of missing gas from separator and stock tank oil are approximately identical ($\boldsymbol{\rho_{mg\ STK}}$ = 0.61 gr/cm3, $\rho_{mg\ Sep}$= 0.59 gr/cm3) missing gas flow rate

from first stage separator and stock tank oil can be added together. So, the average normalized and unnormalized CGR for development well 63058-A2H can be calculated as following:

$$CGR_{Unnormalized} = \frac{Q_{C\ STK}}{Q_{mg\ Sep}} = 13.80\ STB/MMSCF$$

$$CGR_{Normalized} = \frac{Q_{C\ STK}}{Q_{mg\ Sep+}Q_{mg\ STK}} = 12.91\ STB/MMSCF$$

4.1.3 Accuracy of condensate to gas ratios (CGRs) of candidate development wells from Ormen Lange field

Tables 4.5 and 4.6 show the analyses of nine development wells, and for each development well, the average normalized CGR was calculated with regards to the approach which was explained in subchapter 3.2. Although In all of these nine wells the relative error between average normalized and unnormalized condensate to the gas ratios (CGRs) is very insignificant (around 5 % error) (see table 4.4 and **Appendix 6.1.1**), there are some fields that this error is very considerable (approximately 30 or 40 % errors). Also, some oil company engineers do not pay attention to normalize the condensate to the gas ratio (CGR), and as a result of this there might be significant uncertainties in their results as compared to their previous estimations, then they make decisions based on these uncertain outcomes which may have substantial losses.

Finally, by calculating the normalized condensate to gas ratio (CGR) for each candidate development well, the average normalized CGR of nine development wells can be achieved, which is around **12.76 STB/MMSCF**.

Table 4.4. Accuracy of Condensate to gas ratios (CGRs) of selected development wells from the Ormen Lange field.

Well no.	Average Unnormalized CGR (STB/MMSCF)	Average Normalized CGR (STB/MMSCF)	Accuracy (%)	Well no.	Average Unnormalized CGR (STB/MMSCF)	Average Normalized CGR (STB/MMSCF)	Accuracy (%)
63058A2H	13.80	12.91	93.12	**63058A4H**	10.47	10.05	96.02
63058A7H	16.00	15.50	96.77	**63058A6H**	11.83	11.33	95.58
63055/B3H	16.5	16.09	97.45	**63058B7H**	3.55	3.40	97.06
63055BA2H	14.50	13.62	93.53	**63058B6H**	11.67	11.17	95.52
63058A5H	19.85	19.33	97.41				

Table 4.5. Summary of cleanup test data of 4 development wells (Ormen Lange Field).

Well no.	63058_A2H	63058_A7H	63055_B3H	63055_B2AH
Date MM/DD/YYYY	7/20/2007	8/7/2007 to 8/8/2007	9/17/2008	9/7/2008
Time HH:MM: SS	3:50 to 6:00	22:40 to 1:10	11:00 to 1:30	4:00 to 5:30
Choke Size 64th	62	80	80	92
Avg Pressure (bar)	76.59	90.60	65.27	79.44
Avg Temperature ©	12.81	8.63	6.46	9.85
Avg Gas SG (SEP)	0.59	0.591	0.58	0.59
Avg Oil SG (STK)	0.77	0.79	0.80	0.82
AVG Gas gravity (STK)	0.69	0.65	0.69	0.69
AVG Oil gravity (SEP)	0.75	0.77	0.79	0.82
Avg Corrected Q_g SEP (MMm^3/day)	1.48	2.55	2.46	2.86
Avg Q_o STK (m^3/day)	108.75	222.17	223.25	218.92
Avg Q_g STK (m^3/day)	60.43		7.59	74.52
Avg Uncorrected Q_o SEP (m^3/day)	167.73	328.81	242.62	282.88
Total Volume Correction Factor (TVCF)	0.62	0.85	0.96	0.76
Avg Corrected Q_o SEP(m^3/day)	104.43	281.78	233.31	217.34
Unnormalized Avg CGR (STB/MMSCF)	13.80	16.00	16.5	14.50
Normalized Avg CGR (STB/MMSCF)	12.91	15.50	16.09	13.62

Table 4.6.Summary of cleanup test data of 5 development wells (Ormen Lange Field).

Well no.	63058_A5H	63058_B7H	63058_A4H	63058_B6H	63058_A6H
Date MM/DD/YYYY	2/9/2009to 3/9 /2009	9/28/2009	8/24/2009 to 8/25/2009	10/7/2009	3/10/2008
Time HH:MM: SS	21:00 to 2:40	11:00 to 1:00	23:00 to 4:00	15:30 to 20:30	10:18 to 15:38
Choke Size 64th	96	64	96	94	88
Avg Pressure (bar)	55.19	60.85	54.7654	65.24	85.48
Avg Temperature ©	16.88	21.83	16.61	17.58	19.93
Avg Gas SG (SEP)	0.61	0.60	0.61	0.60	0.59
Avg Oil SG (STK)	0.74	0.79	0.77	0.79	0.80
AVG Gas (STK)	0.69	0.65	0.7	0.68	0.7
AVG Oil (SEP)	0.77	0.78	0.76	0.77	0.8
Avg Corrected Q_g SEP (MMm^3/day)	2.6	1.58	2.65	2.36	2.71
Avg Q_o STK (m^3/day)	283.18	30.36	149.71	147.50	172.76
Avg Q_g STK (m^3/day)	84.94	9.45		66.39	83.91
Avg Uncorrected Q_o SEP (m^3/day)	373.62	38.84	198.77	210.25	246.89
Total Volume Correction Factor (TVCF)	0.66	0.80	0.77	0.71	0.74
Avg Corrected Q_o SEP(m^3/day)	248.21	31.24	154.17	150.54	184.39
Unnormalized Avg CGR (STB/MMSCF)	19.85	3.55	10.47	11.67	11.83
Normalized Avg CGR (STB/MMSCF)	19.33	3.40	10.05	11.17	11.33

4.1.4 Validity check of stable choke size

For calculating condensate to gas ratios of all candidate development wells, the most stable choke size should be chosen. In other words, when the size of the choke is constant for a long time period, the fluctuation in measurement is lower, and the accuracy of condensate to the gas ratio is more precise. Therefore, based on subchapter 3.2.1, the most constant choke size belongs to the last period of each candidate development well. So, by analyzing the condensate to gas ratios in all different choke sizes, this principle can be verified. Figure 4.10 shows the variation of choke size and normalized CGR of development well 63058-A7H through the cleanup test process, and the last choke size (84/64") is the most constant choke with the highest stability of normalized condensate to the gas ratio (**15.50 STB/MMSCF**). Furthermore, the alteration of choke size and normalized CGR of the other development wells are located in **Appendix 1** (see subchapter 6.1.2).

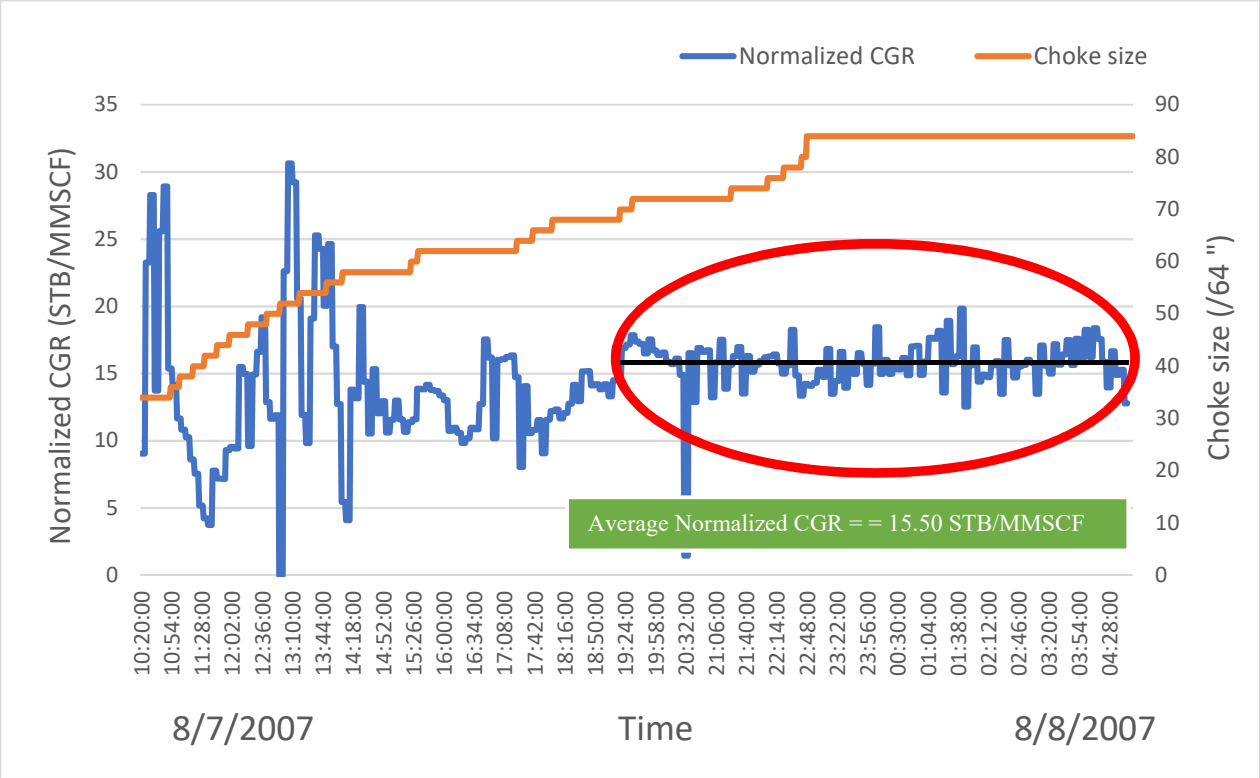

Figure 4.10. Schematic diagram of Normalized CGR and Choke size variation of development well 63058-A-7H (Ormen Lange field) through the cleanup test process.

4.1.5 Validity check of calculated condensate to gas ratio (CGR) by Actual production data

The average normalized condensate to gas ratio (CGR) of candidate development wells from Ormen Lange field was calculated with cleanup test data which was provided by EXPRO from 2007 to 2009, and it was approximately **12.76 STB/MMSCF** (see subchapter 4.1.3). So, by considering the actual production data assembled by Norwegian Petroleum Directorate (NPD) from the Ormen Lange field (see **Appendix 1**, subchapter 6.1.3), the quantification of condensate to the gas ratio which was computed by cleanup test data can be analyzed. Figure 4.11 indicates the actual condensate to the gas ratio from 2007 to the end of 2018. However, by taking the average of condensate to gas ratio in the first three years when cleanup test process was carried out by EXPRO (2007 to 2009), it can be understood that the average actual condensate to the gas ratio (CGR) was around **13.73 STB/MMSCF**. Therefore, the calculated normalized CGR from cleanup test data is so close to actual CGR by accuracy around 93% and 0.97 STB/MMSCF standard deviation (see figure 4.11).

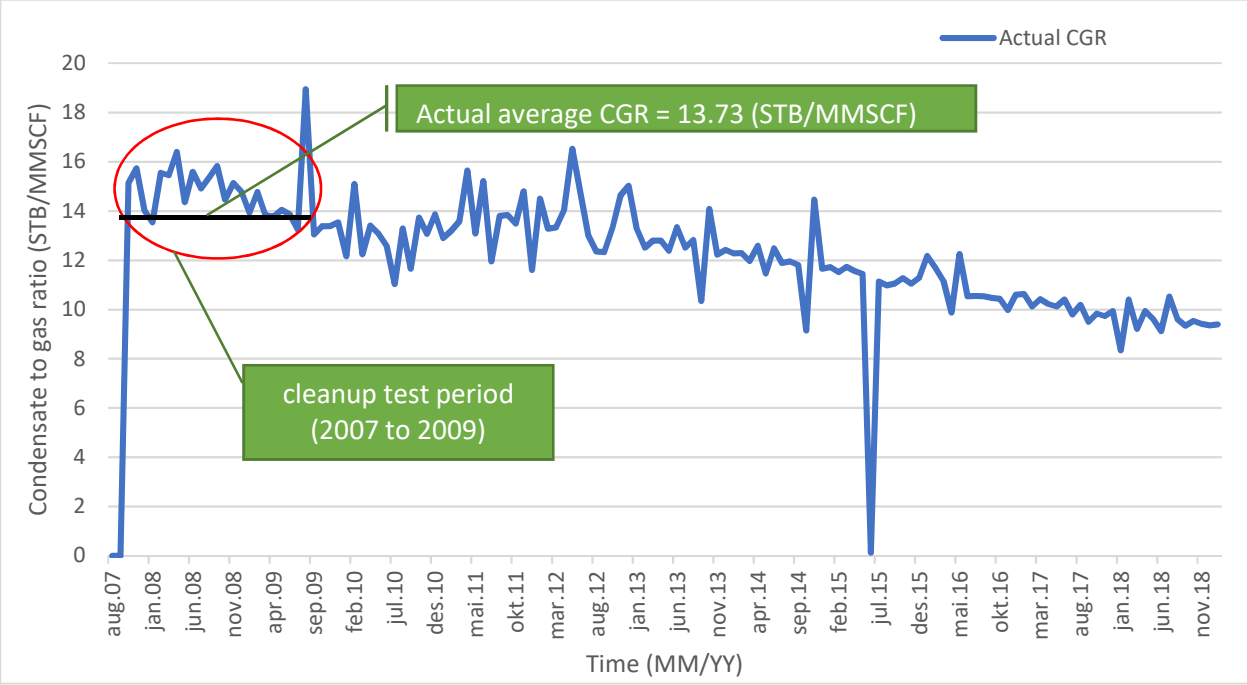

Figure 4.11. Schematic diagram of actual condensate to the gas ratios (CGR) of the Ormen Lange field from August of 2007 to December of 2018.

4.2 PVT analysis of candidate sample from the cleanup test process

Laboratory of EXPRO in Haugesund provided compositional data of fluid samples which were collected from the separator of the cleanup test process as a test separator sample, which is a type of surface fluid sampling method. Therefore, by considering the average normalized CGR from development wells (Ormen Lange field), which was calculated in subchapter 4.1.3, the liquid and gas phases can be recombined by PVT.SIM software. Then, the accuracy of the CGR of each sample from different exploration wells can be evaluated apparently.

4.2.1 Quality control of cleanup test sample

For checking the quality of the sample, Hoffmann plot is one of the most precise approaches which can be used for cleanup test sample (Ormen Lange field). In subchapter 2.5.2, this method was explained clearly. Figure 4.12 illustrates the high quality of cleanup test sample because plotting the K values of components versus Hoffmann factors (F_i) creates a linear relationship which can show that the sample from cleanup test separator is consistent, and the R-squared value on chart is around 0.99 which shows the high accuracy of compositional data of cleanup test sample (test separator sample). Besides, the pressure and temperature of separator are 71 bar and 14 C, respectively which are the average pressure and temperature of the separators of nine candidate development wells in cleanup test process (EXPRO).

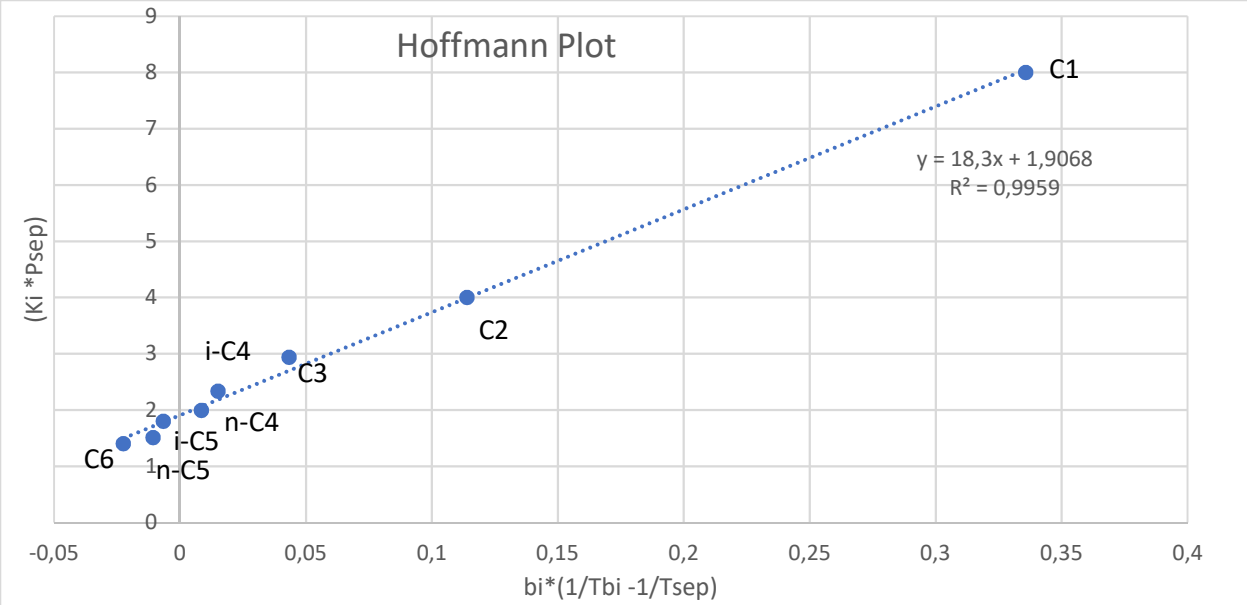

Figure 4.12. Hoffmann Plot of cleanup test sample of development wells from Ormen Lange field (**Appendix 2**, subchapter 6.2.1).

4.2.2 Simulation of PVT-Data for candidate cleanup test sample

By utilizing PVT.SIM software, the recombination of liquid and gas phases of the cleanup test sample with calculated average CGR can be achieved. Then, PT diagram of the recombined sample can show a phase envelope curve of the particular sample fluid, and by contemplating the reservoir conditions on the PT diagram, it can be understood that the cleanup test sample is single phase fluid at reservoir pressure (287 bar) (see figure 4.13).

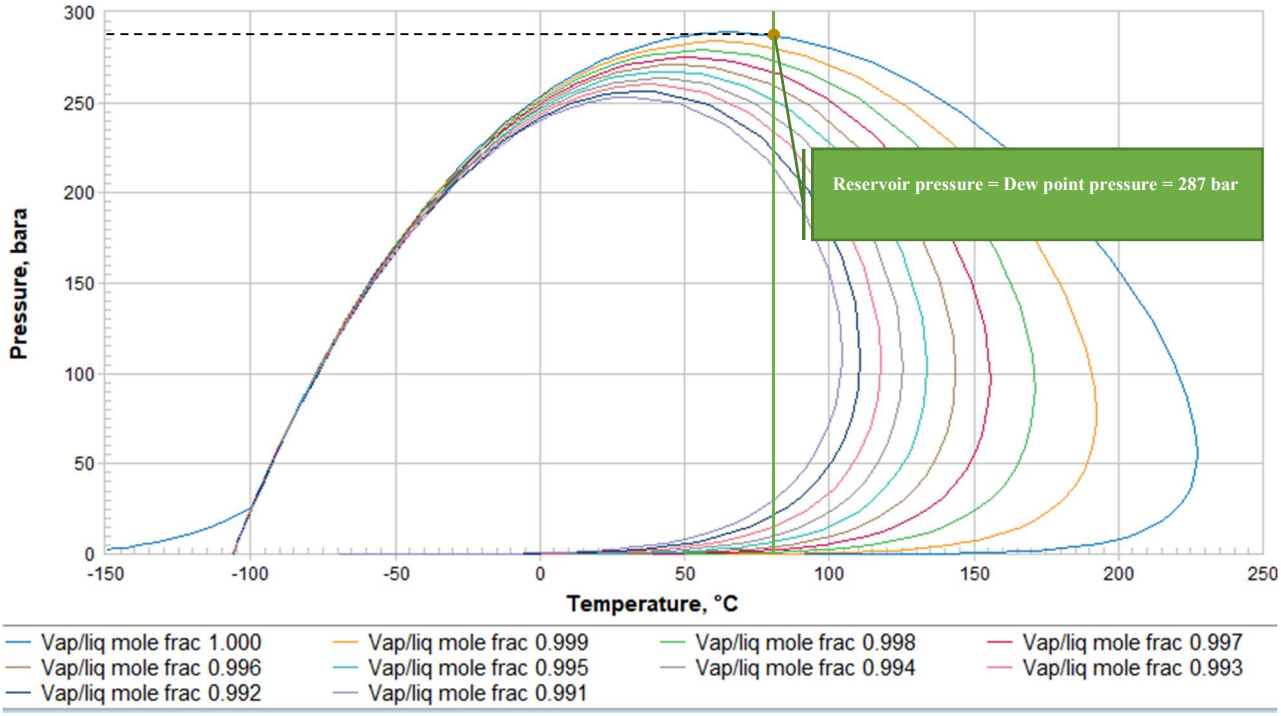

Figure 4.13. PT diagram of the cleanup test sample of development wells from the Ormen Lange field by PVT.SIM software.

One of the most significant segments of PVT simulation is an adjustment or tuning the simulator. So, by considering the laboratory data, we can calibrate the Equation of State (EOS). For example, tuning by constant mass expansion data (CME) from the laboratory which was used for the entire this thesis. Figure 4.14 indicates relative volume (V/Vd) VS. Pressure before and after tuning. Also, this figure specifies the quality of the simulation because the relative volume (V/Vd) of simulation after tuning is wholly matched with relative volume (V/Vd) curve versus pressure.

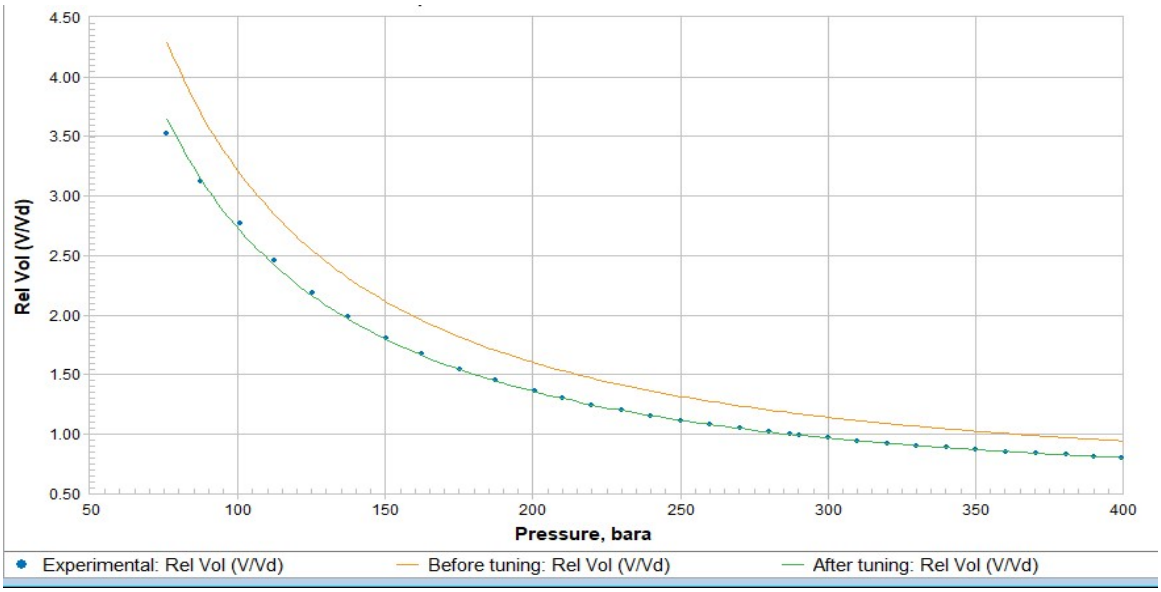

Figure 4.14. Relative volume (V/Vd) Vs. Pressure before and after tuning of the cleanup test sample.

After tuning the simulator, we can simulate the dropout liquid of a representative fluid sample which was collected from the separator of the cleanup test process. Then, we can compute the maximum volume of the condensate (/Vd) from the fluid sample by decreasing the pressure stepwise. Figure 4.15 illustrates that the maximum dropout liquid volume is approximately 1.78% of the dew point volume at a pressure around 120.1 bar.

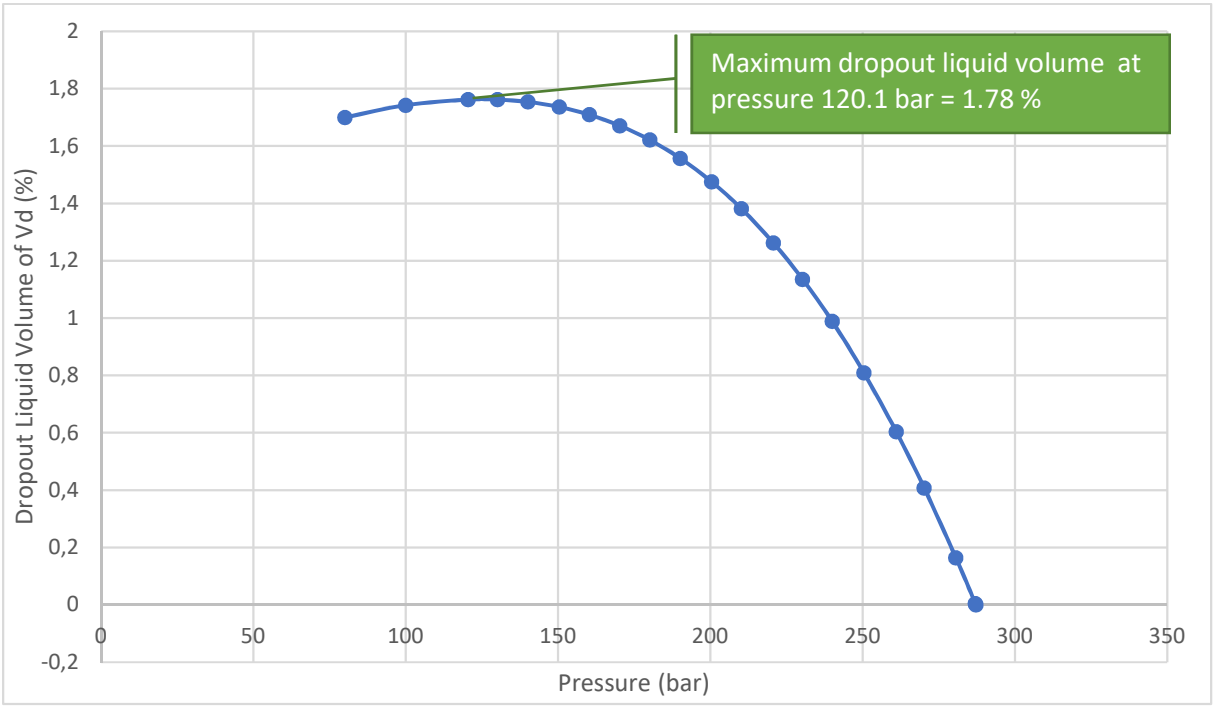

Figure 4.15. Schematic diagram of Dropout liquid volume of dew point volume Vs pressure (cleanup test sample).

4.3 PVT analysis of exploration Wells

One of the most efficient approaches for analyzing the condensate to the gas ratio (CGR) is the evaluation of representative fluid samples from the reservoir. Therefore, in this project, some fluid samples which were taken of candidate exploration wells from the Ormen Lange field are analyzed accurately.

4.3.1 Exploration well 6305/5-1

Five fluid samples were collected by the most advanced wireline fluid sampling (MDT) in 1998 from exploration well 6305/5-1. Table 4.7 illustrates that all five samples were collected from formation Våle in-depth interval 2747m to 2777m (30m) at the same pressure and temperature (287 bar, 81 C).

Table 4.7. Specifications of five MDT samples of exploration well 6305/5-1 from Ormen Lange field.

Specification	TS-18204	PT-1087	TS-2008	E-3468	TS-18211
MDT chamber number	756	607	67	132	45
Formation	Våle	Våle	Våle	Våle	Våle
Depth point (m)	2777	2747	2747	2763.5	2770.3
Initial reservoir pressure (bar)	287	287	287	287	287
Initial reservoir temperature ©	81	81	81	81	81
Date of sampling	24.09.1997	15.09.1997	15.09.1997	15.09.1997	24.09.1997
Sample type	Gas	Gas	Gas	Gas	Gas
CGR (STB/MMSCF)	5.93	8.294	2.45	6.474	6.759
Dew point pressure (bar)	325	287	287	287	287

After collecting the fluid samples, they were brought to the laboratory for PVT analyses. Constant mass expansion (CME), which was explained in subchapter 2.4.2 was one of the techniques for measuring the dew point pressure. After flashing the representative fluid samples from reservoir conditions to standard conditions (1 bar, 60 °F), Liquid and gas phases were transmitted to GC analysis for achieving the compositional data (**Appendix 2**). Here, in this project, we recombined the liquid and gas phases of each sample with measured CGR by utilizing PVT.SIM software. Also, by using constant mass expansion data (CME) from the laboratory, the simulator for each sample was modified. Then, by determining the reliable samples, the accuracy of CGR for each sample was computed.

4.3.1.1. Quality control of MDT samples of exploration well 6305/5-1:

Firstly, the quality of samples is checked, so based on the approach which was explained in subchapter 2.5.1. The dew point pressure of each sample at the reservoir and ambient temperatures should be the same with accuracy around 97%. Therefore, by utilizing PVT.SIM software we can flash each sample from reservoir conditions to standard conditions at reservoir temperature (81C) and ambient temperature (25C). Table 4.8 illustrates this analysis and it can be understood two samples: TS-18204 and TS-2008 are not reliable fluid samples of reservoir fluid because the accuracy of dew point pressures at reservoir and ambient temperatures of two samples as compared to the dew point pressure of cleanup test sample (test separator sample) is 72.56 % and 90.88%, respectively.

Table 4.8. Quality control of MDT samples of exploration well 6305/5-1 from Ormen Lange field.

Samples number	Dew point pressure (bar) @ reservoir temperature (81C)	Dew point pressure(bar) @ ambient temperature (25C)	Accuracy (%) at reservoir temperature	Accuracy (%) at ambient temperature
TS-18204	325	351.75	72.56	72.56
PT-1087	287.15	279.1	98.87	98.87
TS-2008	287.85	301.43	90.88	90.78
E-3468	287.32	276.34	99.87	99.87
TS-18211	287.11	276.14	99.95	99.95

4.3.1.2. Characterization of MDT samples of exploration well 6305/5-1:

By recombining the liquid and gas phases of each sample with measured CGR from the laboratory, the phase envelope of each fluid sample can be achieved by PVT.SIM software. According to the analysis which was explained in last subchapter (4.3.1.1), sample TS-18204 showed a huge relative error (28%) in dew point pressure at the reservoir and ambient temperature as compared to the dew point pressure from cleanup test sample (test separator sample). So, by contemplating the phase envelope (see figure 4.16), it can be understood that the fluid sample is two-phase fluid because the measured dew point pressure at the reservoir condition is higher than reservoir pressure around 38 bar. Figure 4.16 illustrates this difference in dew point pressure clearly, and reservoir condition is exactly in the two-phase envelope. The laboratory of NORSK HYDRO Company also concluded sample TS-18204 consists of contaminants and filtrate; therefore, it cannot be considered as a representative fluid sample of in-situ reservoir fluid.

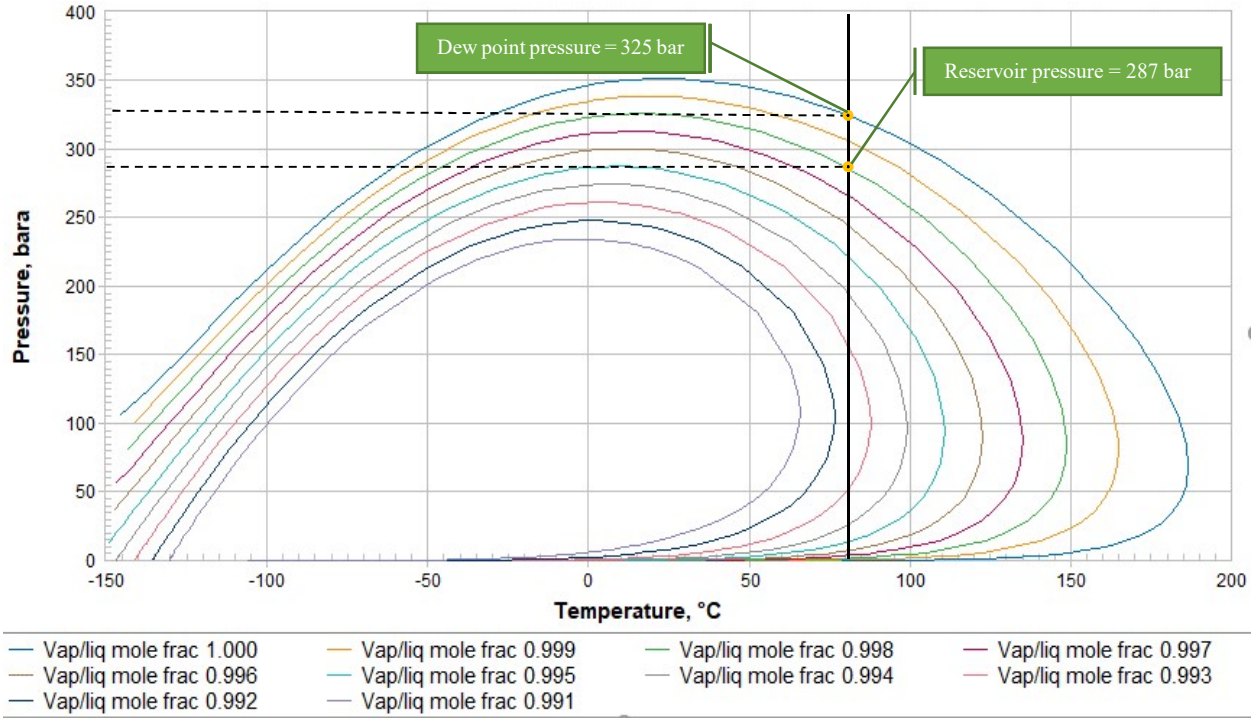

Figure 4.16. Phase envelop of sample TS-18204 of exploration well 6305/5-1 by PVT.SIM software.

Although the dew point pressure at reservoir temperature in sample TS-2008 is so close to the dew point pressure of representative sample at reservoir temperature, there is a significant

relative error around 9.12 % in dew point pressure at ambient temperature. Therefore, it cannot be selected as a consistent sample of reservoir fluid (see figure 4.17).

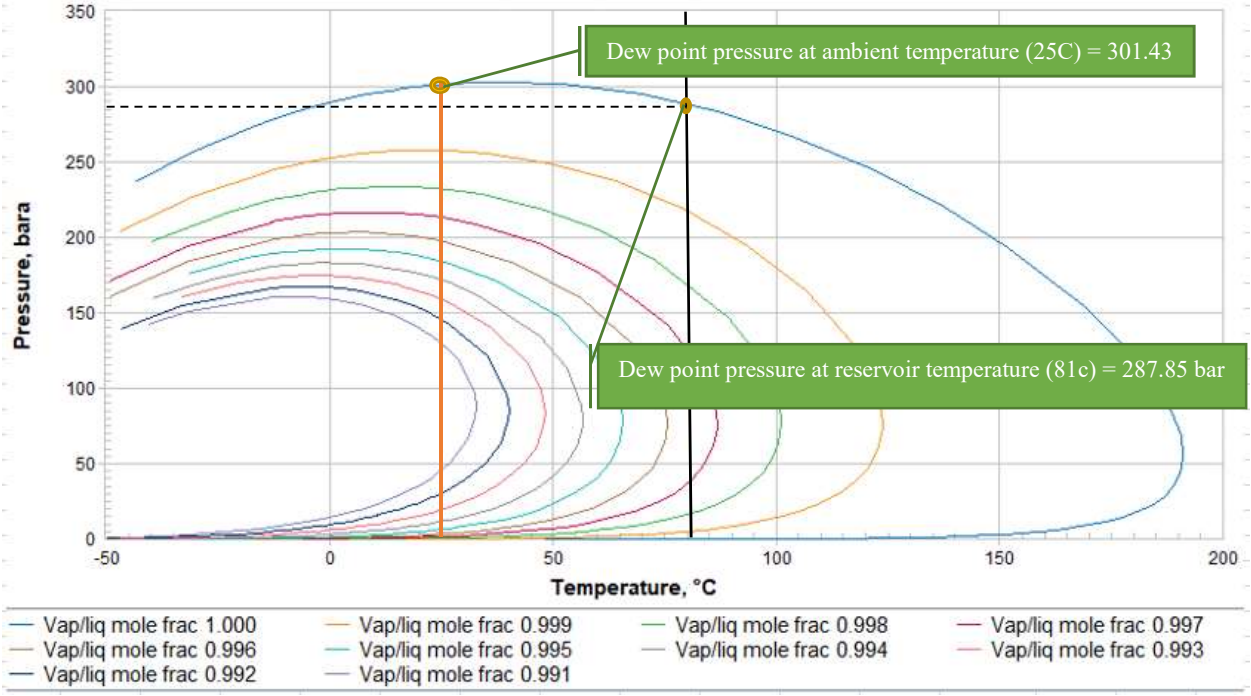

Figure 4.17. Phase envelop of sample TS-2008 of exploration well 6305/5-1 by PVT.SIM software

Thus, the other three samples; PT-1087, E-3468, and TS-18211 are reliable samples by high accuracy around 99% for CGR analysis in this project.

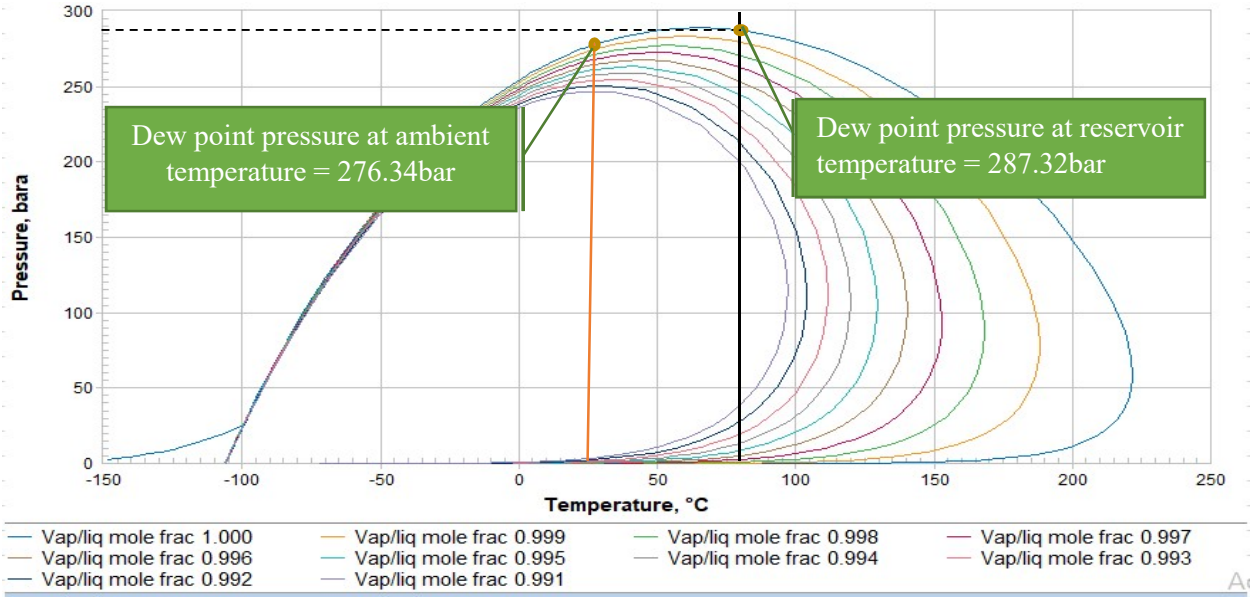

Figure 4.18. PT diagram of sample E-3468 of exploration well 6305/5-1 by PVT.SIM software.

4.3.2 Exploration well 6305/7-1

For this appraisal well, one drill stem test was also carried out. DST is more accurate than MDT method in very lean gas condensate reservoirs. because in the DST method, one specific depth interval will be considered for collecting reservoir fluid sample; however, the MDT method is so cheaper than the DST method. Sample MPSRBA-927 is one of the MDT samples from well 6305/7-1, which is evaluated in this project for analyzing the CGR. Table 4.9 illustrates the specifications of candidate samples from MDT and DST methods of exploration well 6305/7-1.

Table 4.9. Specifications of MDT and DST samples of exploration well 6305/7-1 from Ormen Lange field.

Sample number	Test Type	Formation	Depth point (m)	Reservoir pressure (bar)	Reservoir temperature ©	Sample type	CGR (STB/MMSCF)
MPSRBA-927	MDT	Egga	2937	287	90	Gas	15.93
1-39(gas phase),1-41(liquid phase)	DST	Egga	2915 to 2931	287	90	Gas	15.5

4.3.2.1. Quality control of MDT and DST samples of exploration well 6305/7-1:

Simulating the sample MPSRBA-927 by utilizing PVT.SIM software specifies that this MDT sample cannot be a representative sample of reservoir fluid because there is a considerable relative error around 6 % in dew point pressure at reservoir temperature, although, DST sample has a high accuracy approximately 97% in dew point pressure at the reservoir and ambient temperature. (See table 4.10).

Table 4.10. Dew point pressure of MDT and DST samples at reservoir and ambient temperature and relative errors (PVT.SIM).

Samples number	Dew point pressure (bar) @ reservoir temperature (90 C)	Dew point pressure(bar) @ ambient temperature (25C)	Accuracy (%) at reservoir temperature	Accuracy (%) at ambient temperature
MPSRBA-927 (MDT)	303.87	316.20	94.12	85.43
1-39(gas phase), 1-41(liquid phase) (DST)	290.28	285	97	96.73

PT diagram of MDT sample MPSRBA-927 shows that the dew point pressure which is simulated by PVT.SIM software is higher than the reservoir pressure around 16 bar (see figure 4.19). It means that the collected sample was two-phase, but the sample which was collected by the DST method illustrates lighter components. So, by analyzing the compositions of recombined fluids from different fluid sampling methods (MDT and DST) which were simulated with certain CGRs by PVT.SIM software, it can be understood that the mole percentage of the plus fraction (C6+) in MDT sample as compared to DST sample is higher around 0.1%. Because the measured CGR from MDT sample is higher than measured CGR from DST sample (see table 4.9), thus more liquid phase is mixed with gas phase in MDT sample as compared to DST sample. Also, the other reason which supports MDT sample has heavier components is that NORSK HYDRO Company specified MDT sample MPSRBA-927 had gas leakage around 30Cm^3 out of overall volume 330cm^3. Therefore, a substantial volume of sample which was considered as gas phase was missed out.

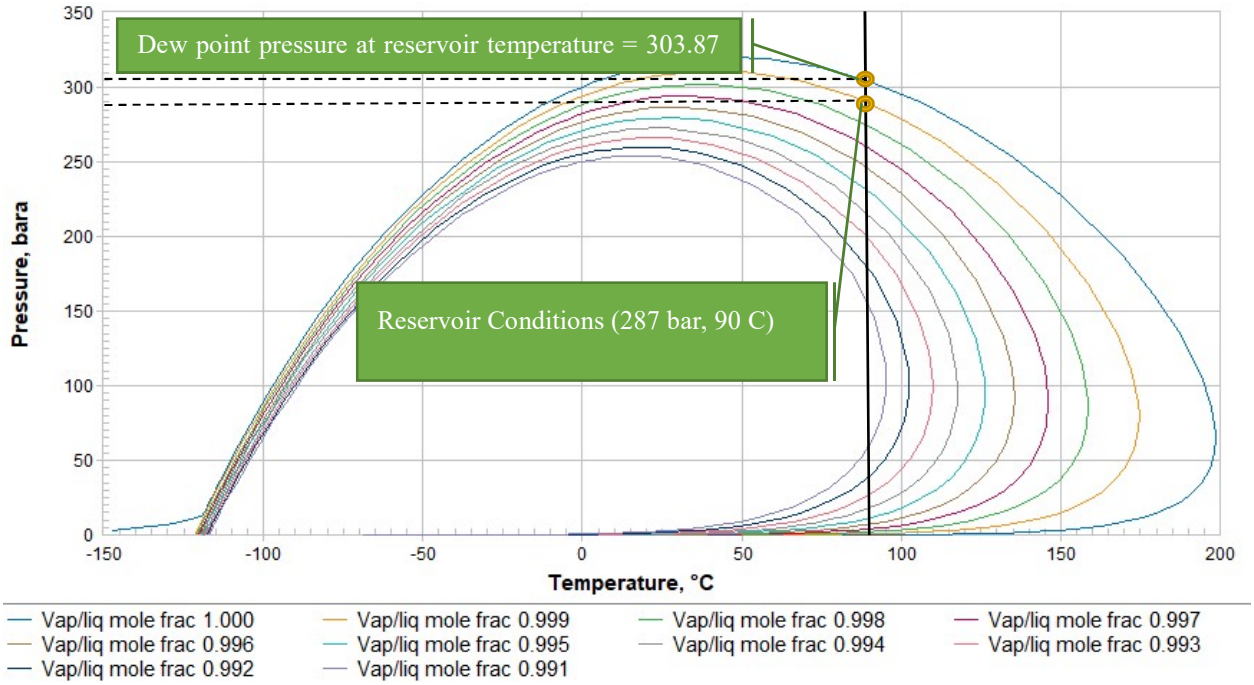

Figure 4.19. PT diagram of MDT sample MPSRBA-927of exploration well 6305/7-1 from Ormen Lange field (PVT.SIM).

On the other hand, Sample (1-39) gas phase and sample (1-41) liquid phase from DST were evaluated, and the quality of gas and liquid samples from separator were validated based on

Hoffmann plot. Figure 4.20 illustrates that there is a linear relationship between the k values of components and Hoffmann factor so the recombined fluid of gas and liquid phases from the separator of DST can be taken into account as a reliable sample of reservoir fluid. The pressure and temperature of the DST separator were approximately 798 psi and 540 R, respectively. Thus, Hoffmann plot is corrected based on the Standing (1979) method (see subchapter 2.5.2).

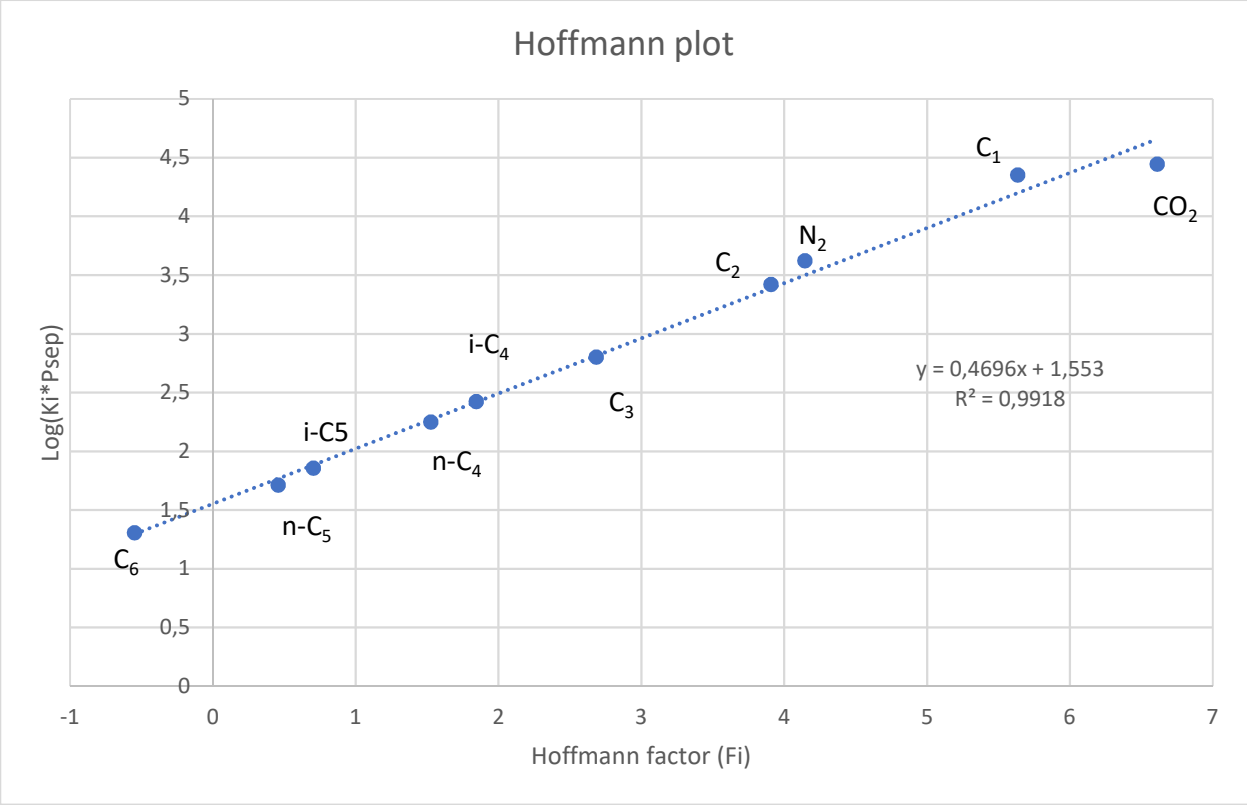

Figure 4.20.Hoffmann Plot of DST sample (1_39 (gas phase), 1_41 (liquid phase)) of exploration well 6305/7-1 from Ormen Lange field (see **Appendix 2**, subchapter 6.2.1).

So, based on the analysis which was carried out for MDT and DST samples for exploration well 6305/7-1 it can be understood that MPSRBA-927 cannot be considered as a reliable sample of reservoir fluid. However, DST sample (1_39, 1_41) is a consistent sample of reservoir fluid and one of the most significant reasons that this sample from DST method was selected for analyses is that BP (British Petroleum) company validated this sample for PVT analyses.

4.3.3 Exploration well 6305/4-1

For samples from exploration well 6305/4-1, constant mass expansion data from the laboratory was not available. So, firstly we check the quality of the DST sample from this exploration well. In addition, The pressure of DST separator was lower than 1000 psi approximately 530 psi and the temperature was around 520 R, so based on Standing (1979) approach which is modified Hoffmann plot, it can be figured out the efficiency of DST separator was high enough for collecting the representative fluid sample of DST separator (see figure 4.21 & 4.22) .

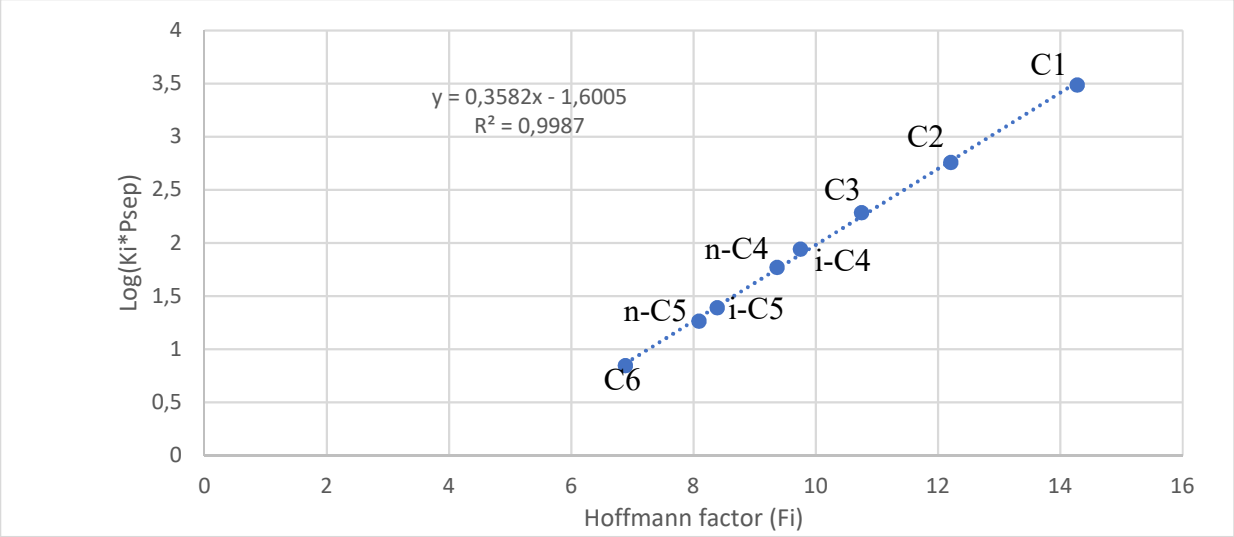

Figure 4.21. Hoffmann plot of organic hydrocarbon compositions of DST sample of exploration well 6305/4-1 (Ormen Lange field) (See **Appendix 1**, subchapter 6.2.1).

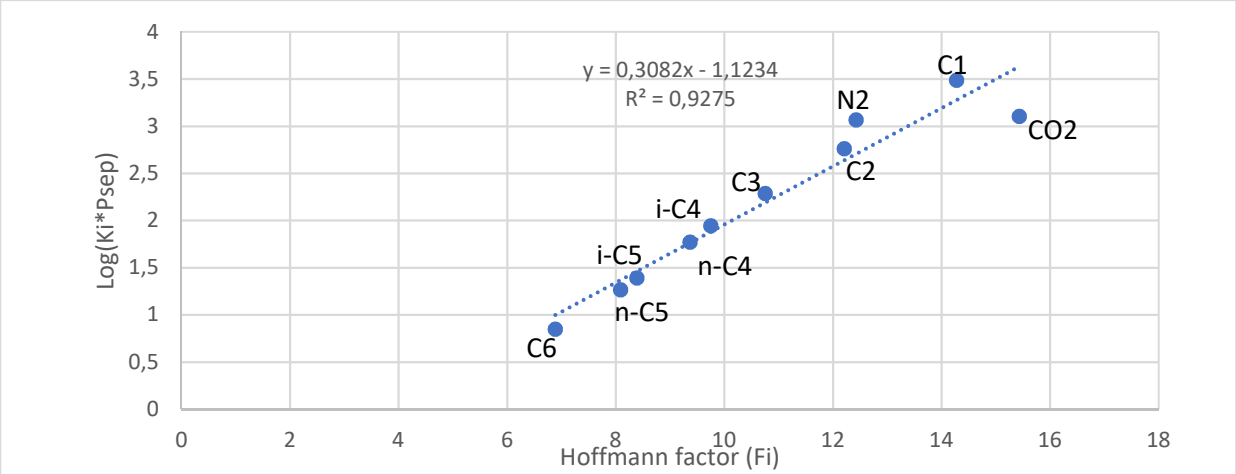

Figure 4.22. Hoffmann plot of organic and inorganic hydrocarbon compositions of DST sample of exploration well 6305/4-1 (Ormen Lange field) (See **Appendix 1**, subchapter 6.2.1).

So, because of lacks information about constant mass expansion (CME) data for tuning the simulator for achieving the correct dew point pressure, we checked the quality of DST sample, which was explained above. Secondly, by recombining the liquid phase and gas phase from DST separator with measured CGR (14.5 STB/MMSCF) by PVT.SIM simulator, the PT diagram of recombined fluid can be attained (see figure 4.23). Then, by implementing one straight line at reservoir temperature (81C) which is parallel with pressure axis, the intersection of dew point curve and the straight line is dew point pressure, which is 237.5 bar. Also, the dew point pressure at ambient temperature is 254 bar. However, this dew point pressure at the reservoir and ambient temperatures is not the actual dew point pressure of reservoir fluid due to the unavailable CME data. Moreover, the reason for achieving the dew point pressure was for checking the quality of MDT sample (MPRS-756), which was collected from exploration well 6305/4-1.

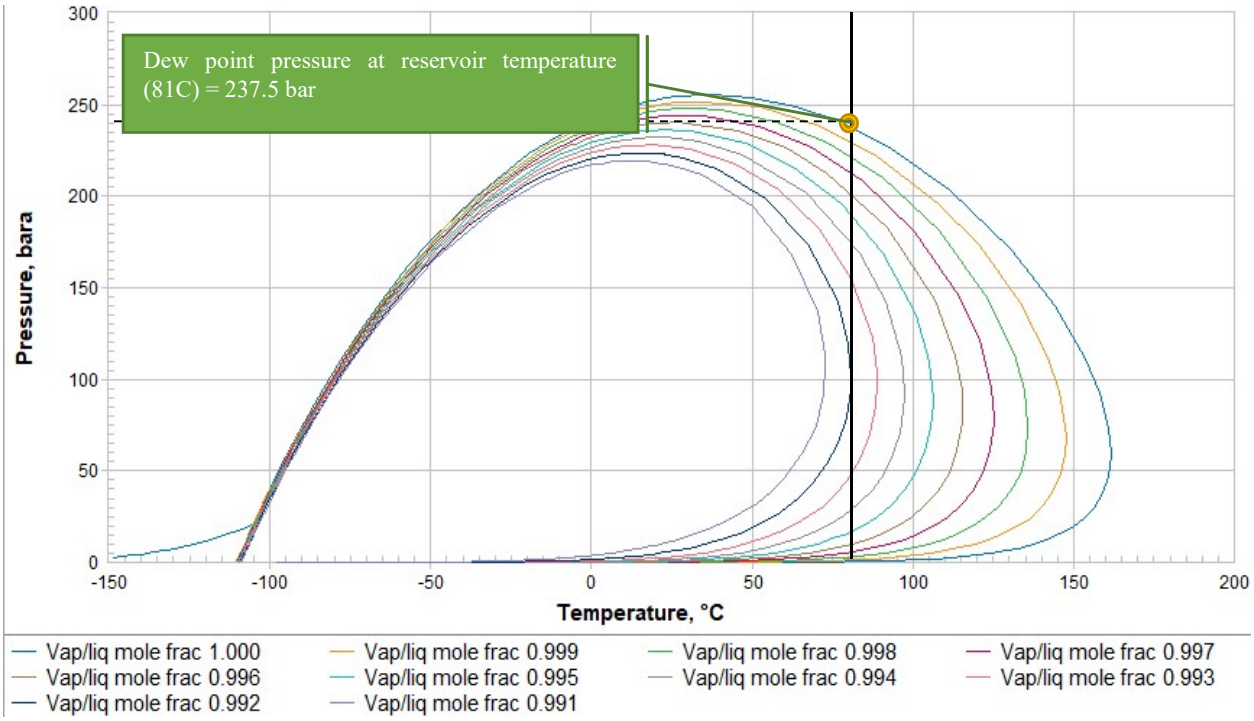

Figure 4.23. PT diagram of DST sample of exploration well 6305/4-1 from Ormen Lange field by PVT.SIM software.

Thus, for controlling the quality of MDT sample, the same as before by mixing the liquid and gas phases of the sample with certain CGR (5.714 STB/MMSCF) by the simulator, the dew point pressure at the reservoir and ambient temperature can be achieved. Figure 4.24 shows that the dew point pressures at ambient and reservoir temperatures, which are around 230 bar and 249

bar, respectively. Therefore, the accuracy of dew point pressure of MDT sample (230 bar at reservoir temperature and 249 bar at ambient temperature) as compared to the dew point pressure of DST sample (237.5 bar at reservoir temperature and 254 bar at ambient temperature) at reservoir and ambient temperature is around 98%. Consequently, based on the approving DST sample as a reliable sample of reservoir fluid which was explained before, the relative error between dew point pressure of DST sample and MDT sample at the reservoir and ambient temperature was around 2%, so MDT sample can be considered as consistent sample of reservoir fluid (see figure 4.24).

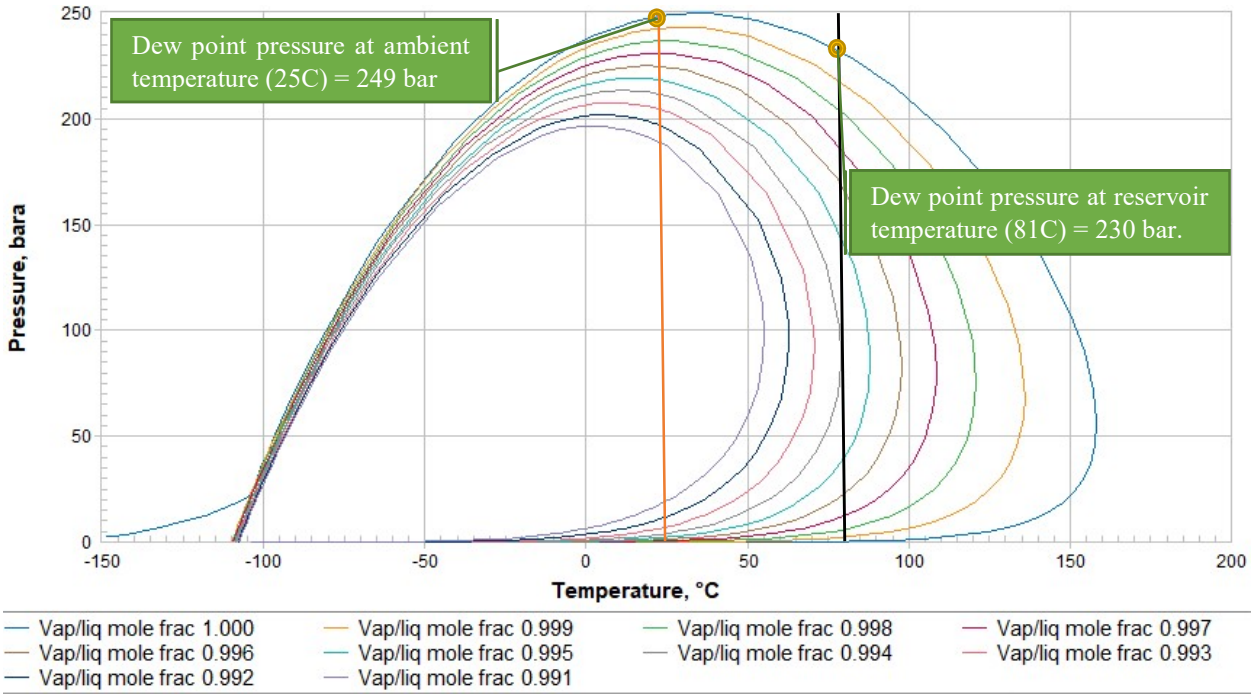

Figure 4.24.PT diagram of MDT sample (MPRS-756) of exploration well 6305/4-1 from Ormen Lange field by PVT.SIM software.

4.4 Compositional analyses of reliable MDT and DST samples

In subchapter 4.3, the quality of MDT and DST samples was checked, and the consistent samples were determined (see table 4.11). In this subchapter, the compositions of liquid and gas phases of DST and MDT samples at standard conditions and the compositions of recombined fluid at reservoir conditions will be checked.

Table 4.11. Reliable MDT and DST samples of exploration wells from the Ormen Lange field.

Sample number	PT- 1087	E-3468	TS-18211	Gas phase (1-39) Liquid phase (1-41)	MPRS-756	Minilab
Type of test	MDT	MDT	MDT	DST	MDT	DST
Well number	6305/5-1	6305/5-1	6305/5-1	6305/7-1	6305/4-1	6305/4-1
Reservoir pressure (bar)	287	287	287	287	287	287
Reservoir temperature ©	81	81	81	90	81	81
Date of sample	15.09.1997	15.09.1997	24.09.1997	22.08.1998	28.04.2002	20.05.2002
Type of sample	Gas	Gas	Gas	Gas	Gas	Gas
Dew point pressure @ reservoir condition (bar)	287	287	287	290.28	230	237.5
Measured CGR (STB/MMSCF)	8.294	6.759	6.474	15.5	5.714	14.5

4.4.1 Compositional analyses of liquid phase of consistent MDT and DST samples

By simulating the phase envelope of the liquid phase of each fluid sampling method and cleanup test, it can be understood that there is a considerable difference in critical points between MDT and DST samples (see table 4.12). Because the mole fraction of C_{10+} (around 57 %) in MDT samples is more than the mole fraction of C_{10+} (approximately 45%) in DST samples (see figure 4.25, red color circle). However, the mole fraction of C_4-C_8 in DST and cleanup test (test separator sample) samples is higher than the mole fraction of C_4-C_8 in the MDT samples, which results in

higher CGRs in DST samples. Figure 2.26 illustrates PT diagram of liquid phase of reliable fluid samples which were collected by different fluid sampling methods (MDT& DST). The critical points of the liquid phase of DST samples are so close to the critical point of cleanup test sample (test separator sample) precisely, DST (minilab) which is the most precise fluid sampling method as compared to the other fluid sampling method. So, the relative error between liquid phase compositions of DST samples and cleanup test is negligible (see figure 4.25).

Table 4.12. Critical point (pressure and temperature) of MDT, DST, and cleanup test samples (Ormen Lange field).

	Cleanup test	MDT (E-3468)	MDT (PT-1087)	MDT (TS-18211)	MDT (MPRS-756)	DST (1-41)	DST (minilab)
Critical pressure (bar)	35.34	29.01	28.81	27.16	28.99	32.97	33.31
Critical temperature ©	375.63	435.73	412.33	404.28	409.75	366.99	381.82

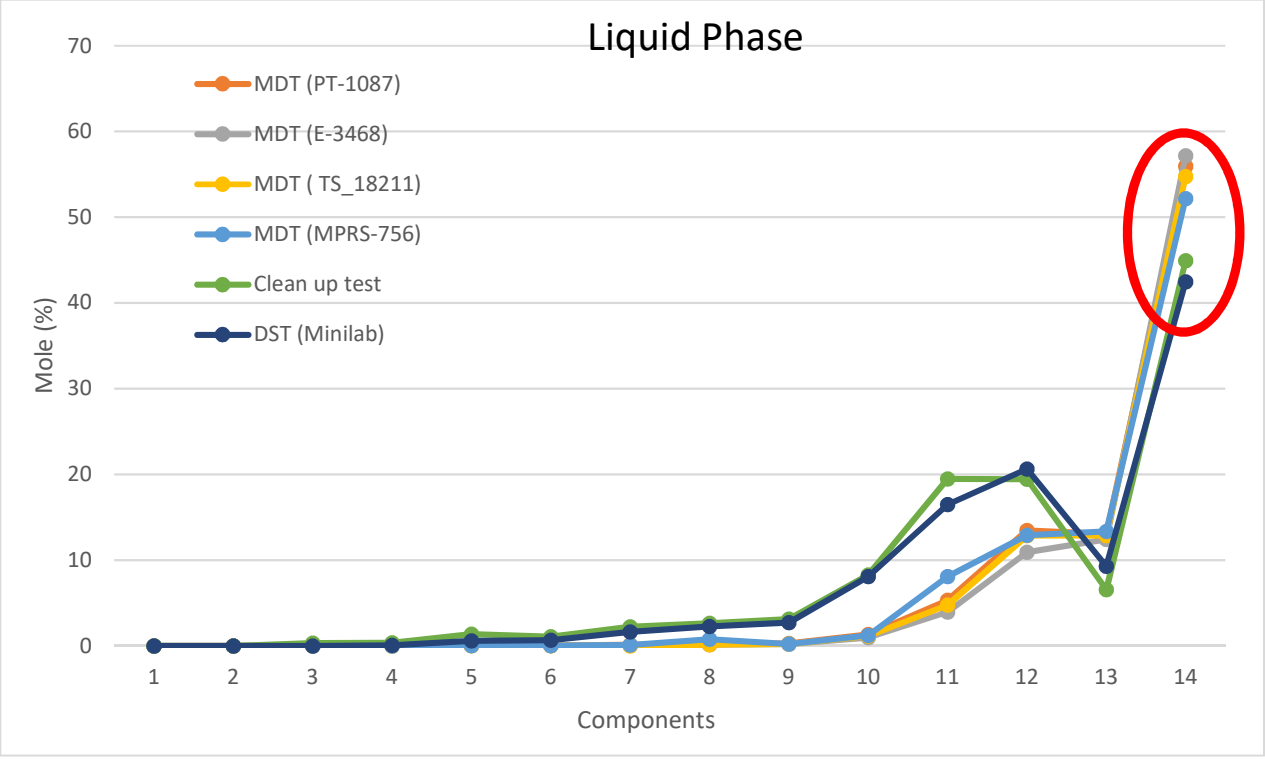

Figure 4.25. Mole fractions of components of MDT, DST and Cleanup test samples (Ormen Lange field).

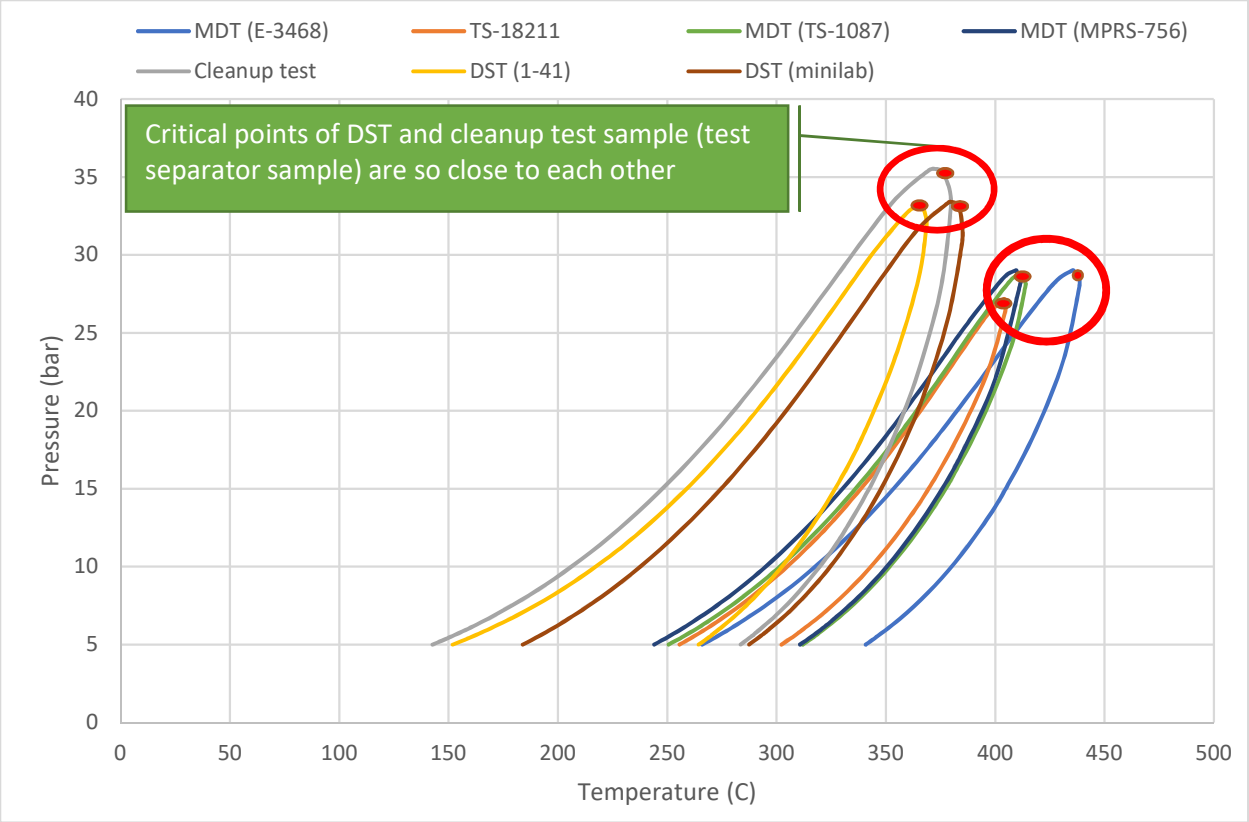

Figure 4.26. PT diagram of the liquid phase of DST, MDT, and cleanup test samples (Ormen Lange field).

4.4.2 Compositional analyses of the gas phase of reliable MDT and DST samples

In DST and test separator methods since the separation was carried out in two stages (primary separator and stoke tank oil), the compositional data of missing gas from stoke tank oil was not available for analyzing and comparing the phase envelopes of the gas phase of test separator sample with MDT samples. However, figure 4.26 has appropriately shown that the critical points of DST and test separator samples (cleanup test sample) are so close; thus, it means that the measured CGRs of DST samples and test separator can support each other.

4.5 Flashing the recombined fluids of different fluid sampling methods (MDT, DST and Test Separator)

When the compositions of reliable fluid samples of different fluid sampling methods were analyzed in last subchapter (4.4), the Condensate to the gas ratio (CGR) which was measured in each fluid samples should be evaluated. So, by utilizing PVT.SIM software, we can flash recombined fluids of different fluid sampling techniques (reported by NORSK HYDRO laboratory) to standard conditions (1 bar, 60 °F) for calculating CGR. Therefore, following the bar chart (see figure 4.27) illustrates the difference between measured and calculated CGR by PVT.SIM software. By considering the calculated CGRs with PVT.SIM software, it can be understood that there is a big difference between calculated and measured CGR in MDT samples. In other words, the CGR of each MDT sample was not measured accurately. This is one of the approaches for checking the quality of CGR measurement.

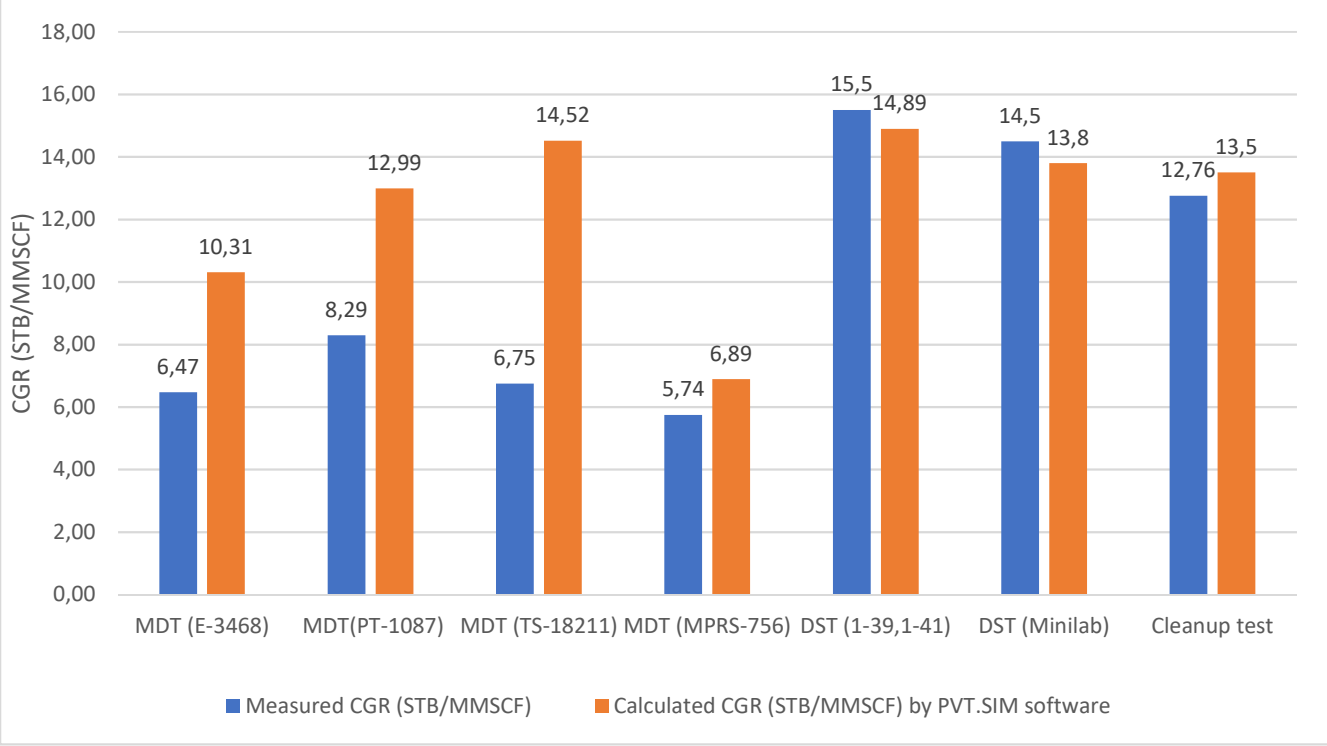

Figure 4.27. Difference between measured and calculated CGRs of MDT, DST, and Test separator samples.

4.6 Simulating the constant volume depletion (CVD) of MDT and DST samples

Based on subchapter (2.4.3), constant volume depletion is the technique for measuring the dropout liquid volume or vaporization due to the natural pressure depletion in gas condensate reservoir. For simulating the constant volume depletion (CVD) with PVT.SIM software, liquid and gas phases of each sample were recombined with measured CGRs. Hence, the volume of the liquid phase, which is proportional to the volume of the reservoir fluid in dew point conditions can be estimated. Also based on Fevang and Whitson (1996), gas condensate reservoirs which undergo natural depletion consists of three regions. Region one which is close to the reservoir includes single-phase reservoir fluid because the reservoir pressure is higher than the dew point pressure but in region two because of the natural depletion phenomenon, there will be two-phase flow and liquid phase is immobile because the condensate saturation is not high enough for movement. In region three near to the wellbore, condensate and gas flow at the same time by different flow rates. Figure 4.28 illustrates the dropout liquid volume of each fluid sample. MDT samples show the lowest dropout liquid volume as compared to cleanup test sample and DST sample (Minilab). If we assume that the gas condensate reservoir is homogenous ultimately and the relative permeability is identical throughout the reservoir, we can figure out that making the decision based on MDT samples with maximum dropout liquid volume (at pressure 120 bar) around 1.3% of reservoir fluid volume at dew point conditions is wrong. Because cleanup test sample (test separator sample) and DST sample from minilab which are the most precise fluid sampling methods for gas condensate reservoir show the liquid dropout volume around 1.78 % at pressure 120 bar. Thus, by considering the amount of liquid dropout volume from MDT and DST samples, it can be understood that the banking issue, which is the result of dropout liquid in reservoir based on MDT samples can affect production more than DST samples.

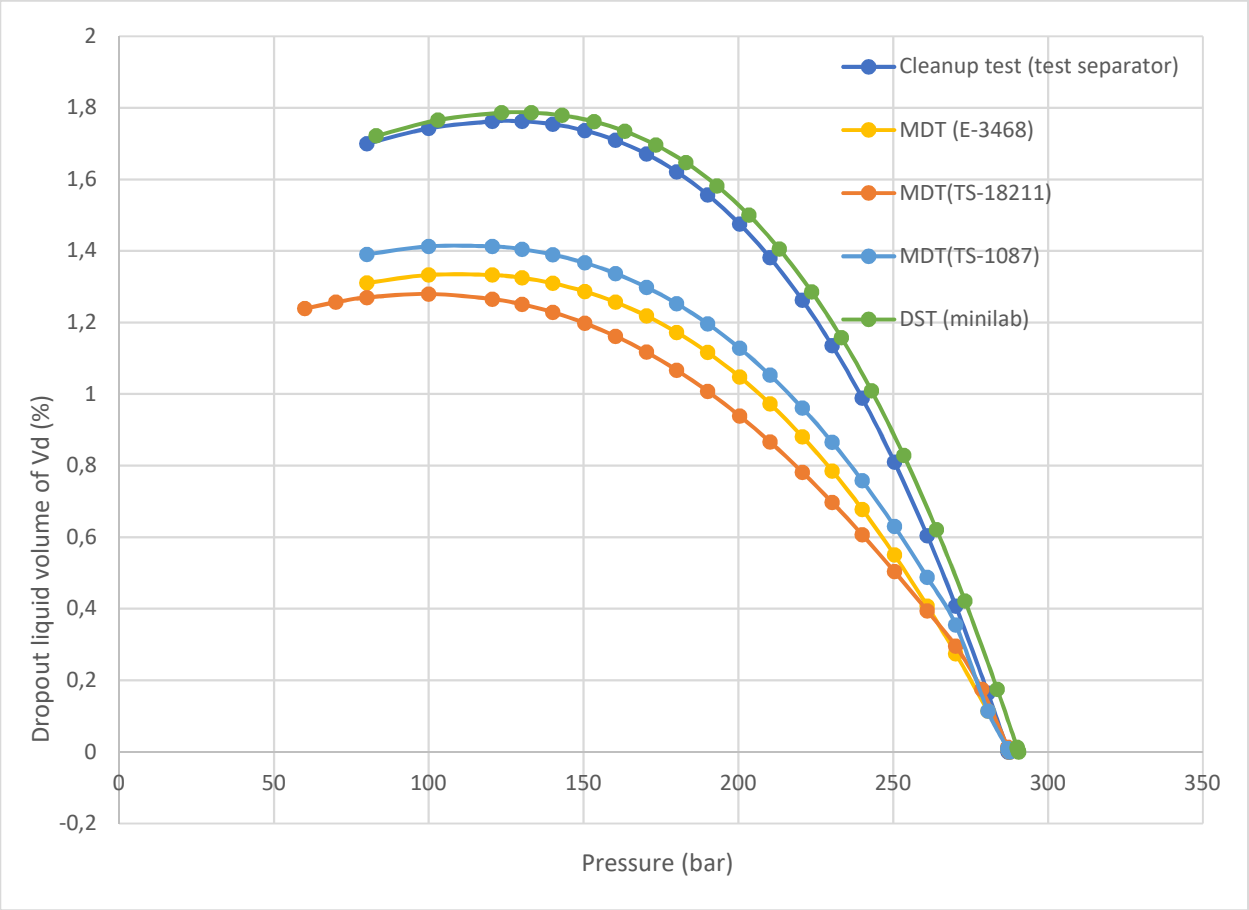

Figure 4.28. Schematic diagram of Dropout liquid volume of MDT and DST samples Vs pressure (Ormen Lange field).

5 . Chapter 5 Conclusion

5.1 . Conclusion

- This study has shown that changing pressure and temperature of oil and gas outlets of cleanup test separators can affect gas and oil flow rates. Specifically, pressure loss results in precipitation of gas and then shrinkage of oil. Hence, based on the results (see table 4.1), it can be figured out there was a considerable error around 20% in oil flow rates due to the fluid conditions.

- The difference between normalized and unnormalized condensate to gas ratios (CGRs) of development wells from the Ormen Lange field was negligible with high accuracy around 95 %, and the standard deviation was approximately 0.5 STB/MMSCF. Because the reservoir of Ormen Lange field was very lean gas condensate reservoir, so most of the volume of gas phase was removed from first stage separator, and the volume of missing gas from stoke tank oil was not noticeable.

- Based on the results which were achieved from PVT analyses in this study, the measured CGRs of MDT samples need more investigation due to the considerable average relative error around 40% as compared to the calculated CGRs from flashing the MDT samples. However, this average relative error in measured CGRs of DST samples and test separator sample (cleanup test sample) was around ± 5%.

- Simulating the constant volume depletion (CVD) of MDT and DST samples has indicated that the maximum dropout liquid volume of MDT samples was around 0.5% lower than the maximum dropout liquid volume of DST and cleanup test samples (see figure 4.28) because the liquid and gas phases of MDT samples recombined with inaccurate CGRs. So, the volume of the liquid phase of the reservoir fluid due to the natural pressure depletion in region two of reservoir valued inaccurately. Eventually, the production of the reservoir might be estimated wrongfully.

5.2 Probable reasons for considerable relative errors in measured CGRs from MDT samples

There are some probable reasons that the measured CGRs from MDT samples are different from DST and test separator samples as following:

- MDT method, which is the most time efficient and advanced fluid sampling methods among the other wireline fluid sampling methods, can collect limited volume samples from preselected formations as representative fluid samples. However, surface fluid sampling methods such as test separator method can support a vast volume of the reservoir fluid from the separator. Also, Ormen Lange field based on the calculated CGRs (**12.76 STB/MMSCF**) from development wells is a very lean gas condensate field. Hence, the error in measured CGRs from MDT samples is higher than measured CGRs from surface sampling methods due to the volume limitation in fluid sampling.

- Transferring the fluid samples from MDT sample chambers to laboratory compartments might create some errors. Because even if one droplet of liquid phase remains in MDT sample chambers during the transferring, it can make a noticeable error in CGR measurement, specifically MDT samples from very lean gas condensate field like Ormen Lange.

- The other possible reason might be human error in measuring the CGRs from MDT fluid samples or in transferring the fluid samples from MDT chambers to laboratory compartments. Also, the errors from measurement equipment and MDT methods should be considered.

5.3 Future Study

In this study, Ormen Lange field was the case study, and the reservoir fluid was very lean gas condensate. So, the missing gas of stoke tank oil in the cleanup test which was performed by EXPRO was negligible. However, there are some fields that the volume of missing gas is very noticeable, and petroleum companies do not consider it, which will result in wrong CGR measurement. Checking the accuracy of CGR from **rich gas condensate reservoir** fluid can be a new study for analyzing the accuracy of CGR based on fluid sampling.

5.4 . References

- Badry, R., Head, E., Morris, C., & Traboulay, I. (1993). *New Wireline Formation Tester Techniques And Applications*. Paper presented at the SPWLA 34th Annual Logging Symposium, Calgary, Alberta. https://doi.org/
- Bentley, J. P. (2005). *Principles of measurement systems*: Pearson Education.
- Bjørn Dybdahl, & Hans Petter Hjermstad. (2001). *A systematic Approach to Sampling during Well Testing*. Paper presented at the SPE Latin American and Caribbean Petroleum Engineering Conference, Buenos Aires, Argentina. https://doi.org/10.2118/69427-MS
- Burke, N. E., Chea, C. K., Hobbs, R. D., & Tran, H. T. (1991). *Extended Analysis of Live Reservoir Oils by Gas Chromatography*. Paper presented at the SPE International Symposium on Oilfield Chemistry, Anaheim, California. https://doi.org/10.2118/21003-MS
- Expro. (2007). *Well tesing,*. In *Choke manifold* (Vol. 2, pp. 1-2): Expro.
- Fevang, Ø., & Whitson, C. H. (1996). Modeling Gas-Condensate Well Deliverability. *SPE Reservoir Engineering, 11*(04), 221-230. Retrieved from https://doi.org/10.2118/30714-PA. doi:10.2118/30714-PA
- Freyss, H., Guieze, P., Varotsis, N., Khakoo, A., Lestelle, K., & Simper, D. J. T. T. R. (1989). PVT analysis for oil reservoirs. *37*, 4-15.
- GPSA. (1998). *Engineering data book,* . Tulsa, Oklahoma 74145.
- Gundersen, I. S. (2015). *Data Accuracy from Well Test Operations.* (Mastre degree), University of Stavanger,
- Hoffman, A. E., Crump, J. S., & Hocott, C. R. (1953). Equilibrium Constants for a Gas-Condensate System. *Journal of Petroleum Technology, 5*(01), 1-10. Retrieved from https://doi.org/10.2118/219-G. doi:10.2118/219-G
- Kool, H., Azari, M., Soliman, M. Y., Proett, M. A., Irani, C. A., & Dybdahl, B. (2001). *Testing of Gas Condensate Reservoirs - Sampling, Test Design and Analysis*. Paper presented at the SPE Asia Pacific Oil and Gas Conference and Exhibition, Jakarta, Indonesia. https://doi.org/10.2118/68668-MS
- Minhas, H. N., Fakharuddin, M., Gibrata, M. A., Bt M Nordin, N. S., Cheong, B. C., Daungkaew, S., & Sinnappu, S. (2009). *Advanced Formation Testing and PVT Sampling*

in Deep Gas Condensate Reservoir: Case Study from Malaysia. Paper presented at the International Petroleum Technology Conference, Doha, Qatar. https://doi.org/10.2523/IPTC-13623-MS

- Mp, S., Indra, T. B., & Prasetyo, I. A. (1999). *The Application of Modular Formation Dynamics Tester -MDT* with a Dual Packer Module in Difficult Conditions in Indonesia*. Paper presented at the SPE Asia Pacific Oil and Gas Conference and Exhibition, Jakarta, Indonesia. https://doi.org/10.2118/54273-MS
- Nagarajan, Narayana Rao, Honarpour, Matt, M., Sampath, & Krishnaswamy. (2006). *Reservoir Fluid Sampling and Characterization—Key to Efficient Reservoir Management*. Paper presented at the Abu Dhabi International Petroleum Exhibition and Conference, Abu Dhabi, UAE. https://doi.org/10.2118/101517-MS
- Norwegian Petroleum Directorate. (2019). *Ormen Lange Field Specialization,*. Retrieved from http://factpages.npd.no/factpages/Default.aspx?culture=no
- Proett, M. A., Gilbert, G. N., Chin, W. C., & Monroe, M. L. (1999). *New Wireline Formation Testing Tool with Advanced Sampling Technology*. Paper presented at the SPE Annual Technical Conference and Exhibition, Houston, Texas. https://doi.org/10.2118/56711-MS
- René MIGNOT. (2003). *Reservoir Fluid Properties,* . IFP School: IFP School,.
- Roussennac, B. (2001). *Gas condensate well test analysis.* Stanford University,
- Schlumberger. (2002). *MDT Modular Formation Dynamics Tester*,. In (pp. 1-11): Schlumberger.
- Shi, C. (2009). *Flow behavior of gas-condensate wells*: Stanford University Stanford, California.
- Standing, M. B. (1977). *Volumetric and phase behavior of oil field hydrocarbon systems*: Society of petroleum engineers of AIME.
- Theodosia Fiotodimitraki. (February 2016,). *Quality controlled oil reservoirs PVT data.* (Postgraduate program in Petroleum Engineering,), Technical University of Crete,, Retrieved from https://dias.library.tuc.gr/view/manf/63591
- Wall, C. G. (1982). Characteristics of gas condensate reservoirs and traditional production methods. *Oyez scientific and technical service*

1-12.

- Whitson, C. H. (1983). Characterizing Hydrocarbon Plus Fractions. *Society of Petroleum Engineers Journal, 23*(04), 683-694. Retrieved from https://doi.org/10.2118/12233-PA. doi:10.2118/12233-PA
- Whitson, C. H., & Brulé, M. R. J. S. o. P. E. (2000). Phase Behavior, Monograph Series.
- Whitson, C. H. J. F. d., & Hydro, t. N. (1998). Fluid sampling & laboratory data.
- Witt, C. J., Crombie, A., & Vaziri, S. (1999). *A Comparison of Wireline and Drillstem Test Fluid Samples From a Deepwater Gas-Condensate Exploration Well*. Paper presented at the SPE Annual Technical Conference and Exhibition, Houston, Texas. https://doi.org/10.2118/56714-MS
- Worth, G. J. O., EUA. (2003). Engineering data Book, (electronic).

6. Chapter 6 Appendices

6.1 Appendix 1

6.1.1 Normalized and unnormalized CGRs of development wells from Ormen Lange field

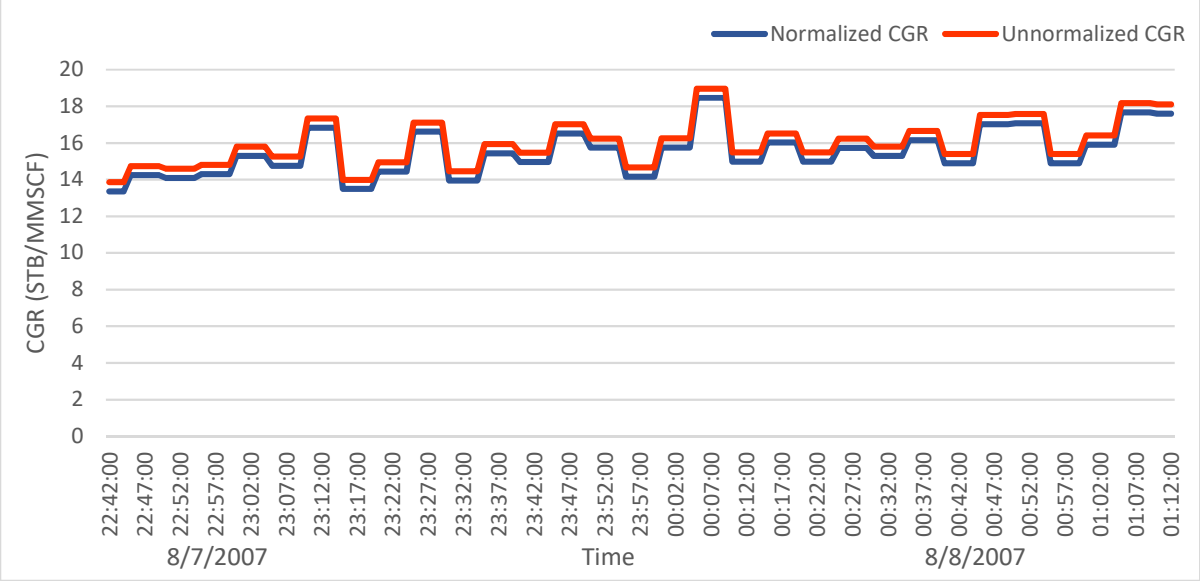

Figure 6.1. Normalized and unnormalized CGRs of development well 63058-A7H from Ormen Lange field.

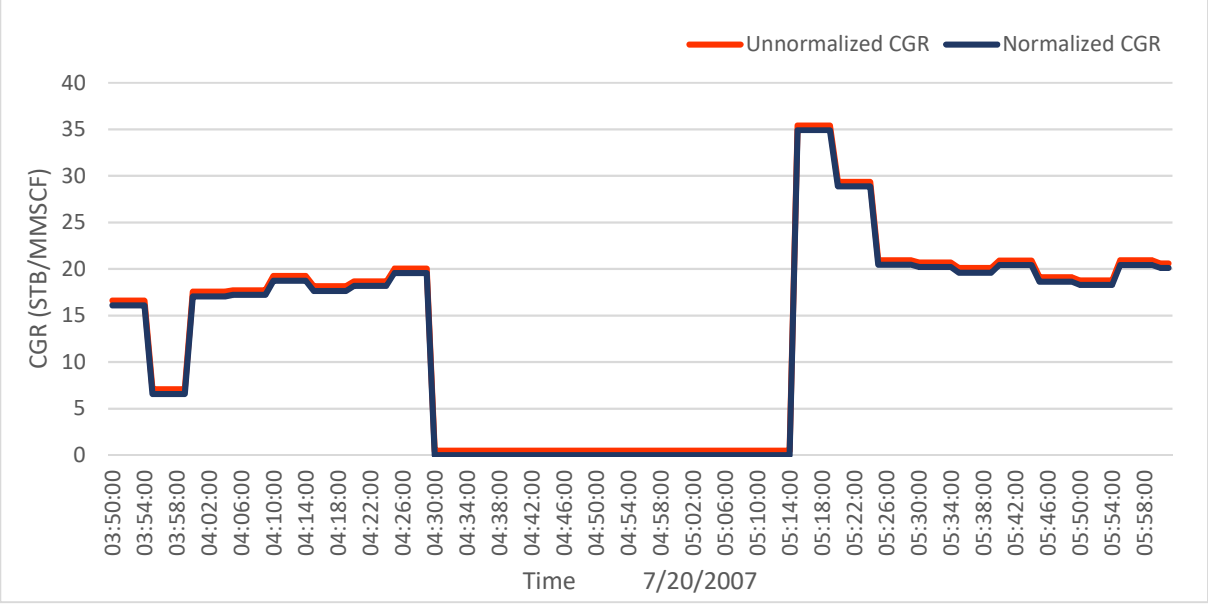

Figure 6.2. Normalized and unnormalized CGRs of development well 63058-A2H from Ormen Lange field.

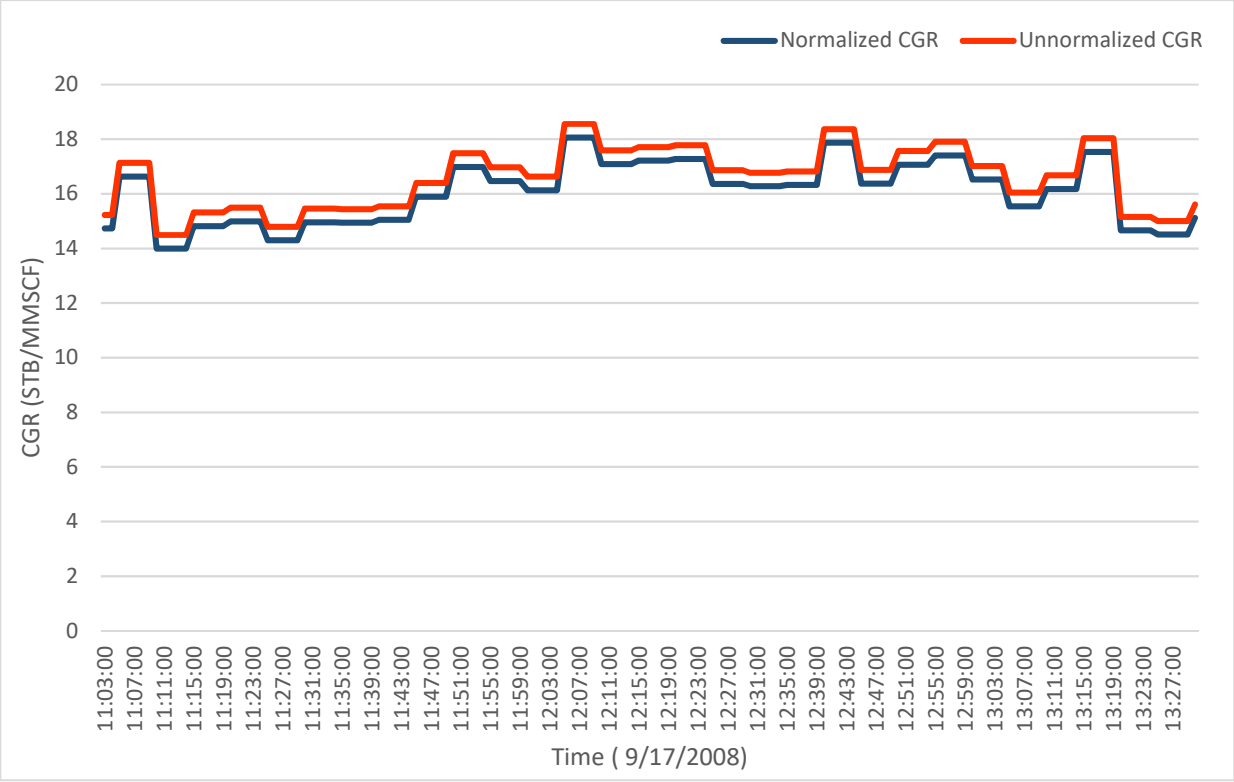

Figure 6.3. Normalized and unnormalized CGRs of development well 63055-B3H from Ormen Lange field.

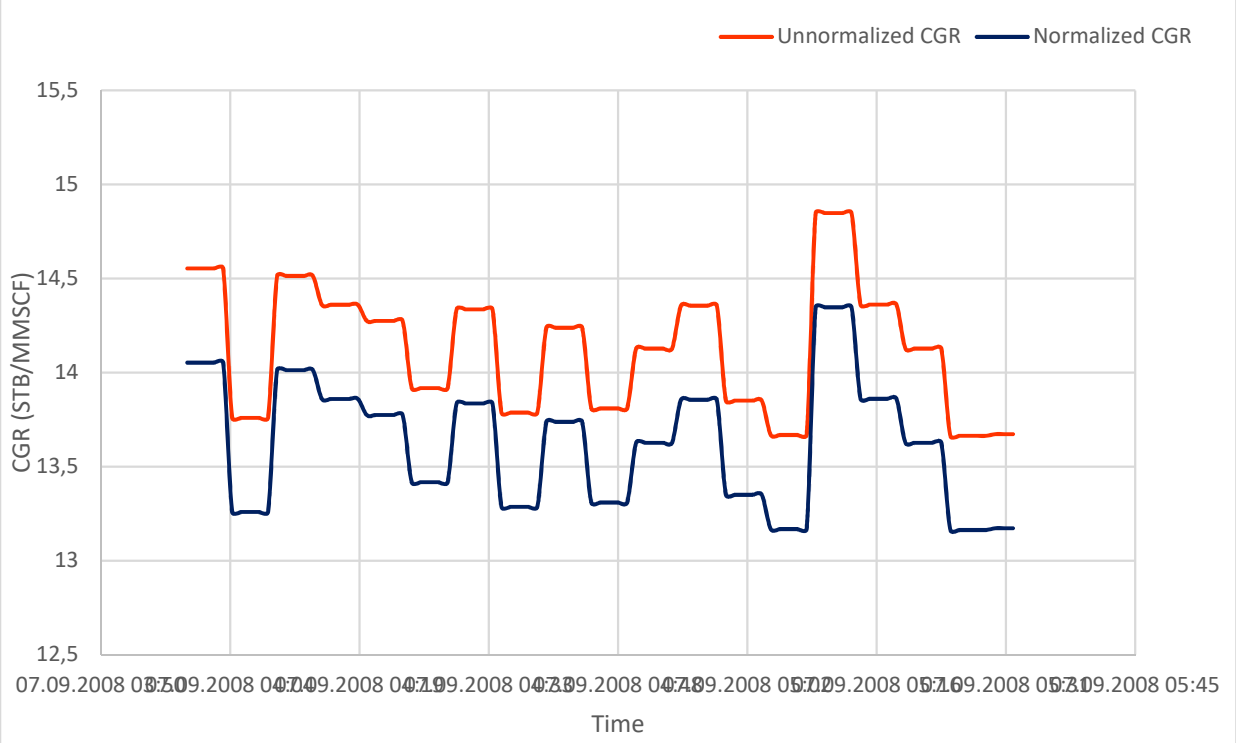

Figure 6.4. Normalized and unnormalized CGRs of development well 63055-B-2AH from Ormen Lange field.

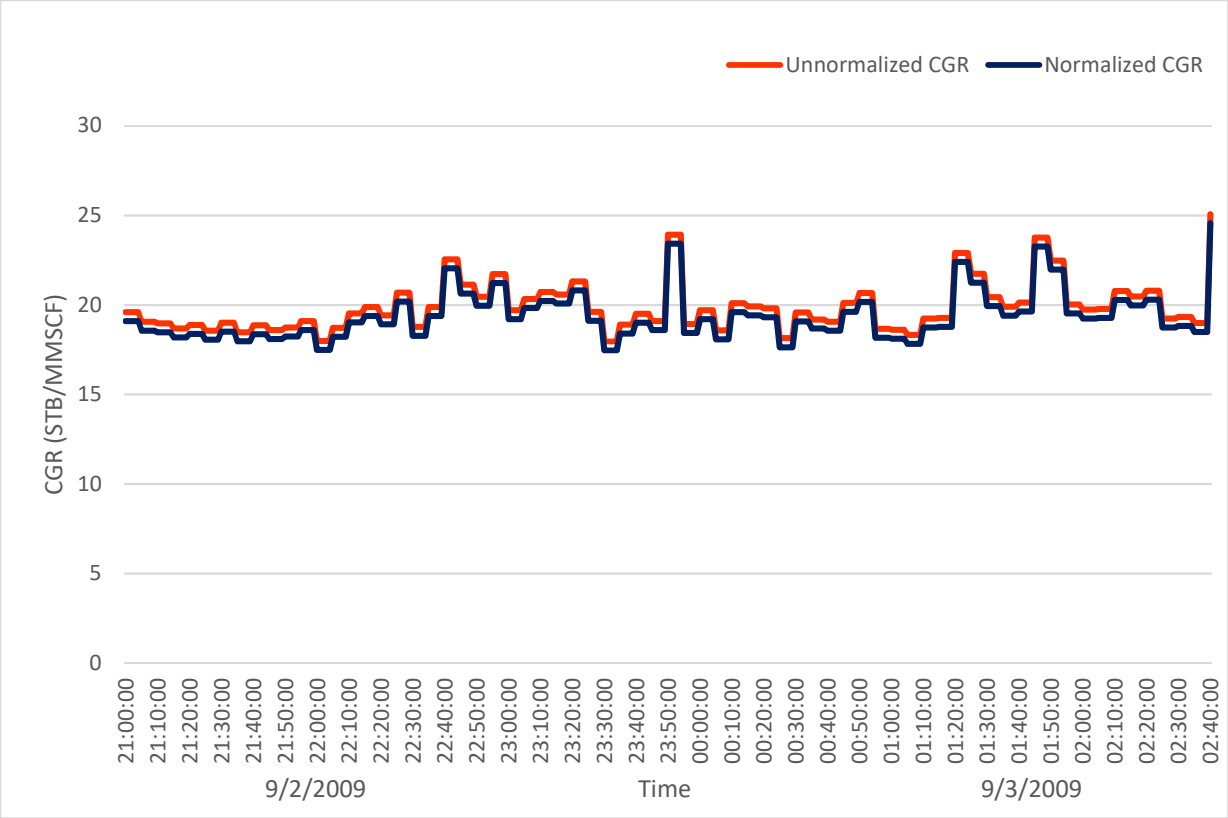

Figure 6.5. Normalized and unnormalized CGRs of development well 63058-A5H from Ormen Lange field.

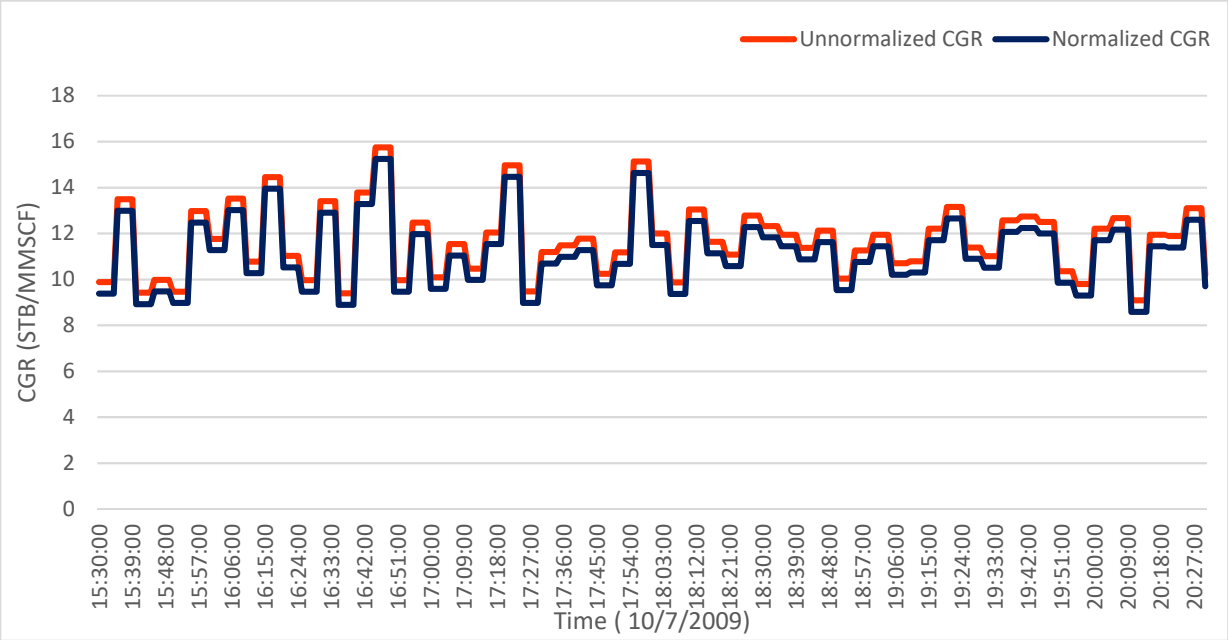

Figure 6.6. Normalized and unnormalized CGRs of development well 63058-B6H from Ormen Lange field.

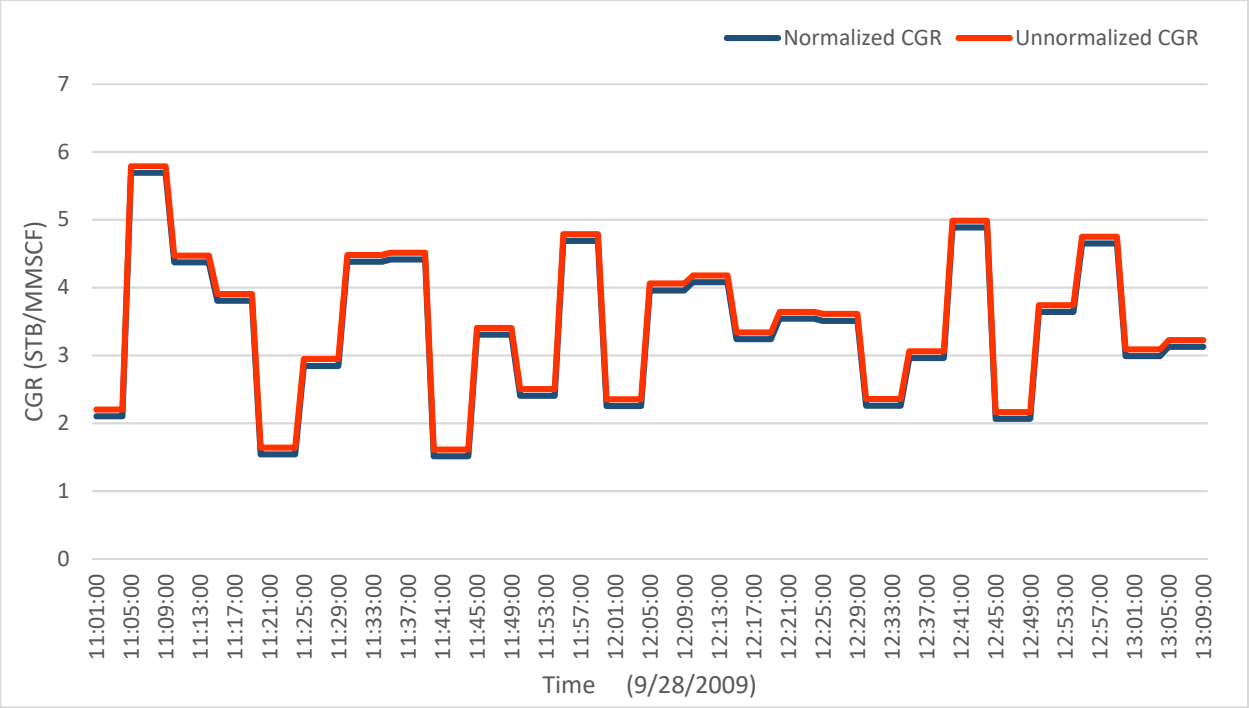

Figure 6.7. Normalized and unnormalized CGRs of development well 63058-B7H from Ormen Lange field.

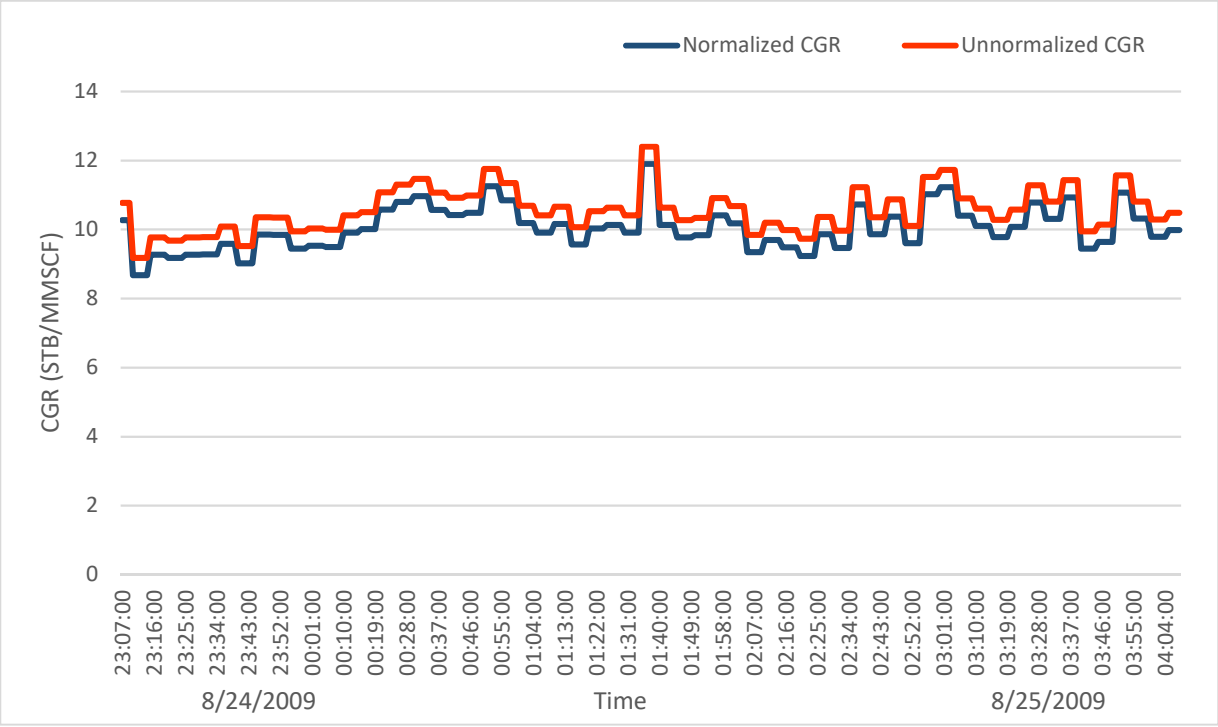

Figure 6.8. Normalized and unnormalized CGRs of development well 63058-A4H from Ormen Lange field.

6.1.2 Normalized CGR and Choke size variation of development wells from Ormen Lange field

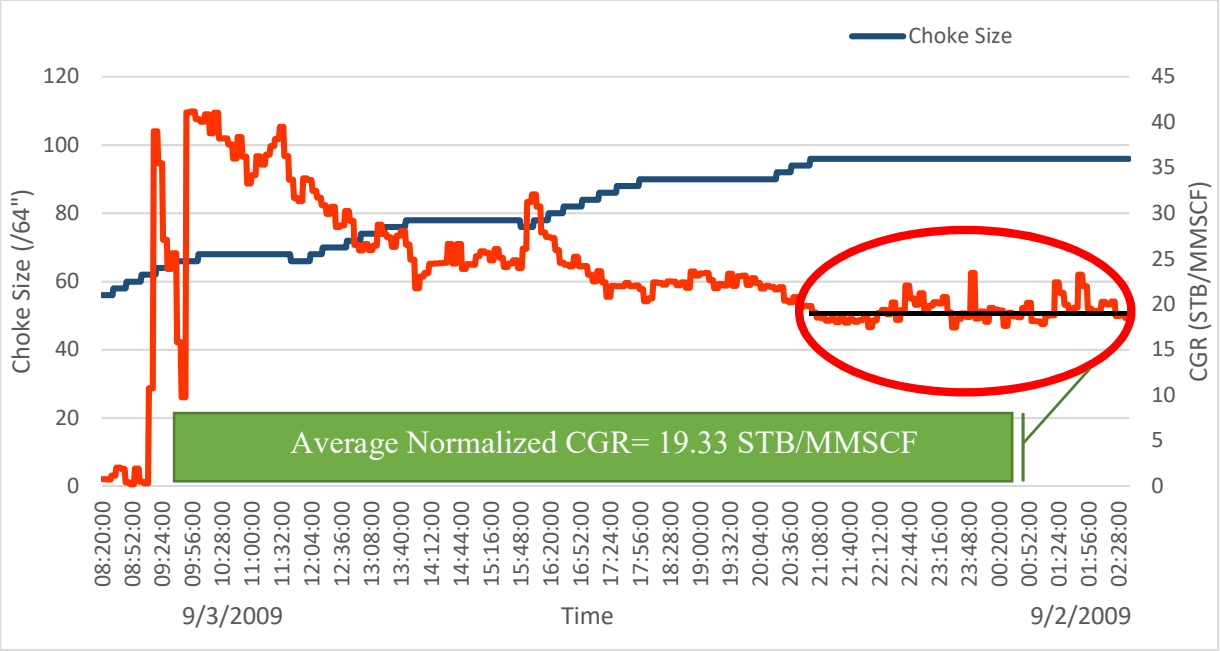

Figure 6.9. Schematic diagram of Normalized CGR and Choke size variation of development well 63058-A5H (Ormen Lange field) through cleanup test process.

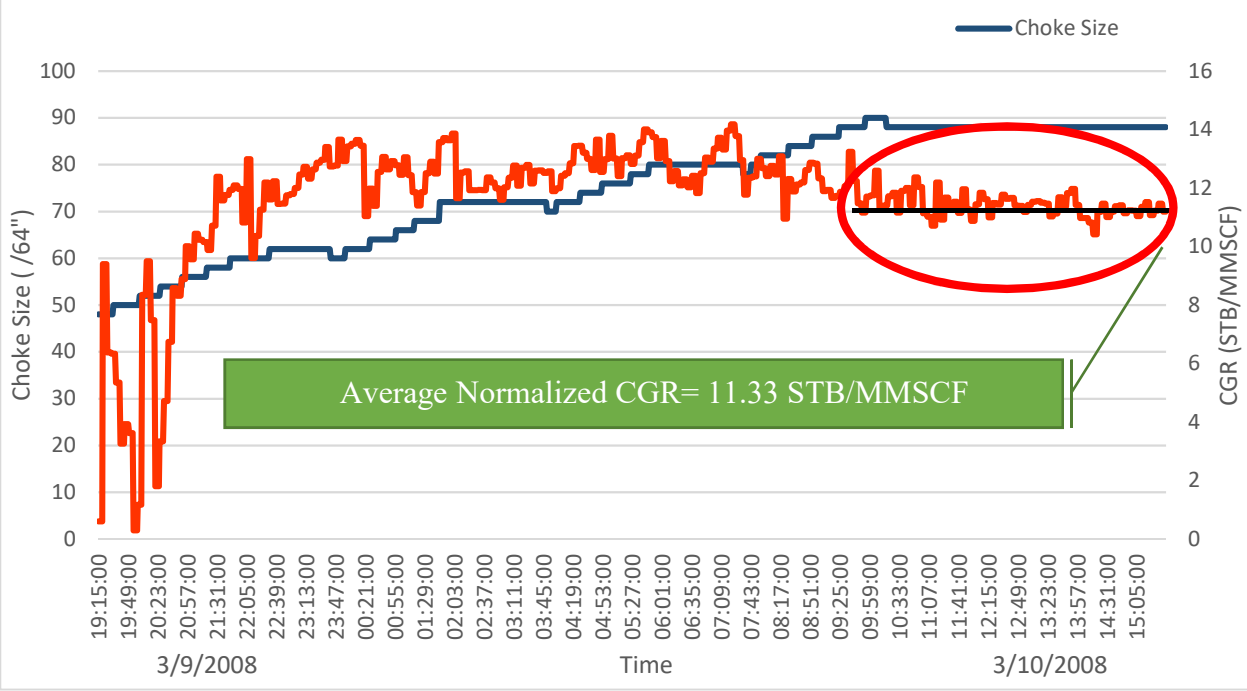

Figure 6.10. Schematic diagram of Normalized CGR and Choke size variation of development well 63058-A6H (Ormen Lange field) through cleanup test process.

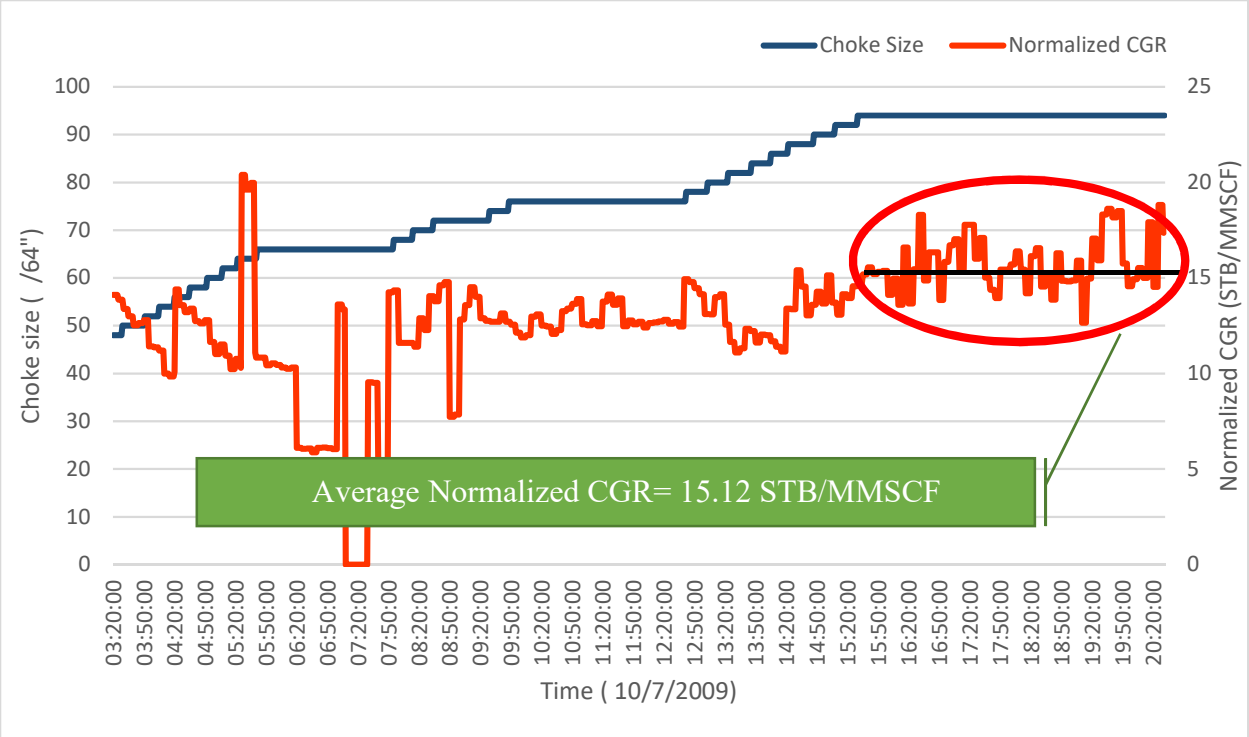

Figure 6.11. Schematic diagram of Normalized CGR and Choke size variation of development well 63058-B6H (Ormen Lange field) through cleanup test process.

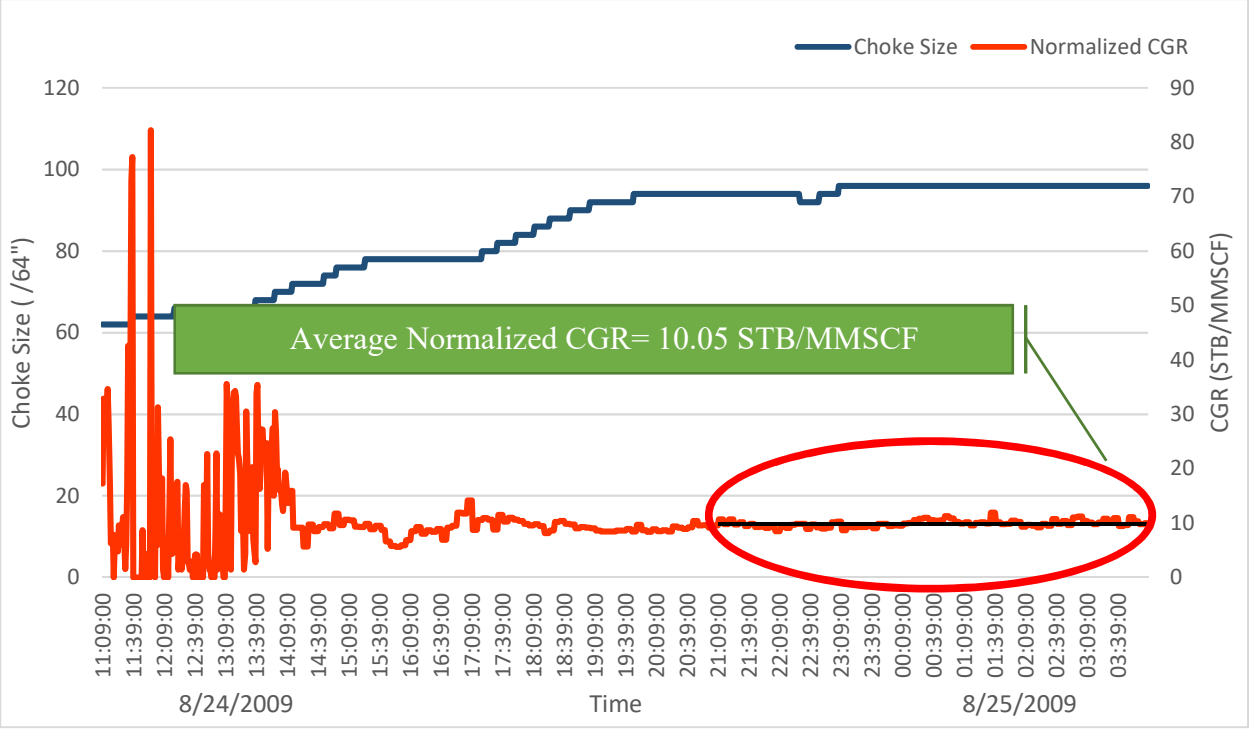

Figure 6.12. Schematic diagram of Normalized CGR and Choke size variation of development well 63058-A4H (Ormen Lange field) through cleanup test process.

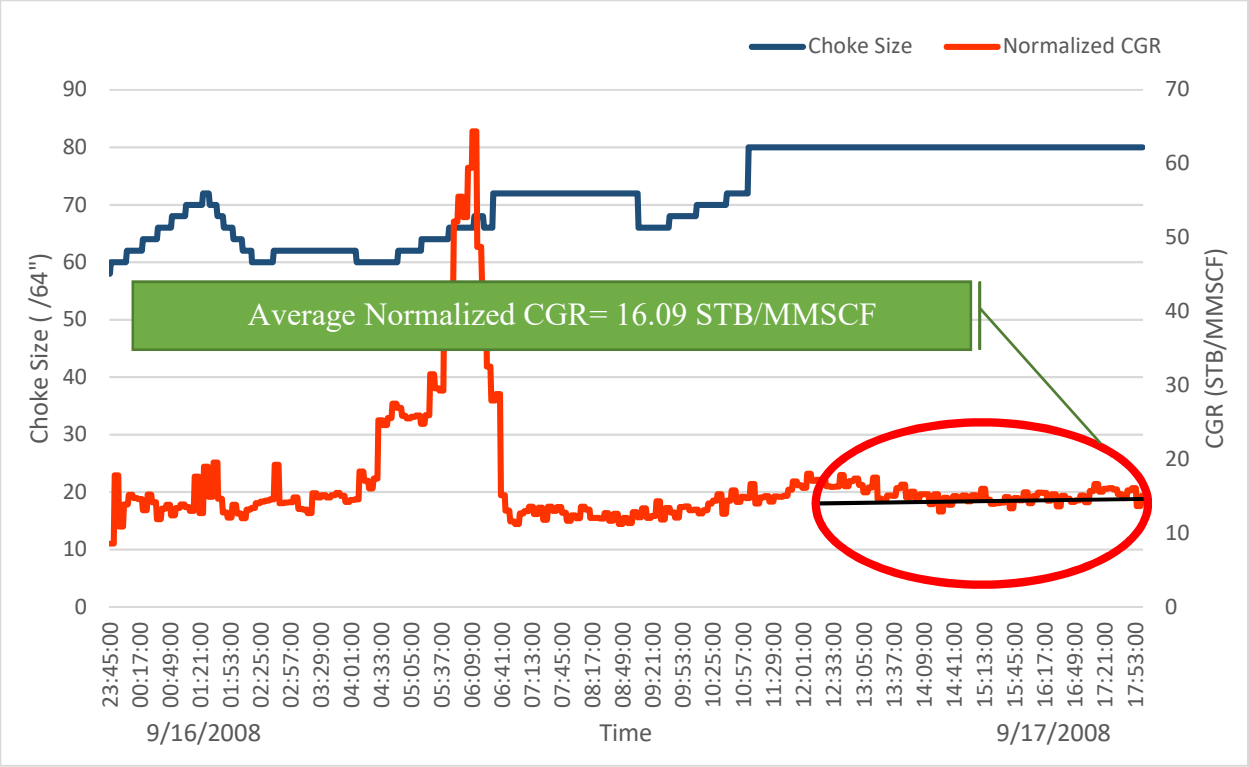

Figure 6.13. Schematic diagram of Normalized CGR and Choke size variation of development well 63058-B3H (Ormen Lange field) through cleanup test process.

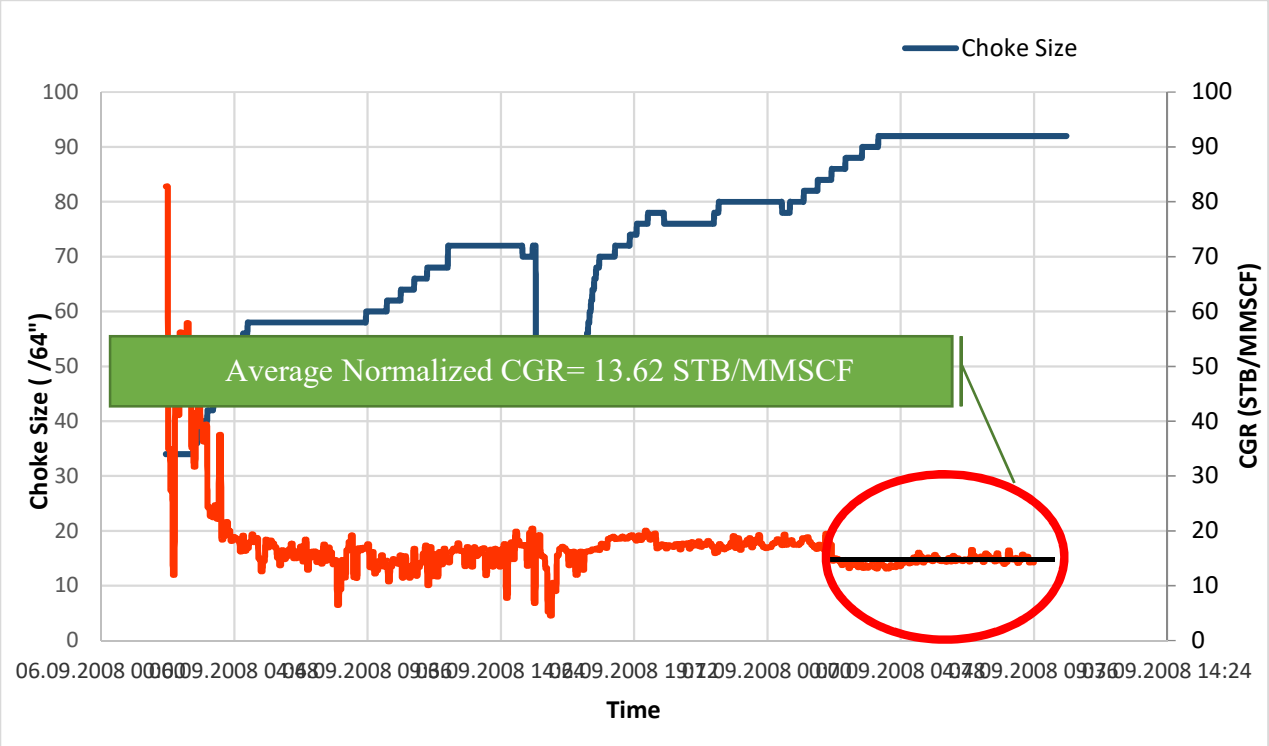

Figure 6.14. Schematic diagram of Normalized CGR and Choke size variation of development well 63055-B-2AH (Ormen Lange field) through cleanup test process.

6.1.3 . Actual production data of development wells from Ormen Lange field

Table 6.1. Actual production data of development wells from Ormen Lange field (2016 to 2019).

Year	Month	Gas (MMsm3)	Condensate	CGR (sm3/sm3)	CGR (STB/MMSCF)
2019	1	1.25	66.20	52.77	9.39
2018	1	1.39	65.01	46.91	8.35
	2	1.27	74.27	58.46	10.41
	3	1.29	66.87	51.78	9.22
	4	1.34	74.95	55.88	9.95
	5	1.36	73.77	54.06	9.62
	6	1.27	65.09	51.25	9.12
	7	1.35	79.66	59.14	10.53
	8	1.31	70.81	54.02	9.62
	9	1.26	66.27	52.53	9.35
	10	1.28	68.72	53.60	9.54
	11	1.23	64.91	52.95	9.43
	12	1.24	65.07	52.57	9.36
2017	1	1.46	86.88	59.69	10.63
	2	1.24	70.28	56.90	10.13
	3	1.43	83.77	58.55	10.42
	4	1.38	79.39	57.44	10.22
	5	1.07	60.77	56.84	10.12
	6	1.34	78.61	58.47	10.41
	7	1.40	77.23	55.07	9.80
	8	1.39	79.78	57.23	10.19
	9	1.39	73.99	53.35	9.50
	10	1.34	74.25	55.24	9.83
	11	1.38	75.49	54.69	9.73
	12	1.42	79.47	55.83	9.94
2016	1	1.55	106.14	68.43	12.18
	2	1.48	97.40	65.81	11.71
	3	1.52	95.41	62.72	11.16
	4	1.27	70.72	55.47	9.87
	5	1.42	97.97	68.82	12.25
	6	1.50	88.73	59.19	10.54
	7	1.51	89.38	59.32	10.56
	8	1.50	88.55	59.22	10.54
	9	1.19	70.20	58.83	10.47
	10	1.50	87.72	58.60	10.43
	11	1.37	76.49	56.03	9.97
	12	1.46	87.04	59.58	10.61

Table 6.2. Actual production data of development wells from Ormen Lange field (2013 to 2015).

Year	Month	Gas (MMsm3)	Condensate	CGR (sm3/MMsm3)	CGR (STB/MMSCF)
			(Sm3)		
2015	1	1.65	108.86	65.86	11.72
	2	1.54	99.54	64.70	11.52
	3	1.69	111.30	65.95	11.74
	4	1.63	105.70	64.97	11.57
	5	0.94	60.50	64.34	11.45
	6	0.07	0.05	0.74	0.13
	7	1.61	100.77	62.60	11.14
	8	1.48	91.50	61.68	10.98
	9	1.54	95.53	62.11	11.06
	10	1.46	92.25	63.37	11.28
	11	1.58	98.22	62.08	11.05
	12	1.62	102.64	63.46	11.30
2014	1	1.85	127.25	68.96	12.28
	2	1.64	113.54	69.08	12.30
	3	1.55	104.06	67.27	11.97
	4	1.72	121.63	70.72	12.59
	5	1.36	87.54	64.40	11.46
	6	1.75	122.72	70.19	12.49
	7	1.77	118.11	66.79	11.89
	8	1.77	119.13	67.17	11.96
	9	1.70	112.86	66.34	11.81
	10	1.75	89.77	51.39	9.15
	11	1.68	136.52	81.22	14.46
	12	1.69	110.65	65.47	11.65
2013	1	1.96	146.13	74.71	13.30
	2	1.78	124.90	70.30	12.51
	3	1.74	125.13	71.89	12.80
	4	1.89	136.03	71.91	12.80
	5	1.57	109.56	69.56	12.38
	6	1.70	127.39	74.98	13.35
	7	1.86	130.96	70.27	12.51
	8	1.85	132.97	72.02	12.82
	9	1.80	104.57	58.14	10.35
	10	1.87	147.97	79.14	14.09
	11	1.70	116.94	68.68	12.23

Table 6.3. Actual production data of development wells from Ormen Lange field (2010 to 2012).

Year	Month	Gas (MMsm3)	Condensate	CGR (sm3/MMsm3)	CGR (STB/MMSCF)
			(Sm3)		
2012	1	2.02	164.31	81.47	14.50
	2	1.93	144.13	74.58	13.28
	3	1.97	147.31	74.88	13.33
	4	1.87	147.06	78.81	14.03
	5	1.51	140.56	92.82	16.52
	6	1.91	158.09	82.89	14.76
	7	1.96	143.29	73.04	13.00
	8	1.80	124.88	69.44	12.36
	9	1.88	129.97	69.30	12.34
	10	1.71	128.40	74.90	13.33
	11	1.87	153.61	82.30	14.65
	12	1.80	151.98	84.41	15.03
2011	1	2.00	144.98	72.51	12.91
	2	1.76	130.25	74.11	13.19
	3	1.95	148.76	76.27	13.58
	4	1.81	159.12	87.89	15.65
	5	1.88	138.40	73.50	13.08
	6	0.73	62.21	85.47	15.21
	7	1.77	119.26	67.20	11.96
	8	2.10	162.60	77.53	13.80
	9	2.01	156.21	77.74	13.84
	10	1.99	150.75	75.78	13.49
	11	2.04	169.54	83.18	14.81
	12	1.72	112.16	65.20	11.61
2010	1	1.80	123.10	68.30	12.16
	2	1.87	158.54	84.79	15.09
	3	1.88	128.99	68.74	12.24
	4	2.00	150.34	75.33	13.41
	5	1.86	136.82	73.49	13.08
	6	1.77	125.22	70.66	12.58
	7	1.05	65.16	61.97	11.03
	8	0.95	70.70	74.67	13.29
	9	1.49	97.23	65.46	11.65
	10	2.08	160.71	77.18	13.74
	11	2.06	151.14	73.42	13.07

Table 6.4. Actual production data of development wells from Ormen Lange field (2007 to 2009).

Year	Month	Gas (MMsm3)	Condensate	CGR (sm3/MMsm3)	CGR (STB/MMSCF)
			(Sm3)		
2009	1	1.73	135.76	78.27	13.93
	2	1.63	135.14	82.96	14.77
	3	1.69	131.40	77.67	13.83
	4	1.67	129.41	77.39	13.78
	5	1.74	137.54	78.93	14.05
	6	1.51	117.39	77.89	13.86
	7	1.61	119.66	74.46	13.25
	8	1.53	162.66	106.39	18.94
	9	1.59	116.34	73.26	13.04
	10	1.93	145.28	75.17	13.38
	11	2.03	152.90	75.22	13.39
	12	2.13	162.30	76.09	13.54
2008	1	0.77	58.62	76.05	13.54
	2	0.76	66.65	87.41	15.56
	3	0.76	66.04	86.78	15.45
	4	0.83	76.02	92.11	16.40
	5	0.87	70.35	80.67	14.36
	6	0.78	68.35	87.61	15.59
	7	0.93	78.02	83.77	14.91
	8	0.93	80.35	86.27	15.36
	9	0.79	70.67	88.89	15.82
	10	0.95	77.37	81.21	14.46
	11	1.41	120.12	85.04	15.14
	12	1.62	134.93	83.05	14.78
2007	1	-0.01	0.00	0.00	0.00
	2	0.07	0.00	0.00	0.00
	3	0.37	31.30	85.02	15.13
	4	0.62	54.98	88.43	15.74

6.2 Appendix 2

6.2.1 Quality control of cleanup test and DST samples from Ormen Lange field

Table 6.5. Hoffmann plot data of DST sample (1_39 (gas phase), 1_41 (liquid phase)) of exploration well 6305/7-1 from Ormen Lange field.

Components	Pci (psi)	Psp(psi)	Tci®	Tsp®	Tbi®	Fi	Yi	Xi
Co2	7382.00	797.80	547.56	540.09	350.37	2.63	0.42	0.08
N2	3399.00	797.80	227.00	540.09	139.25	4.54	0.35	0.01
C1	4604.00	797.80	343.01	540.09	200.95	3.78	93.55	3.32
C2	4880.00	797.80	549.79	540.09	332.25	2.45	3.44	1.04
C3	4249.00	797.80	665.70	540.09	415.96	1.51	1.17	1.47
i-C4	3648.00	797.80	734.65	540.09	470.43	0.86	0.25	0.75
n-C4	3797.00	797.80	765.31	540.09	490.81	0.61	0.29	1.30
i-C5	3381.00	797.80	828.72	540.09	541.80	-0.02	0.12	1.33
n-C5	3369.00	797.80	845.30	540.09	556.60	-0.21	0.10	1.55
C6	3012.00	797.80	913.34	540.09	615.42	-0.99	0.11	4.33

Components	Log (Pci/Psc)	((1/Tbi)-(1/Tci))	((1/Tbi)-(1/Tsep))	Fi*A1+A0	Ki	Log(Ki*Psep)
Co2	2.70	0.00103	0.00100	4.14	5.25	3.62
N2	2.36	0.00278	0.00533	6.61	35.00	4.45
C1	2.50	0.00206	0.00312	5.63	28.18	4.35
C2	2.52	0.00119	0.00116	3.91	3.31	3.42
C3	2.46	0.00090	0.00055	2.69	0.80	2.80
i-C4	2.39	0.00076	0.00027	1.84	0.33	2.42
n-C4	2.41	0.00073	0.00019	1.53	0.22	2.25
i-C5	2.36	0.00064	-0.00001	0.70	0.09	1.86
n-C5	2.36	0.00061	-0.00005	0.46	0.06	1.71
C6	2.31	0.00053	-0.00023	-0.55	0.03	1.31

Table 6.6. . Hoffmann plot data of cleanup test sample from Ormen Lange field.

Components	Pci (psi)	Psp(psi)	Tci®	Tsp®	Tbi®	Fi	Yi	Xi
Co2	7382.00	1043.70	547.56	516.87	350.37	2.42	0.46	0.00
N2	3399.00	1043.70	227.00	516.88	139.25	4.47	0.44	0.00
C1	4604.00	1043.70	343.01	516.89	200.95	3.68	92.57	0.09
C2	4880.00	1043.70	549.79	516.90	332.25	2.28	3.28	0.00
C3	4249.00	1043.70	665.70	516.91	415.96	1.28	1.26	1.51
i-C4	3648.00	1043.70	734.65	516.92	470.43	0.60	0.35	1.70
n-C4	3797.00	1043.70	765.31	516.93	490.81	0.34	0.32	3.34
i-C5	3381.00	1043.70	828.72	516.94	541.80	-0.33	0.21	3.40
n-C5	3369.00	1043.70	845.30	516.95	556.60	-0.53	0.14	4.40
C6	3012.00	1043.70	913.34	516.96	615.42	-1.35	0.23	9.55

Components	Log (Pci/Psc)	((1/Tbi)-(1/Tci))	((1/Tbi)-(1/Tsep))	Fi*A1+A0	Ki	Log(Ki*Psep)
Co2	2.70	0.0010	0.0009	5.10	0.00	0.00
N2	2.36	0.0028	0.0052	8.86	0.00	0.00
C1	2.50	0.0021	0.0030	7.43	1017.21	6.03
C2	2.52	0.0012	0.0011	4.85	0.00	0.00
C3	2.46	0.0009	0.0005	3.02	0.83	2.94
i-C4	2.39	0.0008	0.0002	1.77	0.21	2.34
n-C4	2.41	0.0007	0.0001	1.30	0.09	1.99
i-C5	2.36	0.0006	-0.0001	0.07	0.06	1.80
n-C5	2.36	0.0006	-0.0001	0.30	0.03	1.51
C6	2.31	0.0005	-0.0003	1.80	0.02	1.40

Table 6.7. . Hoffmann plot data of DST sample of exploration well 6305/4-1 from Ormen Lange field.

Components	Pci (psi)	Psp(psi)	Tci®	Tsp®	Tbi®	Fi	Yi	Xi
Co2	7382.00	529.20	547.56	520.47	350.37	2.45	0.19	0.08
N2	3399.00	529.20	227.00	520.47	139.25	4.48	0.36	0.16
C1	4604.00	529.20	343.01	520.47	200.95	3.70	94.03	16.19
C2	4880.00	529.20	549.79	520.47	332.25	2.30	3.32	3.05
C3	4249.00	529.20	665.70	520.47	415.96	1.32	1.19	3.25
i-C4	3648.00	529.20	734.65	520.47	470.43	0.64	0.23	1.38
n-C4	3797.00	529.20	765.31	520.47	490.81	0.38	0.28	2.51
i-C5	3381.00	529.20	828.72	520.47	541.80	-0.28	0.11	2.36
n-C5	3369.00	529.20	845.30	520.47	556.60	-0.48	0.09	2.64
C6	3012.00	529.20	913.34	520.47	615.42	-1.29	0.09	6.61

Components	Log (Pci/Psc)	((1/Tbi)-(1/Tci))	((1/Tbi)-(1/Tsep))	Fi*A1+A0	Ki	Log(Ki*Psep)
Co2	2.70	0.0010	0.0009	3.42	2.40	3.10
N2	2.36	0.0028	0.0053	5.02	2.20	3.07
C1	2.50	0.0021	0.0031	4.40	5.81	3.49
C2	2.52	0.0012	0.0011	3.30	1.09	2.76
C3	2.46	0.0009	0.0005	2.52	0.36	2.29
i-C4	2.39	0.0008	0.0002	1.99	0.17	1.94
n-C4	2.41	0.0007	0.0001	1.78	0.11	1.77
i-C5	2.36	0.0006	-0.0001	1.26	0.05	1.39
n-C5	2.36	0.0006	-0.0001	1.10	0.03	1.27
C6	2.31	0.0005	-0.0003	0.46	0.01	0.85

6.2.2 Compositional data of fluid samples of Exploration wells from Ormen Lange field

Table 6.8. Compositional data of MDT sample (PT-1087) of exploration well 63058/5-1 from Ormen Lange field.

composition	Gas		Condensate		Density	Recombined
						Laboratory
	Mole%	MW	Mole%	Mw	g/cm3	Mole %
N2	0.181		0.000			0.179
Co2	1.279		0.000			1.272
C1	92.258		0.028			91.756
C2	3.167		0.023			3.150
C3	1.161		0.074			1.155
i-C4	0.328		0.058			0.326
n-C4	0.292		0.137			0.291
i-C5	0.193		0.204			0.193
n-C5	0.127		0.289			0.128
C6.P	0.204	85.600	1.305	85.600	0.666	0.210
C6.N	0.015	85.600	0.040	85.600	0.666	0.015
C6.A	0.000	85.600	0.000	85.600	0.666	0.000
C7.P	0.158	94.800	3.130	94.800	0.723	0.175
C7.N	0.145	94.800	2.139	94.800	0.723	0.156
C7.A	0.005	94.800	0.064	94.800	0.723	0.005
C8.P	0.053	107.800	6.499	107.800	0.749	0.089
C8.N	0.206	107.800	6.040	107.800	0.749	0.237
C8.A	0.025	107.800	0.944	107.800	0.749	0.030
C9.P	0.023	121.600	8.473	121.600	0.760	0.069
C9.N	0.002	121.600	2.105	121.600	0.760	0.013
C9.A	0.005	121.600	2.498	121.600	0.760	0.018
C10+	0.174	156.000	55.947	189.500	0.813	0.533

Table 6.9. Compositional data of recombined fluid by PVT.SIM simulator of MDT sample (PT-1087) of exploration well 63058/5-1 from Ormen Lange field.

Recombined fluid by PVT.SIM simulation			
Component	Mol %	Mol wt	Liquid Density g/cm³
N2	0.18	28.014	
CO2	1.272	44.01	
C1	91.762	16.043	
C2	3.15	30.07	
C3	1.155	44.097	
iC4	0.327	58.124	
nC4	0.291	58.124	
iC5	0.193	72.151	
nC5	0.128	72.151	
C6	0.21	86.178	0.66
c-C6	0.015	84.162	0.78
c-C7	0.161	98.189	0.81
c-C8	0.267	112.216	0.83
Mesitylene	0.032	120.195	0.86
C7	0.174	96	0.72
C8	0.088	107	0.74
C9	0.068	121	0.76
C10	0.127	134	0.77
C11	0.096	147	0.78
C12	0.073	161	0.79
C13	0.056	175	0.80
C14	0.042	190	0.81
C15	0.032	206	0.82
C16-C17	0.043	228.473	0.83
C18-C20	0.033	260.823	0.85
C21-C54	0.025	334.269	0.8886

Table 6.10. Compositional data of MDT sample (TS-2008) of exploration well 63058/5-1 from Ormen Lange field.

composition	Gas		Condensate		Density	Recombined
						Laboratory
	Mole%	MW	Mole%	Mw	g/cm3	Mole %
N2	0.36		0.00	85.60		0.36
Co2	0.20		0.00	85.60		0.20
C1	93.46		0.02	85.60		93.32
C2	3.23		0.01	94.80		3.22
C3	1.18		0.04	94.80		1.17
i-C4	0.33		0.04	94.80		0.33
n-C4	0.29		0.00	107.80		0.29
i-C5	0.19		0.15	107.80		0.19
n-C5	0.13		0.22	107.80		0.13
C6,P	0.19	85.60	1.03	121.60	0.67	0.20
C6,N	0.01	85.60	0.03	121.60		0.01
C6,A	0.00	85.60	0.00	121.60		0.00
C7,P	0.02	94.80	2.54	200.90	0.72	0.02
C7,N	0.16	94.80	1.72	85.60		0.16
C7,A	0.00	94.80	0.06	85.60		0.00
C8,P	0.05	107.80	6.12	85.60	0.75	0.05
C8,N	0.16	107.80	5.23	94.80		0.17
C8,A	0.00	107.80	0.84	94.80		0.00
C9,P	0.02	121.60	10.25	94.80	0.76	0.04
C9,N	0.00	121.60	2.20	107.80		0.00
C9,A	0.01	121.60	2.85	107.80		0.02
C10+	0.00	156.00	66.66	107.80	0.83	0.11

Table 6.11. Compositional data of recombined fluid by PVT.SIM simulator of MDT sample (TS-2008) of exploration well 63058/5-1 from Ormen Lange field.

Recombined fluid by PVT.SIM simulation			
Component	Mol %	Mol wt	Liquid Density g/cm³
N2	0.36	28.01	
CO2	0.20	44.01	
C1	93.32	16.04	
C2	3.22	30.07	
C3	1.17	44.10	
iC4	0.33	58.12	
nC4	0.29	58.12	
iC5	0.19	72.15	
nC5	0.13	72.15	
C6	0.20	86.18	0.67
c-C6	0.02	84.16	0.67
c-C7	0.17	98.19	0.72
c-C8	0.17	112.22	0.75
c-C9	0.02	120.20	0.76
C7	0.02	96.00	0.72
C8	0.06	107.00	0.75
C9	0.04	121.35	0.76
C10	0.02	134.00	0.77
C11	0.02	147.00	0.79
C12-C13	0.02	167.33	0.80
C14	0.01	190.00	0.82
C15-C16	0.01	213.23	0.83
C17-C18	0.01	243.33	0.85
C19-C20	0.01	268.42	0.86
C21-C25	0.01	312.91	0.88
C26-C117	0.01	425.53	0.93

Table 6.12. Compositional data of MDT sample (E-3468) of exploration well 63058/5-1 from Ormen Lange field.

composition	Gas		Condensate		Density	Recombined
						Laboratory
	Mole%	MW	Mole%	Mw	g/cm3	Mole %
N2	0.41		0.00			0.41
Co2	0.20		0.00			0.20
C1	93.10		0.00			92.72
C2	3.25		0.01			3.24
C3	1.17		0.03			1.17
i-C4	0.33		0.03			0.33
n-C4	0.29		0.09			0.29
i-C5	0.19		0.14			0.19
n-C5	0.13		0.21			0.12
C6,P	0.20	85.60	0.94	85.60	0.67	0.20
C6,N	0.01	85.60	0.03	85.60	0.67	0.02
C6,A	0.00	85.60	0.00	85.60	0.67	0.00
C7,P	0.15	94.80	2.33	94.80	0.72	0.16
C7,N	0.13	94.80	1.59	94.80	0.72	0.14
C7,A	0.00	94.80	0.05	94.80	0.72	0.00
C8,P	0.05	107.70	5.42	107.70	0.75	0.07
C8,N	0.19	107.70	4.75	107.70	0.75	0.21
C8,A	0.03	107.70	0.75	107.70	0.75	0.03
C9,P	0.03	121.10	7.71	121.10	0.76	0.06
C9,N	0.01	121.10	2.24	121.10	0.76	0.02
C9,A	0.02	121.10	2.49	121.10	0.76	0.03
C10+	0.11	156.00	57.19	201.20	0.83	0.40

Table 6.13. Compositional data of recombined fluid by PVT.SIM simulator of MDT sample (E-3468) of exploration well 63058/5-1 from Ormen Lange field.

Recombined fluid by PVT.SIM simulation			
Component	Mol %	Mol wt	Liquid Density g/cm³
N2	0.41	28.01	
CO2	0.20	44.01	
C1	92.72	16.04	
C2	3.24	30.07	
C3	1.17	44.10	
iC4	0.33	58.12	
nC4	0.29	58.12	
iC5	0.19	72.15	
nC5	0.13	72.15	
C6	0.20	86.18	0.67
c-C6	0.02	84.16	0.67
c-C7	0.15	98.19	0.72
c-C8	0.24	112.22	0.75
nC9	0.04	128.26	0.76
C7	0.16	96.00	0.72
C8	0.07	107.00	0.75
C9	0.06	121.00	0.76
C10	0.08	134.00	0.78
C11	0.06	147.00	0.79
C12	0.05	161.00	0.81
C13	0.04	175.00	0.82
C14	0.03	190.00	0.83
C15-C16	0.05	213.09	0.84
C17-C18	0.03	243.20	0.86
C19-C22	0.03	279.50	0.88
C23-C102	0.04	371.94	0.93

Table 6.14. Compositional data of MDT sample (TS-18211) of exploration well 63058/5-1 from Ormen Lange field.

composition	Gas		Condensate		Density	Recombined
						Laboratory
	Mole%	MW	Mole%	Mw	g/cm3	Mole %
N2	0.72		0.00			0.72
Co2	0.22		0.00			0.22
C1	92.17		0.01			91.73
C2	3.45		0.01			3.44
C3	1.20		0.03			1.19
i-C4	0.34		0.04			0.34
n-C4	0.30		0.00			0.30
i-C5	0.20		0.16			0.20
n-C5	0.13		0.24			0.13
C6,P	0.21	85.60	1.13	85.60	0.67	0.21
C6,N	0.02	85.60	0.03	85.60		0.02
C6,A	0.00	85.60	0.00	85.60		0.00
C7,P	0.15	94.80	2.85	94.80	0.72	0.17
C7,N	0.14	94.80	1.93	94.80		0.15
C7,A	0.00	94.80	0.01	94.80		0.01
C8,P	0.05	107.50	6.23	107.50	0.75	0.08
C8,N	0.20	107.50	5.73	107.50		0.22
C8,A	0.03	107.50	0.91	107.50		0.03
C9,P	0.02	121.00	8.24	121.00	0.76	0.06
C9,N	0.00	121.00	2.06	121.00		0.01
C9,A	0.00	121.00	2.58	121.00		0.02
C10+	0.21	156.00	55.75	194.32	0.80	0.54

Table 6.15. Compositional data of recombined fluid by PVT.SIM simulator of MDT sample (TS-18211) of exploration well 63058/5-1 from Ormen Lange field.

Recombined fluid by PVT.SIM simulation			
Component	Mol %	Mol wt	Liquid Density g/cm³
N2	0.72	28.01	
CO2	0.22	44.01	
C1	91.99	16.04	
C2	3.44	30.07	
C3	1.20	44.10	
iC4	0.34	58.12	
nC4	0.30	58.12	
iC5	0.20	72.15	
nC5	0.13	72.15	
C6	0.21	86.18	0.67
c-C6	0.02	84.16	0.67
c-C7	0.16	98.19	0.72
c-C8	0.25	112.22	0.75
nC9	0.03	128.26	0.76
C7	0.17	96.00	0.72
C8	0.08	107.00	0.75
C9	0.06	121.00	0.76
C10	0.12	134.00	0.77
C11	0.09	147.00	0.78
C12	0.07	161.00	0.79
C13	0.05	175.00	0.79
C14	0.04	190.00	0.80
C15	0.03	206.00	0.81
C16-C17	0.04	228.47	0.81
C18-C20	0.03	260.81	0.83
C21-C87	0.02	333.89	0.85

Table 6.16. Compositional data of MDT sample (TS-18204) of exploration well 63058/5-1 from Ormen Lange field.

composition	Gas		Condensate		Density	Recombined
						Laboratory
	Mole%	MW	Mole%	Mw	g/cm3	Mole %
N2	0.36		0.00			0.36
Co2	0.21		0.00			0.20
C1	92.99		0.05			92.60
C2	3.36		0.03			3.35
C3	1.25		0.07			1.24
i-C4	0.35		0.06			0.35
n-C4	0.31		0.14			0.31
i-C5	0.21		0.27			0.21
n-C5	0.13		0.42			0.14
C6,P	0.23	85.60	2.17	85.60	0.67	0.24
C6,N	0.02	85.60	0.06	85.60	0.67	0.02
C6,A	0.00	85.60	0.00	85.60	0.67	0.00
C7,P	0.07	94.60	4.97	94.60	0.72	0.09
C7,N	0.06	94.60	3.54	94.60	0.72	0.07
C7,A	0.01	94.60	0.11	94.60	0.72	0.01
C8,P	0.04	107.10	9.23	107.10	0.75	0.08
C8,N	0.17	107.10	9.07	107.10	0.75	0.21
C8,A	0.03	107.10	1.44	107.10	0.75	0.03
C9,P	0.02	121.00	11.00	121.00	0.76	0.06
C9,N	0.00	121.00	2.83	121.00	0.76	0.01
C9,A	0.01	121.00	3.41	121.00	0.76	0.00
C10+	0.17	156.00	51.15	187.00	0.82	0.39

Table 6.17. Compositional data of recombined fluid by PVT.SIM simulator of MDT sample (TS-18204) of exploration well 63058/5-1 from Ormen Lange field.

Recombined fluid by PVT.SIM simulation			
Component	Mol %	Mol wt	Liquid Density g/cm³
N2	0.07	28.01	
CO2	0.21	44.01	
C1	93.59	16.04	
C2	3.32	30.07	
C3	1.17	44.10	
iC4	0.23	58.12	
nC4	0.29	58.12	
iC5	0.12	72.15	
nC5	0.10	72.15	
C6	0.10	84.00	0.67
c-C6	0.01	84.16	0.67
c-C7	0.07	98.19	0.72
c-C8	0.08	112.22	0.75
nC9	0.04	121.00	0.76
C7	0.04	91.10	0.72
C8	0.06	107.00	0.75
C9	0.07	121.00	0.76
C10	0.11	134.00	0.77
C11	0.08	147.00	0.78
C12	0.06	161.00	0.79
C13	0.05	175.00	0.79
C14	0.03	190.00	0.80
C15	0.03	206.00	0.81
C16	0.02	222.00	0.81
C17-C19	0.04	247.93	0.83
C20-C86	0.03	319.20	0.85

Table 6.18.Compositional data of MDT sample (MPSRBA-927) of exploration well 6305/7-1 from Ormen Lange field.

	Gas (mole%)	Liquid(mole %)	Recombined (Mole %)
H2	0	0	0
H2S	0	0	0
Co2	0.36	0	0.36
N2	0.38	0	0.37
C1	93.65	0	92.5
C2	3.42	0	3.38
C3	1.22	0.02	1.2
i-C4	0.24	0.11	0.24
n-C4	0.3	0.44	0.31
i-C5	0	0.01	0
n-C5	0.12	1.43	0.13
Neo-C5	0.1	2.2	0.12
C6	0.09	7.4	0.17
M,C,C5	0.02	2.88	0.05
Benzene	0	0.37	0.01
C-C6	0.03	4.16	0.08
C7	0.02	9.42	0.14
m,c,C6	0.02	8.22	0.12
Toluene	0	1.9	0.03
C8	0.01	11.43	0.15
eth,benzene	0	0.63	0.01
meta,para-xylene	0	2.05	0.03
Ortho-xylene	0	0.7	0.01
C9	0.01	7.94	0.11
Tri-me-benzene	0	0.73	0.01
C10	0.01	7.73	0.1
C11	0	6.23	0.08
C12	0	4.83	0.06
C13	0	4.2	0.05
C14	0	3.69	0.04
C15	0	3.13	0.04
C16	0	2.3	0.03
C17	0	1.71	0.02
C18	0	1.46	0.02
C19	0	0.95	0.01
C20	0	0.61	0.01
C21	0	0.44	0.01

C22	0	0.25	0
C23	0	0.16	0
C24	0	0.1	0
C25	0	0.06	0
C26	0	0.04	0
C27	0	0.03	0
C28	0	0.02	0
C29	0	0.01	0
C30	0	0	0
C31	0	0	0
C32	0	0	0
C33	0	0.01	0
C34	0	0	0
C35	0	0	0
C36+	0	0	0
	100	100	100
C7+			
Mole%	0.12	88.39	1.22
Mw	99.7	139	134
Density	0.75	0.77	0.77
C20+			
Mole%	0	1.73	0.02
Mw	0	300	300
Density	0	0.871	0.87
Total			
Mw	17.5	132	18.9
Density	0	0.76	

Table 6.19. Compositional data of DST sample (1-39, 1-41) of exploration well 63058/7-1 from Ormen Lange field.

Component	Separator liquid		Separator Gas	Recombined Laboratory	
Mole	Weight (%)	Mole (%)	Mole (%)	weight (%)	Mole(%)
Hydrogen	0	0	0	0	0
Hydrogen Sulphide	0	0	0	0	0
Carbon Dioxide	0,18	0,08	0,42	0,42	0,96
Nitrogen	0,04	0,01	0,35	0,34	0,51
Methane	20,57	3,32	93,55	92,31	78
Ethane	3,43	1,04	3,44	3,44	5,45
Propane	3,32	1,47	1,17	1,21	2,8
i-Butane	1,28	0,75	0,25	0,27	0,82
n-Butane	2,23	1,3	0,29	0,32	0,99
neo-Pentane	0,05	0,04	0	0	0
i-Pentane	1,83	1,33	0,12	0,15	0,57
n-Pentane	2,14	1,55	0,1	0,13	0,51
Hexanes	4,99	4,33	0,11	0,19	0,87
Me-Cyclo-pentane	1,87	1,58	0,03	0,06	0,27
Benzene	0,25	0,19	0	0	0,02
Cyclo-hexane	2,78	2,36	0,04	0,09	0,38
Heptanes	5,86	5,91	0,04	0,14	0,73
Me-Cyclo-hexane	5,55	5,49	0,04	0,13	0,69
Toluene	1,24	1,16	0,01	0,03	0,15
Octanes	7,41	8,53	0,02	0,15	0,87
Ethyl-benzene	0,41	0,44	0	0,01	0,04
Meta/Para-xylene	1,47	1,57	0	0,02	0,14
Ortho-xylene	0,48	0,51	0	0,01	0,05
Nonanes	5,38	6,96	0,01	0,1	0,68
Tri-Me-benzene	0,52	0,63	0	0,01	0,06
Decanes	5,3	7,6	0,01	0,1	0,75
Undecanes	4,37	6,47	0	0,07	0,57
Dodecanes	3,41	5,53	0	0,06	0,49
Tridecanes	2,97	5,24	0	0,05	0,46
Tetradecanes	2,57	4,92	0	0,04	0,44
Pentadecanes	2,18	4,53	0	0,04	0,4
Hexadecanes	1,58	3,54	0	0,03	0,31
Heptadecanes	1,2	2,87	0	0,02	0,25
Octadecanes	1,07	2,71	0	0,02	0,24
Nonadecanes	0,71	1,89	0	0,01	0,17
Eicosanes	0,46	1,28	0	0,01	0,11
Heneicosanes	0,32	0,94	0	0,01	0,08
Docosanes	0,21	0,66	0	0	0,06
Tricosanes	0,14	0,45	0	0	0,04
Tetracosanes	0,09	0,3	0	0	0,03

Pentacosanes	0,06	0,2	0	0	0,02
Hexacosanes	0,03	0,12	0	0	0,01
Heptacosanes	0,02	0,08	0	0	0,01
Octacosanes	0,01	0,05	0	0	0
Nonacosanes	0,01	0,03	0	0	0
Triacontanes	0,01	0,02	0	0	0
Hentriacontanes	0	0,01	0	0	0
Dotriacontanes	0	0,01	0	0	0
Tritriacontanes	0	0	0	0	0
Total	100	100	100	99,99	100

Table 6.20. Compositional data of recombined fluid by PVT.SIM simulator of DST sample (1-39, 1-41) of exploration well 63058/7-1 from Ormen Lange field.

Recombined by Simulation		
Component	Mole (%)	MW
N2	0,346	28,014
CO2	0,416	44,01
C1	92,513	16,043
C2	3,412	30,07
C3	1,173	44,097
iC4	0,256	58,124
nC4	0,302	58,124
iC5	0,134	72,151
nC5	0,117	72,151
C6	0,159	86,178
C7	0,306	96
C8	0,226	107
C9	0,167	121
C10	0,123	134
C11	0,091	147
C12	0,067	161
C13	0,05	175
C14	0,037	190
C15	0,027	206
C16	0,02	222
C17-C19	0,034	247,739
C20-C79	0,023	315,497

Table 6.21. Compositional data of MDT sample (MPRS-756) of exploration well 63058/4-1 from Ormen Lange field.

Component	Stock tank gas	stock tank oil	Recombined Laboratory	Dsty kg/m3	MW g/mole*
	(mole%)	liq.(mole%)	mole %		
N2	0,39	0,00	0,39		28,01
CO2	0,19	0,00	0,19		44,01
H2S	0,00	0,00	0,00		0,00
C1	93,73	0,00	93,40		16,04
C2	3,26	0,00	3,25		30,07
C3	1,14	0,04	1,13		44,10
IC4	0,22	0,04	0,22		58,12
NC4	0,28	0,11	0,27		58,12
IC5	0,12	0,79	0,13		72,15
NC5	0,11	0,25	0,11		72,15
C6 total	0,15	1,22	0,15	0,67	85,30
P	0,14	1,13	0,14		85,30
N	0,01	0,09	0,01		85,30
C7 total	0,19	8,10	0,22	0,71	92,20
P	0,05	5,81	0,07		92,20
N	0,13	2,21	0,14		92,20
A	0,01	0,08	0,01		92,20
C8 total	0,15	12,91	0,20	0,74	104,80
P	0,06	6,96	0,08		104,80
N	0,08	4,91	0,10		104,80
A	0,02	1,05	0,02		104,80
C9 total	0,05	13,36	0,09	0,76	119,10
P	0,02	7,13	0,05		119,10
N	0,02	3,28	0,03		119,10
A	0,01	2,95	0,02		119,10
C10+	0,04	63,18	0,26	0,81	198,50
Sum	100,00	100,00	100,00		
Total					
MW g/mole	17,70	169,8	18,3		
Density kg/m3	0,75	792,2	160,3		
Gas gravity	0,61				

Table 6.22. Compositional data of recombined fluid by PVT.SIM simulator of MDT sample (MPRS-756) of exploration well 63058/4-1 from Ormen Lange field.

Recombined by PVT.SIM		
Component	Mole %	Mw
N2	0,389	28,014
CO2	0,188	44,01
C1	93,388	16,043
C2	3,248	30,07
C3	1,132	44,097
iC4	0,221	58,124
nC4	0,274	58,124
iC5	0,126	72,151
nC5	0,111	72,151
C6	0,141	86,178
c-C6	0,009	84,162
c-C7	0,144	98,189
c-C8	0,114	112,216
nC9	0,047	128,258
C7	0,071	96
C8	0,083	107
C9	0,047	121
C10	0,052	134
C11	0,042	147
C12	0,034	161
C13	0,027	175
C14-C15	0,039	197,138
C16-C17	0,026	228,692
C18-C19	0,017	256,353
C20-C23	0,018	293,415
C24-C107	0,013	389,473

Table 6.23. Compositional data of DST sample (Minilab) of exploration well 63058/4-1 from Ormen Lange field.

Component	Separator gas	Sep.liquid	Recombined Laboratory	Dsty kg/m3	MW g/mole*
	mole%	mole%	mole %		
N2	0,358	0,163	0,356	0,8093	
CO2	0,192	0,08	0,191	0,8226	
H2S	0	0	0	0	
C1	94,033	16,185	93,164	0,3	
C2	3,319	3,052	3,316	0,3581	
C3	1,185	3,25	1,208	0,5083	
IC4	0,229	1,38	0,242	0,5637	
NC4	0,279	2,505	0,304	0,5847	
IC5	0,11	2,359	0,135	0,625	
NC5	0,092	2,638	0,121	0,6316	
C6 total	0,088	6,611	0,161	0,6656	85,3
P	0,082	6,303	0,151		
N	0,007	0,308	0,01		
C7 total	0,061	12,631	0,201	0,7288	92,2
P	0,009	5,673	0,072		
N	0,049	6,661	0,123		
A	0,003	0,297	0,007		
C8 total	0,035	15,261	0,205	0,7504	104,8
P	0,015	6,439	0,087		
N	0,016	7,37	0,098		
A	0,003	1,451	0,02		
C9 total	0,007	6,778	0,083	0,7827	119,1
P	0,007	3,136	0,042		
N	0	1,913	0,021		
A	0	1,729	0,019		
C10+	0,011	27,107	0,313	0,8086	216,9
Sum	100	100	100		
Total					
MW g/mole	17,4	111,8	18,5	*recomb. MW	
Density kg/m3	0,737	-	-	**stabil. Dsty	
Gas gravity	0,602	-	-		

Table 6.24. Compositional data of recombined fluid by PVT.SIM simulator of DST sample (Minilab) of exploration well 63058/4-1 from Ormen Lange field.

Recombined by PVT.SIM		
Component	Mole (%)	MW
N2	0,356	28,014
CO2	0,191	44,01
C1	93,159	16,043
C2	3,316	30,07
C3	1,208	44,097
iC4	0,242	58,124
nC4	0,304	58,124
iC5	0,135	72,151
nC5	0,121	72,151
C6	0,161	85,774
C7	0,202	93,333
C8	0,206	105,17
C9	0,083	119,258
C10-C11	0,087	139,976
C12	0,034	161
C13	0,029	175
C14-C15	0,046	197,355
C16-C17	0,033	228,896
C18-C19	0,024	256,517
C20-C23	0,03	294,375
C24-C28	0,018	354,835
C29-C135	0,015	481,877

6.2.3 Constant mass expansion (CME) data of exploration wells from Ormen Lange field

Table 6.25. Constant mass expansion data of MDT sample (E-3468) of exploration well 6305/5-1 from Ormen Lange field.

6305/5-1 MDT Recombined*E-3468 ,EOS = SRK Peneloux				
Constant Mass expansion at 81C				
Pressure	Rel Vol		Z Factor	Density
bara	V/Vd			g/cm³
348,30	0,87		1,02	0,22
345,10	0,88		1,01	0,22
340,00	0,89		1,01	0,22
335,10	0,90		1,00	0,21
330,10	0,91		1,00	0,21
325,10	0,92		1,00	0,21
320,10	0,93		0,99	0,21
315,10	0,94		0,99	0,21
310,00	0,95		0,98	0,20
305,20	0,96		0,98	0,20
300,00	0,97		0,97	0,20
295,00	0,98		0,97	0,20
287,32	1,00		0,96	0,19
287,00	1,00			
275,00	1,03			
260,10	1,08			
240,00	1,16			
220,00	1,25			
200,00	1,36			
180,00	1,51			
160,00	1,69			
140,00	1,93			
120,00	2,26			
100,00	2,73			
80,00	3,46			

Table 6.26. Constant mass expansion data of MDT sample (PT-1087) of exploration well 6305/5-1 from Ormen Lange field.

6305/5-1 MDT Recombined PT-1087 ,EOS = SRK Peneloux				
Constant Mass expansion at 81C				
Pressure	Rel Vol		Z Factor	Density
bara	V/Vd			g/cm³
399,80	0,80		1,07	0,25
390,20	0,82		1,06	0,24
380,80	0,83		1,05	0,24
370,00	0,84		1,03	0,24
360,10	0,86		1,02	0,23
350,60	0,87		1,01	0,23
339,90	0,89		1,00	0,22
330,10	0,91		0,99	0,22
319,90	0,93		0,98	0,21
310,80	0,95		0,97	0,21
300,00	0,97		0,96	0,21
290,60	0,99		0,96	0,20
287,41	1,00		0,95	0,20
287,00	1,00			
280,60	1,02			
270,20	1,05			
261,00	1,08			
250,40	1,12			
240,00	1,16			
230,30	1,20			
220,70	1,24			
210,20	1,30			
200,40	1,36			
190,10	1,43			
180,10	1,50			
170,30	1,59			
160,30	1,69			
150,40	1,80			
140,10	1,93			
130,10	2,08			
120,50	2,26			

Table 6.27. Constant mass expansion data of MDT sample (TS-2008) of exploration well 6305/5-1 from Ormen Lange field.

6305/5-1 MDT Recombined TS - 2008 ,EOS = SRK Peneloux				
Constant Mass expansion at 81C				
Pressure	Rel Vol		Z Factor	Density
bara	V/Vd			g/cm³
350,10	0,87		1,03	0,21
340,40	0,89		1,02	0,21
331,60	0,90		1,01	0,20
320,90	0,92		1,00	0,20
310,70	0,94		0,99	0,19
301,30	0,97		0,98	0,19
292,50	0,99		0,97	0,18
287,85	1,00		0,97	0,18
287,00	1,00			
275,30	1,04			
265,20	1,07			
257,30	1,09			
229,30	1,20			
224,50	1,23			
200,10	1,36			
175,00	1,54			
160,00	1,68			
131,70	2,05			
120,10	2,25			
110,00	2,47			
100,00	2,73			
90,10	3,04			
80,10	3,44			

Table 6.28. Constant mass expansion data of MDT sample (TS-18211) of exploration well 6305/5-1 from Ormen Lange field.

6305/5-1 MDT Recombined TS - 18211 ,EOS = SRK Peneloux			
Constant Mass expansion at 81C			
Pressure	Rel Vol	Z Factor	Density
bara	V/Vd		g/cm³
400,10	0,80	1,07	0,24
390,00	0,82	1,06	0,24
380,30	0,83	1,05	0,24
370,20	0,84	1,04	0,23
360,10	0,86	1,03	0,23
350,10	0,87	1,02	0,23
340,20	0,89	1,01	0,22
330,00	0,91	1,00	0,22
320,00	0,93	0,99	0,21
310,00	0,95	0,98	0,21
300,00	0,97	0,97	0,20
290,10	0,99	0,96	0,20
287,11	1,00	0,96	0,20
287,00	1,00		
270,10	1,05		
260,00	1,08		
240,00	1,16		
220,00	1,25		
200,00	1,36		
180,10	1,51		
160,00	1,69		
140,00	1,94		
120,00	2,27		

Table 6.29. Constant mass expansion data of MDT sample (TS-18204) of exploration well 6305/5-1 from Ormen Lange field.

6305/5-1 MDT Recombined TS - 18204 ,EOS = SRK Peneloux			
Constant Mass expansion at 81C			
Pressure	Rel Vol	Z Factor	Density
bara	V/Vd		g/cm³
451,700	0,813	1,132	0,249
426,300	0,841	1,104	0,241
400,700	0,872	1,077	0,232
375,200	0,909	1,050	0,223
351,200	0,949	1,026	0,213
329,600	0,990	1,006	0,204
325,062	1,000	1,001	0,202
325,000	1,000		
304,800	1,048		
271,100	1,148		
241,600	1,263		
212,100	1,416		
181,400	1,637		
151,400	1,953		
121,900	2,434		
91,500	3,278		
62,700	4,866		

Table 6.30. Constant mass expansion data of MDT sample (MPSRBA-927) of exploration well 6305/5-1 from Ormen Lange field.

6305/7-1 MDT Recombined MPSRBA-927,EOS = SRK Peneloux			
Constant Mass expansion at 90C			
Pressure	Rel Vol	Z Factor	Density
bara	V/Vd		g/cm³
477,21	0,75	1,16	0,31
409,18	0,80	1,06	0,29
341,16	0,87	0,96	0,27
285,78	0,96	0,89	0,25
273,13	0,98	0,87	0,24
265,41	1,00	0,86	0,24
257,82	1,02		
256,12	1,02		
252,72	1,03		
245,92	1,05		
239,12	1,08		
232,31	1,10		
225,51	1,12		
211,90	1,18		
198,30	1,25		
184,69	1,33		
157,48	1,55		
130,27	1,89		
116,67	2,13		
89,46	2,87		
62,24	4,31		
48,64	5,66		
41,84	6,67		
30,95	9,22		

Table 6.31. Constant mass expansion data of DST sample (1-39, 1-41) of exploration well 6305/7-1 from Ormen Lange field.

6305/7-1 DST Recombined (1-39 , 1-41), EOS = SRK Peneloux			
Constant Mass expansion at 90C			
Pressure	Rel Vol	Z Factor	Density
bara	V/Vd		g/cm³
408,35	0,82	1,09	0,23
374,41	0,87	1,05	0,22
340,46	0,92	1,02	0,21
306,52	0,99	0,99	0,19
304,25	1,00	0,99	0,19
287,85	1,04		
286,15	1,05		
282,76	1,06		
279,36	1,07		
272,57	1,09		
265,78	1,11		
259,00	1,14		
245,42	1,19		
231,84	1,25		
218,26	1,32		
204,68	1,40		
191,11	1,49		
163,95	1,72		
136,80	2,07		
109,64	2,59		
82,48	3,48		
65,51	4,43		
48,54	6,04		

Table 6.32. Constant mass expansion data of MDT sample (MPRS-756) of exploration well 6305/4-1 from Ormen Lange field.

6305/4-1 MDT Recombined MPRS-756 , EOS = SRK Peneloux			
Constant Mass expansion at 90C			
Pressure	Rel Vol	Z Factor	Density
bara	V/Vd		g/cm³
350,100	0,725	1,027	0,212
340,400	0,739	1,018	0,208
331,600	0,753	1,010	0,204
320,900	0,770	1,000	0,199
310,700	0,788	0,991	0,195
301,300	0,806	0,982	0,191
292,500	0,824	0,975	0,186
287,000	0,836	0,970	0,184
275,300	0,863	0,961	0,178
265,200	0,889	0,953	0,173
257,300	0,911	0,948	0,169
229,927	1,000	0,930	0,154
229,300	1,002		
224,500	1,021		
200,100	1,134		
175,000	1,287		
160,000	1,405		
131,700	1,710		
120,100	1,880		
110,000	2,059		
100,000	2,274		
90,100	2,536		
80,100	2,869		

Table 6.33. Constant mass expansion data of DST sample (Minilab) of exploration well 6305/4-1 from Ormen Lange field.

6305/4-1 DST Recombined Minilab , EOS = SRK Peneloux				
Constant Mass expansion at 90C				
Pressure	Rel Vol		Z Factor	Density
bara	V/Vd			g/cm³
350,10	0,75		1,03	0,21
340,40	0,76		1,02	0,21
331,60	0,77		1,01	0,21
320,90	0,79		1,00	0,20
310,70	0,81		0,99	0,20
301,30	0,83		0,98	0,19
292,50	0,85		0,97	0,19
287,00	0,86		0,97	0,19
275,30	0,89		0,96	0,18
265,20	0,91		0,95	0,18
257,30	0,94		0,95	0,17
237,33	1,00		0,93	0,16
229,30	1,03			
224,50	1,05			
200,10	1,17			
175,00	1,32			
160,00	1,45			
131,70	1,76			
120,10	1,94			
110,00	2,12			
100,00	2,34			
90,10	2,61			
80,10	2,95			

6.2.4 Constant volume depletion (CVD) data of exploration wells from Ormen Lange field

Table 6.34. Constant volume depletion data of MDT sample (E-3468) of exploration well 6305/5-1 from Ormen Lange field.

6305/5-1 MDT Recombined, E-3468 EOS = SRK Peneloux					
Constant volume depletion at 90 C					
Pressure	Liq Vol	%Prod	Z Factor	Z Factor	Viscosity
bara	% of Vd	Mole	Gas	Two Phase	cP
325,06		0,00	0,97		0,02
320,90		0,00	0,97		0,02
310,70		0,00	0,97	0,97	0,02
301,30		0,00	0,97	0,97	0,02
292,50		0,00	0,96	0,96	0,02
287.59	0	0,00	0,95	0,95	0,02
287.41	0.003	9,94	0,95	0,95	0,02
287.16	0.007	13,15	0,94	0,94	0,02
287	0.009	16,23	0,94	0,94	0,02
280.6	0.113	19,34	0,93	0,93	0,02
270.2	0.274	22,82	0,93	0,93	0,02
261	0.407	26,14	0,92	0,92	0,02
250.4	0.550	29,70	0,92	0,92	0,02
240	0.677	33,23	0,92	0,92	0,02
230.3	0.785	36,74	0,92	0,92	0,02
220.7	0.880	40,37	0,92	0,92	0,02
210.2	0.973	44,01	0,92	0,92	0,02
200.4	1.048	47,84	0,92	0,92	0,02
190.1	1.116	51,59	0,92	0,92	0,02
180.1	1.172	55,21	0,92	0,92	0,02

Table 6.35. Constant volume depletion data of MDT sample (TS-18211) of exploration well 6305/5-1 from Ormen Lange field.

6305/5-1 MDT Recombined, TS-18211 EOS = SRK Peneloux					
Constant volume depletion at 90 C					
Pressure	Liq Vol	%Prod	Z Factor	Z Factor	Viscosity
bara	% of Vd	Mole	Gas	Two Phase	cP
319,90		0,00	0,99		0,03
310,80		0,00	0,98		0,03
300,00		0,00	0,97		0,03
290,60		0,00	0,96		0,03
287,41		0,00	0,96		0,02
287.49	0	0,00	0,96	0,96	0,02
287.41	0.001	0,07	0,96	0,96	0,02
287.16	0.008	1,81	0,96	0,96	0,02
287	0.01	4,72	0,95	0,95	0,02
278.6	0.175	7,36	0,94	0,94	0,02
270.2	0.295	10,50	0,93	0,94	0,02
261	0.394	13,66	0,93	0,93	0,02
250.4	0.504	16,70	0,92	0,92	0,02
240	0.606	19,78	0,92	0,92	0,02
230.3	0.697	23,22	0,92	0,92	0,02
220.7	0.781	26,52	0,91	0,91	0,02
210.2	0.86	30,05	0,91	0,91	0,02
200.4	0.938	33,55	0,91	0,91	0,02
190.1	1.007	37,04	0,91	0,90	0,02
180.1	1.066	40,65	0,91	0,90	0,02
170.3	1.117	44,28	0,91	0,90	0,02
160.3	1.161	48,09	0,91	0,90	0,02
150.4	1.198	51,83	0,91	0,90	0,02
140.1	1.228	55,43	0,91	0,90	0,02

Table 6.36. Constant volume depletion data of MDT sample (PT-1087) of exploration well 6305/5-1 from Ormen Lange field.

6305/5-1 MDT Recombined, PT-1087 EOS = SRK Peneloux					
Constant volume depletion at 90 C					
Pressure	Liq Vol	%Prod	Z Factor	Z Factor	Viscosity
bara	% of Vd	Mole	Gas	Two Phase	cP
319,90		0,00	0,98		0,03
310,80		0,00	0,97		0,03
300,00		0,00	0,96		0,03
290,60		0,00	0,96		0,03
287.59	0	0,00	0,95		0,03
287.41	0.003	0,00	0,95	0,95	0,03
287.16	0.007	0,04	0,95	0,95	0,03
287	0.009	1,80	0,95	0,95	0,02
280.6	0.113	4,72	0,94	0,94	0,02
270.2	0.354	7,37	0,94	0,94	0,02
261	0.487	10,53	0,93	0,93	0,02
250.4	0.630	13,71	0,92	0,92	0,02
240	0.757	16,76	0,92	0,92	0,02
230.3	0.865	19,84	0,92	0,91	0,02
220.7	0.96	23,30	0,91	0,91	0,02
210.2	1.053	26,61	0,91	0,91	0,02
200.4	1.128	30,15	0,91	0,90	0,02
190.1	1.196	33,65	0,90	0,90	0,02
180.1	1.252	37,14	0,90	0,90	0,02
170.3	1.298	40,76	0,90	0,90	0,02
160.3	1.33	44,39	0,90	0,90	0,02
150.4	1.366	48,20	0,91	0,90	0,02
140.1	1.389	51,93	0,91	0,90	0,02
130.1	1.404	55,53	0,91	0,90	0,02
120.5	1.412	63,25	0,92	0,90	0,02
100	1.412	70,75	0,93	0,91	0,01

Table 6.37. Constant volume depletion data of DST sample (Minilab) of exploration well 6305/4-1 from Ormen Lange field.

6305/4-1 DST Recombined, Minilab EOS = SRK Peneloux					
Constant volume depletion at 90 C					
Pressure	Liq Vol	%Prod	Z Factor	Z Factor	Viscosity
bara	% of Vd	Mole	Gas	Two Phase	cP
287.4917	0	0,00	0,98		0,02
287.4149	0.001	0,00	0,98		0,02
287.1616	0.008	0,00	0,97		0,02
287	0.012	0,00	0,96		0,02
280.6	0.175	0,00	0,95		0,02
270.2	0.421	0,00	0,95		0,02
261	0.620	0,00	0,94		0,02
250.4	0.828	0,00	0,94	0,94	0,02
240	1.009	3,00	0,94	0,94	0,02
230.3	1.157	7,22	0,93	0,93	0,02
220.7	1.285	11,23	0,93	0,93	0,02
210.2	1.405	15,53	0,93	0,93	0,02
200.4	1.499	19,78	0,93	0,93	0,02
190.1	1.582	24,01	0,92	0,92	0,02
180.1	1.646	28,39	0,92	0,92	0,02
170.3	1.696	32,77	0,92	0,92	0,02
160.3	1.734	37,38	0,92	0,92	0,02
150.4	1.761	41,89	0,92	0,92	0,02
140.1	1.778	46,25	0,93	0,92	0,02
130.1	1.786	55,51	0,93	0,93	0,02
120.5	1.786	64,03	0,94	0,93	0,01
100	1.765	69,24	0,95	0,94	0,01
80	1.721	73,74	0,95	0,94	0,01